AD NUMBER

AD829427

LIMITATION CHANGES

TO:

Approved for public release; distribution is unlimited.

FROM:

**Distribution authorized to U.S. Gov't. agencies and their contractors;
Administrative/Operational Use; OCT 1967. Other requests shall be referred to Air Force Materials Lab., Wright-Patterson AFB, OH 45433.**

AUTHORITY

AFSC ltr 26 May 1972

AFML-TR-67-281

DEVELOPMENT OF MANUFACTURING METHODS FOR IMPROVED DELAY LINES

Authors: Russell T. Mannette, Frank M. Hendry, Beverly A. Shaw

Raytheon Company, Microwave and Power Tube Division
Waltham, Massachusetts

Technical Report AFML-TR-67-281
October 1967

Air Force Materials Laboratory
Research and Technology Division
Air Force Systems Command
Wright-Patterson Air Force Base, Ohio

NOTICES

When U. S. Government drawings, specifications, or other data are used for any purpose other than a difinitely related Government procurement operation, the Government thereby incurs no responsibility nor any obligation whatsoever; and the fact that Government may have formulated, furnished, or in any way supplied the said drawings, specifications, or other data, is not to be regarded by implication or otherwise, as in any manner licensing the holder or any other person or corporation, or conveying any rights or permission to manufacture, use, or sell any patented invention that may be related thereto in any way.

DDC release to CFSTI is NOT authorized because the report contains technology identifiable with items on the strategic embargo lists excluded from export or re-export under U. S. Export Control Act of 1949 (63 STAT. 7), as amended (50 U.S.C. App. 2020-2031), as implemented by AFR 400-10, AFR 310-2, and AFSCR 80-20.

Qualified requesters may obtain copies from DDC, Document Service Center, Cameron Station, Alexandria, Virginia 22314. Orders will be expedited if placed through the librarian or other person designated to request documents from DDC.

Reproduction in whole or in part is prohibited except with the permission of the Manufacturing Technology Division. However, DDC is authorized to reproduce the document for "U. S. Government purposes".

Do not return this copy unless return is requested by security considerations, contractual obligations, or notice on a specific document.

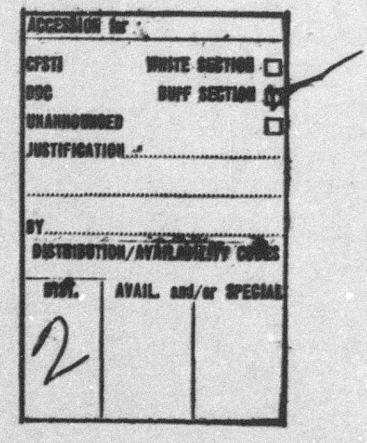

AFML-TR-67-281

DEVELOPMENT OF MANUFACTURING METHODS FOR IMPROVED DELAY LINES

Russell T. Mannette, Frank M. Hendry,
and Beverly A. Shaw

Raytheon Company, Microwave and Power Tube Division
Waltham, Massachusetts

FOREWORD

This final report covers the work performed under Contract Number AF33(615)-2044 from 1 August 1964 to 31 May 1967 relating to the development of methods for the manufacture of photocopied slow-wave structures for C-band microwave tubes. It is published for information only and does not necessarily represent the recommendation, conclusions or approval of the Air Force.

This contract with Raytheon Company, Lexington, Massachusetts, was initiated under Manufacturing Methods Project 8-142, "Development of Manufacturing Methods for Improved Delay Lines." The work was done at the Microwave and Power Tube Division, Waltham, Massachusetts, and was carried out under the general supervision of Mr. L. L. Clampitt, Manager of Engineering, Microwave Tube Operation, and Mr. J. H. Schussele, Manager, Crossed-Field Oscillator Group. Mr. R. T. Mannette, Engineering Section Head in the Crossed-Field Oscillator Group, served as Project Engineer.

The work was carried out under the technical direction of Captain W. C. Horsfield III, MATE, Manufacturing Technology Division, Air Force Materials Laboratory, Wright-Patterson Air Force Base, Ohio.

This technical report has been reviewed and is approved for publication.

JULES I. WITTEBORT
Chief, Electronics Branch,
Manufacturing Technology Division

ABSTRACT

During the three phases of this manufacturing methods program, the following major objectives were accomplished:

1. A facility was established to manufacture photocopied slow-wave structures.
2. A bonding technique was developed between the metallic slow-wave structure and a beryllia substrate, capable of withstanding the processing and operating conditions of the test vehicles.
3. Ten test vehicles have been constructed and evaluated to demonstrate the reliability of the finished C-band slow-wave structure.
4. One test vehicle has been life tested and accumulated 260 hours before failure.
5. Structures have been evaluated at cold test both at C-band and K-band, demonstrating the wide versatility of the technique.
6. Structures have been environmentally evaluated at an acceleration of 20 g's over a frequency range of 55 to 2000 Hz.

TABLE OF CONTENTS

TABLE OF CONTENTS (Continued)

TABLE OF CONTENTS (Continued)

LIST OF ILLUSTRATIONS

LIST OF ILLUSTRATIONS (Continued)

LIST OF ILLUSTRATIONS (Continued)

LIST OF SYMBOLS

Delay Line Nomenclature

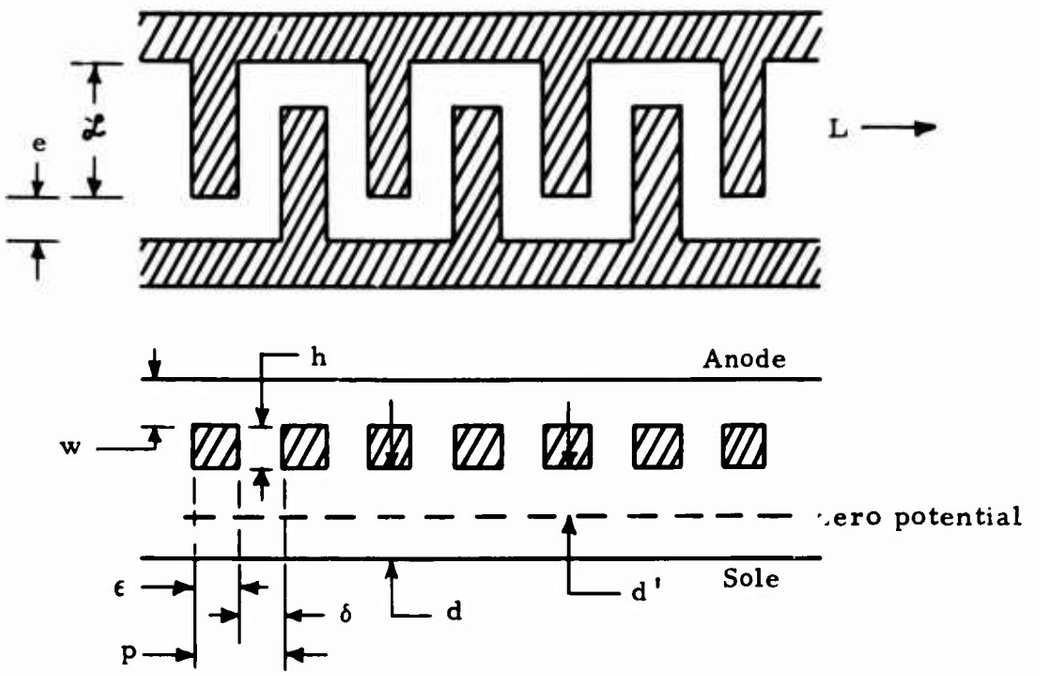

e	=	end spacing
$\mathscr{L}$	=	finger length
L	=	length of line
h	=	finger height
w	=	backwall spacing
ϵ	=	finger thickness
p	=	pitch
δ	=	finger spacing
d	=	sole to anode spacing
d'	=	anode to zero potential line
N	=	number of pitches

1.0 SUMMARY

The objectives of this program were to develop the manufacturing methods, processes and techniques for improving the fabrication of slow-wave structures; to demonstrate the feasibility of the resulting structures by operating one in a test vehicle at C-band; and to evaluate a cold test structure at K-band. This program was concerned with the development of photocopied interdigital delay lines on ceramic substrates.

The initial program was divided into three phases. The detailed objectives of each phase of the work performed are outlined in the revised Statement of Work Exhibit A attached as Appendix A of this report. Phase I consisted of the development of initial structures, establishment of the manufacturing methods and techniques, and evaluation of the product at cold test and hot test at C-band and cold test at K-band. Phase II consisted of the development of a plan for a pilot line to produce ceramic-mounted slow-wave structures. Phase III consisted of operating the pilot line and demonstrating the acceptability of the product by electrical measurements of the slow-wave structure and by the construction, evaluation and life test of test vehicles.

All the objectives of this work statement have been accomplished.

This report describes in detail the work done and results obtained on each of the objectives of the statement of work.

A new technique for the fabrication of slow-wave structures for microwave tubes has been developed and evaluated in the course of this program.

Two major technical difficulties in using such slow-wave structures have been overcome, namely:

1. Achievement of a reliable bond between the ceramic substrate and the thin copper delay line.

2. Reduction in sputtering of the sole material to the delay line, resulting in excess of 200 hours tube life.

A reliable manufacturing technique has been developed for the fabrication of photocopied interdigital delay lines that will result in increased reproducibility, versatility and reliability, while reducing size, weight, and unit cost.

2.0 DISCUSSION

2.1 Purpose and Objectives (Ref: Appendix A, Section IA)

Manufacturing methods, processes, and techniques for improving slow-wave structures in C-band frequency were developed and evaluated during the course of this program. The C-band slow-wave structure selected for this program was a photocopied interdigital delay line on a ceramic substrate.

This design was readily scalable to K-band using the same techniques as were developed for the C-band delay line. It will be shown that the basic technique of fabrication will result in increased reproducibility, versatility and reliability while reducing size, weight and unit cost.

Detailed discussion of the techniques developed and results obtained will be covered in appropriate sections of this report.

2.2 Phase I

2.2.1 Management Control Plan (Ref: Appendix A, Section IB1b(1))

The final version of this chart is attached as Appendix B of this report; the events depicted are directly related to the items of the work statement attached as Appendix A.

2.2.2 Analysis and Selection of Materials (Ref: Appendix A Section IB1b(2)(a))

The slow-wave structures selected for the program were interdigital delay lines for use in an M-type BWO. Since Raytheon Company has had wide experience in conventional interdigital delay lines in C-band M-type backward-wave oscillators, a direct comparison could be made of the parameters of the new technique developed and those of standard interdigital delay lines. This comparison of the new technique vs the old is given in the conclusion of this report.

The initial task was to conduct a study of available materials for use in the photocopied slow-wave structure.

This task logically breaks down into three areas:

a. Materials to be used for the metallic conduction path of the SWS

b. Materials for the dielectric substrate material

c. Materials and techniques to obtain a true bond between the metallic path and the dielectric substrate, capable of withstanding mechanical and thermal stresses.

2.2.2.1 Metallic Conduction Path Analysis

The metallic conduction path that is deposited onto the ceramic substrate requires the following properties:

a. Low vapor pressure

b. High electrical conductivity

c. Reasonable ductility to accommodate thermal expansion mismatch

d. Ability of the material to be electroplated.

Based on the four properties above, the choice of material is limited to silver or copper.

The final differentiation was on the basis of vapor pressure. Silver has a vapor pressure of approximately 10^{-7} mm Hg at 600°C whereas copper is approximately 5×10^{-9} at the same temperature. Copper was therefore chosen as the material for the metallic part of the structure.

2.2.2.2 Support Ceramic

The overall requirements of the support ceramic materials are as follows:

a. Suitable refractoriness to withstand brazing temperatures

b. Sufficiently high tensile, shear and compressive strength to withstand these types of stresses during tube assembly

c. High thermal conductivity

d. Capable of being ground and polished to at least 20 micro-inch finish

e. Capable of being metallized for metal-ceramic joining.

f. General availability

g. Dielectric properties.

A literature search was made at the outset of the program to examine the properties of known ceramic materials, and a comprehensive list of ceramic materials was obtained. A large number of the listed materials could be defined as being unsuitable on the basis of density alone. Considering items (c) and (d) above, those ceramic materials that have been manufactured to produce porous, highly insulating bodies were rejected. The next stage in the selection process was to reject materials not complying with item (a). This rejects certain of the commercial porcelains and certain alumino-silicates.

Those materials remaining as possibilities for the ceramic support structure are shown in Table I.

The major item now left to be considered is item (e) above. Obviously a prolonged study into metal-ceramic sealing techniques for various ceramic materials should be avoided. Within Raytheon, all metal-ceramic sealing techniques developed have been based on the alumina (Al_2O_3) ceramics and beryllia (BeO). The state-of-the-art given in the literature describing bonding techniques to ceramics was surveyed. This yielded no well defined processes for bonding ceramics other than the Al_2O_3 base and BeO. At this point it was decided to confine the investigation of materials to one or more of the following: alumina, sapphire, polycrystalline sapphire or beryllia.

2. 2. 2. 3 Initial Design of Slow-Wave Structure

To complete the selection of the substrate, it was necessary to know the amount of heat dissipation on the delay line for the 50-watt output C-band test vehicle. An initial design of the slow-wave structure (interdigital delay line) was determined by using conventional design techniques and modifying them by the dielectric loading effect of the ceramic substrate. Figure 1 is a sketch of the initial photocopied delay line, with a conventional interdigital delay line shown for comparison. A decision then had to be made as to which substrate to use, based on the work covered in Section 2. 2. 2. 2 of this report. The choice was between BeO and Al_2O_3, based on heat conduction.

First, a line was designed to operate on alumina, and the following dimensions were obtained:

$$\ell = 0.190 \text{ inch}$$
$$p = 0.028 \text{ inch}$$
$$w = 0.080 \text{ inch.}$$

Large signal theory has consistently shown that, assuming normal operation with good beam focusing, the most concentrated beam collection will occur for the most efficient interaction over an area corresponding to 10 interdigital delay line fingers for 50% of the beam. The surface temperature of the SWS was then calculated for three separate conditions using the curves in Figure 2 which were derived from ceramic manufacturers' data. The curves show the hot side temperature (T_H) based on cold side temperatures of 30°C and 100°C, vs a parameter λ' which is defined as

$$\lambda' = \frac{\text{power input}}{\text{area}} \times \text{length of path (watts/inch).}$$

Table I. Candidate Materials Ceramic Support Structure

PROPERTIES		Polycrystalline Glass		Coderite			Zircon	Titania
				Alsimag	Alsimag	Alsimag	$ZrO_2 \cdot S_1O_2$	T_1O_2
Property	Units	9606	9608	202	447	701		
Specific Gravity	---	2.60	2.50	2.1	1.8	2.3	3.7	4.0
Thermal Cond. at 300°C	g. cal/sec/cm²/°C/cm			0.003	0.003	0.008	0.012	0.012
Coef. Ther. Exp	Per °C							
	25-190	7.2×10^{-6}	1.8×10^{-6}	---	---	---	---	---
	25-300	5.68×10^{-6}	1.8×10^{-6}	2.2×10^{-6}	0.6×10^{-6}	2.4×10^{-6}	4.3×10^{-6}	8.3×10^{-6}
	25-500	4.86×10^{-6}	1.97×10^{-6}	---	---	---	---	---
	25-700	---	---	2.8×10^{-6}	1.5×10^{-6}	3.3×10^{-6}	4.8×10^{-6}	9.0×10^{-6}
Thermal Shock Resistance		Good	Good	---	---	---	---	---
Water Absorption	%	0.0	0.0	---	14.0 -17.0	0.02 -1	0.0	0.0
Gas Permeability		Gas-tight	Gas-tight	---	---	---	---	---
Specific Heat	BTU/lb/°F	0.185	0.190	---	---	---	---	---
Density	lb/cu. in.			0.076	0.066	0.083	0.134	0.144
Safe Temp at Con. Heat	°C	---	---	1250	1250	1200	1100	1000
Volume Resistivity	Ohm-Cu							
	25°C	2×10^{16}	6.3×10^{3}	$>10^{14}$	10^{14}	1.0×10^{14}	$>10^{14}$	$>10^{12}$
	100	1.6×10^{3}	1.3×10^{11}	3.0×10^{13}	1.0×10^{13}	2.5×10^{11}	2.0×10^{13}	9.8×10^{11}
	300	2×10^{8}	2×10^{7}	2.0×10^{10}	3.0×10^{9}	3.3×10^{7}	5.5×10^{11}	1.0×10^{9}
	500	2×10^{7}	3.1×10^{5}	9.0×10^{7}	4.9×10^{7}	7.7×10^{5}	5.5×10^{8}	1.7×10^{6}
	700	---	---	3.0×10^{6}	4.7×10^{6}	8.0×10^{4}	1.4×10^{7}	2.5×10^{4}
	900	---	---	3.5×10^{5}	7.0×10^{5}	1.9×10^{4}	8.2×10^{5}	1.0×10^{4}

PROPERTIES		Beryllia		Alumina Al_2O_3			Fosterite	Refractory
		98% . . BeO . . 99.5%		85% . . . . 94% 99.8%			$2MgO \cdot SiO_2$	Mullite
Property	Units							
Specific Gravity	---	2.9	2.88	3.40	3.58	2.40	2.8	3.2
Thermal Cond. at 300°C	g. cal/sec/cm²/°C/cm	0.25	0.28	0.060	0.023	---	0.008	1.4
Coef. Ther. Exp	Per °C							
	25-100	---	---	---	---	---	---	2.8×10^{-6}
	25-300	6.1×10^{-6}	6.0×10^{-6}	6.5×10^{-6}	6.2×10^{-6}	6.6×10^{-6}	10.0×10^{-6}	---
	25-500	---	---	---	7.6×10^{-6}	7.6×10^{-6}	---	---
	25-700	7.8×10^{-6}	7.8×10^{-6}	7.5×10^{-6}	---	---	11.2×10^{-6}	---
							11.7×10^{-6}	---
Thermal Shock Resistance		---	---	---	---	---	---	Good to excellent
Water Absorption	%	0.0	0.0	0.0	0.0	14 - 17	0.0	0.0
Gas Permeability		---	---	---	---	---	---	Impervious
Specific Heat	BTU/lb/°F	---	---	---	---	---	---	
Density	lb/cu. in.	0.105	0.104	0.123	0.129	0.087	0.101	
Safe Temp at Con. Heat	°C	1600	1600	1100	1500	1600	1000	
Volume Resistivity	Ohm-Cu							
	25°C	$>10^{14}$	$>10^{14}$	$>10^{14}$	$>10^{14}$	$>10^{14}$	$>10^{14}$	$10^{14} - 10^{15}$
	100	$>10^{14}$	$>10^{14}$	2.0×10^{13}	$>10^{14}$	$>10^{14}$	5.0×10^{13}	---
	300	6.0×10^{13}	$>10^{14}$	5.0×10^{10}	6.0×10^{12}	$>10^{14}$	7.0×10^{11}	---
	500	1.5×10^{12}	1.0×10^{13}	1.0×10^{8}	1.4×10^{11}	1.0×10^{10}	1.2×10^{10}	---
	700	3.5×10^{10}	1.0×10^{11}	3.0×10^{6}	9.7×10^{8}	2.7×10^{8}	1.0×10^{8}	10^{6}
	900	1.0×10^{9}	3.0×10^{9}	4.6×10^{5}	3.2×10^{7}	8.0×10^{6}	2.0×10^{6}	---

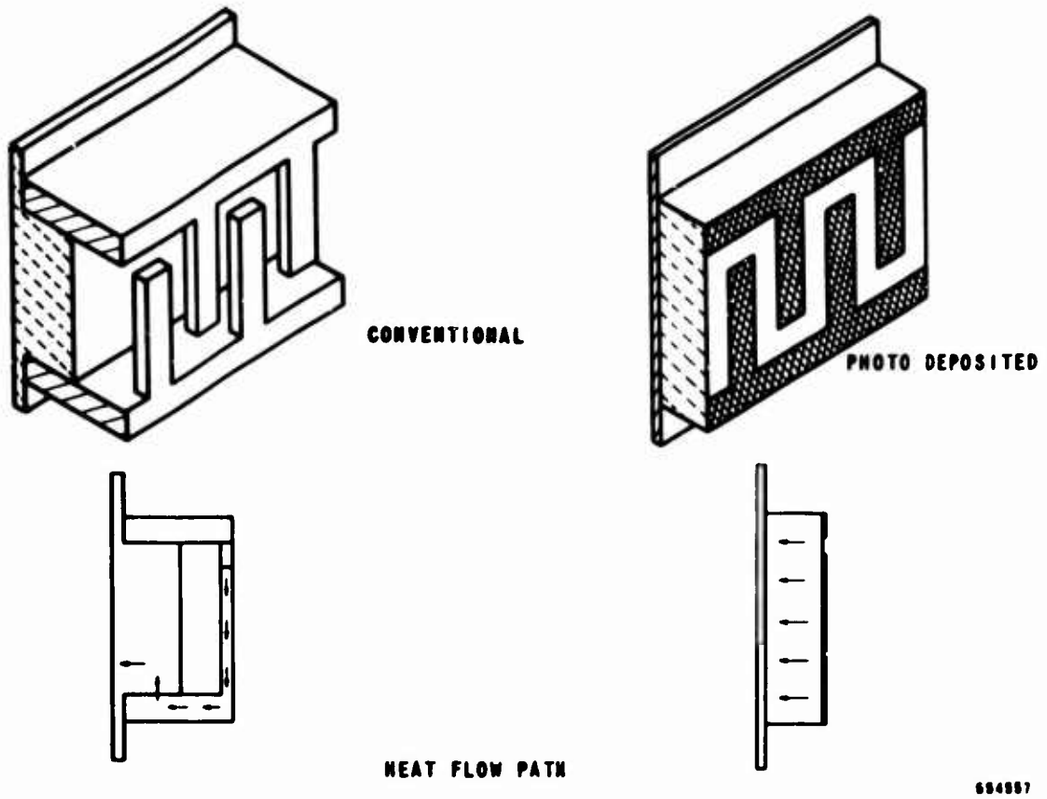

Figure 1. Slow-Wave Structure for MBWO 50-Watt C-Band Test Vehicle

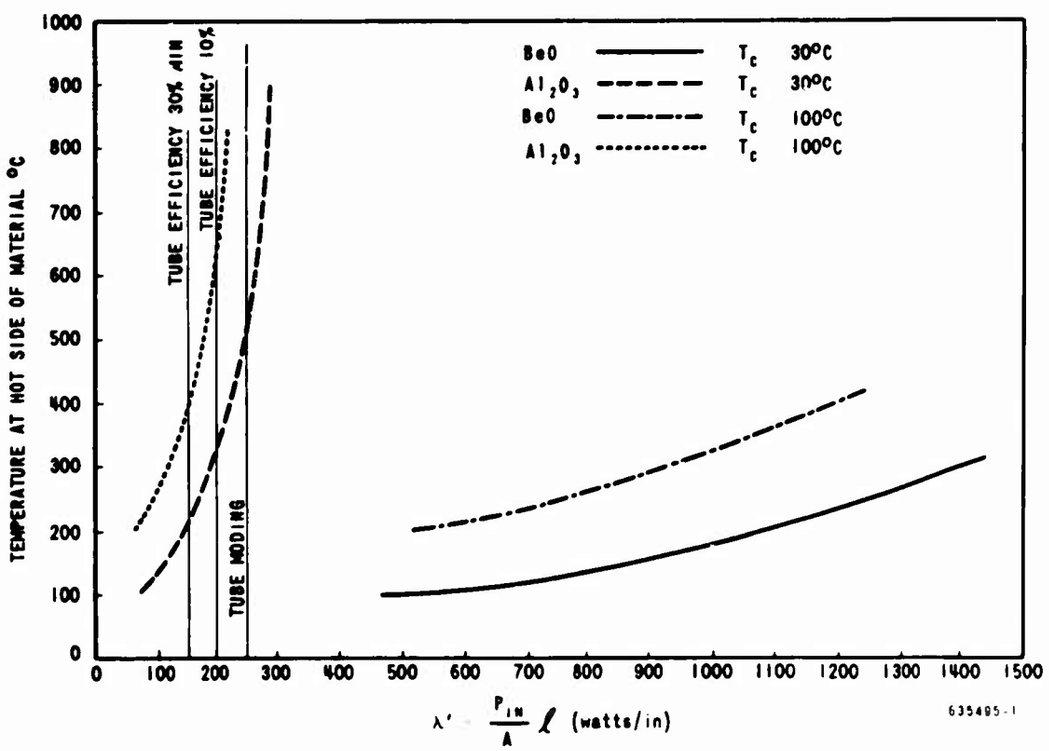

Figure 2. Temperature vs λ'

Values of λ' were then calculated for three values of input power (P_{in}) as follows:

(1) Conservative estimate - Assume 30% minimum efficiency dc to rf conversion.

The portion of the beam collected on the first 10 fingers is assumed to be 10% more efficient in the interaction process than the overall tube efficiency.

Total input power = 1900 volts x 0.175A = 333 watts

P_{in} = (1.0 - 0.4) (0.5) (333) = 100 watts

λ' = 1.515 x 100 = 151.5 watts/in.

From Figure 2:

$T_H(30^\circ)$ = 220°C for Al_2O_3

$T_H(100^\circ)$ = 400°C.

(2) Pessimistic estimate - Tube Operation at 10% efficiency

Also assumed 10% more conversion efficiency over the first 10 fingers.

P_{in} = (1.0 - 0.2) (0.50) (333) = 134 watts

λ' = 134 x 1.515 = 200 watts/in.

From Figure 2:

$T_H(30^\circ)$ = 330°C for Al_2O_3

$T_H(100^\circ)$ = 660°C.

(3) Accident or moding (50% of total beam current collected on first 10 fingers) - Assuming 50% of beam is intercepted over 10 pitches

P = (1.0) (0.5) (333) = 167 watts

= (1.515) (167) = 250 watts/in.

From Figure 2:

$T_H(30°) = 530°C$ for Al_2O_3

$T_H(100°) > 1000°C$.

A line was then designed to operate on a beryllia substrate yielding the following dimensions:

$\ell = 0.198$ inch
p = 0.030 inch
w = 0.100 inch
N = 80 pitches

and a similar thermal analysis was conducted. In all cases T_H was less than 200°C.

It was felt that the maximum temperature that the bond between the substrate and the photodeposited structure could withstand would be 500°C, and, since the possibility of exceeding 500°C would exist with alumina, the decision was made to use beryllia. It was also felt that the use of beryllia would be of more benefit, once the technology was developed, since higher power tubes would eventually be possible with beryllia, whereas the use of alumina would impose a power output restriction of 30 to 50 watts on future tubes.

Slow-wave structures with these dimensions were fabricated in linear form on Stycast* and evaluated.

2.2.3 Basic Photocopy Technique for Producing Slow-Wave Structures (Ref: Appendix A Section IB1b(2)(a))

2.2.3.1 General

The process for producing a slow-wave structure on a ceramic substrate proceeded along two parallel lines. One was concerned with the preparation of a photographic mask; the other, with producing a bonded metallic laminate on one surface of a ceramic substrate. The photographic mask was than used to produce the slow-wave structure from this metal laminate by a process of chemical milling (photo-etching). The initial work during this phase was done on Stycast since the required beryllium oxide substrates were not available. These Stycast-mounted structures served two purposes. First, the techniques developed in preparation of the mask and the procedures used in photo-etching were directly applicable to the later work on beryllia. Secondly, these structures could be used for initial electrical evaluation, as described in Section 2.2.6.2.

2.2.3.2 Preparation of Photo Mask

Based on the physical dimensions of the desired slow-wave structures, photographic transparencies were produced which would later be used to make the photo-etched line.

* Stycast is an epoxy with controlled dielectric manufactured by Emerson Cummings Corp., Canton, Mass.

A master transparency was produced from 30X final size art work. This art work consisted of one element of the desired pattern cut as a stencil on a stripable mylar base laminate (Keuffel and Esser Stabilene film). This was reduced 10X on a (D. W. Mann Co.) reduction camera and the desired line produced by step and repeat using a Mann Photorepeater that introduced an additional 3X reduction and produced the desired number of interdigital line fingers. The basic pitch and cumulative tolerance capability of the photorepeater is given by the manufacturer as less than one half tenth (0.00005) inch. Finger width and spacing are also said to be held to this same tolerance. If the finger widths must be held to a specific dimension, compensation to allow for undercutting must be made in the original art work. (See Section 2.2.3.5)

Since no such compensation was made, the finger width was somewhat narrower than the space between the fingers. This was considered acceptable so long as these widths and spacings remained uniform throughout the line. (The frequency voltage relationship is dependent on the length and pitch of the fingers and is independent of the finger width.)

From the above it is obvious that design changes can be simply and inexpensively accomplished. For complete scaling, where all dimensions are equally reduced or expanded, the same master can be utilized and the changes accomplished photographically. For more complex changes the procedure outlined above is repeated for each design. Should an impedance transformer be required, adjustments can be made to the step and repeat process to attain the required variations.

2.2.3.3 Preparation of Metallic Laminate

Vacuum deposition is used to obtain a metal laminate on a ceramic substrate. Because of the dissimilar atomic lattice spacings of the materials to be bonded (beryllia and copper), the method finally used was one where the lattice spacings were matched by means of a sequence of layers of materials having intermediate lattice spacing dimensions to form a sort of graded bond analogous to a graded seal in glass. In the interests of obtaining initial slow-wave structures as expeditiously as possible for electrical test, the first structures were made by simple evaporation of copper onto beryllia without intermediate layers. Some of these were built up to the final thickness (2-1/2 to 3 mils) entirely by vacuum deposition, and some by electroplating onto an initially vacuum-deposited layer.

2.2.3.4 Photo-etch Process

The initial slow-wave structures were produced by photo-chemical means briefly described as follows:

The metal-coated surface of the beryllia is coated with a light-sensitive plastic-base photoresist. The slow-wave pattern is contact-printed to this resist coating using the transparency mask, contact pressure, and exposure to light. The effect of this operation is to selectively

harden the resist in accordance with the transparent and opaque portions of the mask; those portions under the transparent areas being polymerized and rendered insoluble, while those under the opaque areas are left soluble. These soluble areas are now washed away by immersion in a suitable solvent. This uncovers metal laminate in those areas where it must be removed to produce the desired slow-wave pattern. The removal of this unwanted metal is accomplished by immersion in a suitable chemical solvent or etchant which rapidly attacks and dissolves the metal where uncovered.

2.2.4 Bonding Techniques

2.2.4.1 Mechanical Problems

One of the major problems encountered in the initial processing of these slow-wave structures was the inability to obtain a good bond between the copper delay line and the ceramic substrate.

An investigation was initiated to develop a ceramic-metal bond between substrate and delay line which would possess sufficient mechanical strength to support the circuit during operation and also provide an efficient heat transfer path for the thermal energy imparted to the fingers without increasing the insertion loss of the slow-wave structure. The classic metal-ceramic seal imparts a reacted zone in the ceramic to obtain sufficient adherence to the metalizing. The total thickness of this layer far exceeds the thickness of the final slow-wave structure.

After examining the various methods of bonding, it was concluded that only one mechanism would provide a true bond, namely, a bond that is strongly adherent due to chemical reaction between the ceramic and the bond composite. Since it is rare that the metal and ceramic will react to any extent, the use of an intermediate layer was pursued. This intermediate layer had to react with the ceramic and the metal to provide the interfacial bonding.

Although it was stated in Section 2.2.2.3 that beryllia was selected as the substrate material, alumina test specimens were employed during the initial testings because of their availability and ease of handling. It was felt that initial results obtained on alumina should repeat for beryllia because of the basic similarities of these materials.

The first series of experiments dealt with the straight evaporation of copper onto a cold alumina substrate. This would provide a datum on which to measure the success of other experiments. For this experiment and all other experiments, an 18-inch diameter vertically-raised glass bell jar was used together with supplementary equipment. Results from these initial experiments indicated that a strongly adherent bond to the alumina was obtained. However, these results were misleading in that the bond obtained was not a true interfacial bond (i.e., due to chemical reaction), but was a mechanical bond due to the poor surface finish of the alumina (approximately 60 microinches). This surface roughness was far too severe to allow accurate line production by the photo-etching process.

By grinding and honing, it was possible to obtain a 20-25 microinch finish which proved satisfactory for our initial experiments, i.e., the straight evaporated copper film pulled off the alumina substrate with very little effort.

An Instron tensile tester was used to determine the adherence of the evaporated film. The test specimens were bonded to the specimen holder with epoxy and then mounted on the Instron tester. However, difficulty was encountered in obtaining repeatable results from this set-up. It became quite apparent that there existed so many dependent variables affecting these readings, (e.g., alignment, area contact, epoxy strength, etc.), that this technique of measuring adherence was discontinued.

After reviewing the literature it was found that the most widely used method for determining film adhesion is the adhesive tape method. This method is firmly supported by L. Holland, Head of the Vacuum Deposition Research Division of Edwards High Vacuum Ltd., who is perhaps the foremost authority on evaporated films. The method consists of pressing a piece of transparent adhesive tape firmly against the film surface and then removing it quickly with one thrust. This technique was then used to retest our initial specimens and in every case the film was easily removed.

When the surface finish of the substrate is 25 microinches or better, a chemical reaction must exist between the substrate and film before a strongly adherent bond can be realized. Since it has been established that a 15-20 microinch surface finish on the ID of the beryllia cylinders is required to meet the delay line tolerance specifications, work was directed to obtaining the chemical-type bond mentioned above.

2.2.4.2 Chemical Bond

Work was initiated to study the methods by which the proper bond could be achieved. During this phase of experimentation, attention was focused on obtaining an intermediate layer that would react with the ceramic substrate and the evaporated copper film. At this point in the evaporation tests it was also decided that the bond should be able to withstand temperature cycling up to 860°C. If this could be obtained, it would greatly facilitate the processing of the final tube.

2.2.4.3 Theory of Bonding

In the generalized theory of true metallurgical bonding, there are several influencing parameters. These are:

a. good thermal expansion match between the two bonding components;

b. reasonably close lattice parameter match between the two components;

c. sufficient ductility in one or both of the components to accommodate strain induced by small deviations from (a) and (b) above; and

d. chemical attraction and compatibility between the two atom species present at the interface.

Little is known about these items quantitatively but a study of certain physical constants can yield a basis for a suitable program of empirical study.

For the purposes of this program we have not considered the normal approaches to metallizing ceramics in which item (d) is the predominant factor, i.e., the method of causing considerable chemical reaction between the ceramic and a metallizing material. The metallizing material is generally a mixture of metals and metal oxides which react with the ceramic and provide a surface capable of being plated and finally brazed. It is obvious that such a method creates an area which, because of the process, is very thick; commonly the reacted and affected zone is 0.125 inch thick. The effects on the dielectric properties and thermal conductivity of the ceramic in this area are not known. However, the presence of such a film which is somewhat electrically conductive will cause excessive insertion loss in operation. We therefore confined our investigation to a thin-film approach in which the bonding agent could be kept thin in relation to the thickness of the copper interdigital line.

A schematic diagram of the bond attempted is shown in Figure 3.

Figure 3a shows the effect of simply evaporating copper onto a beryllia substrate and represents the mismatch evident under these conditions.

Figure 3b represents the thin-film-bonded approach. The intermediate layer, generally approximately 100 - 200 Å thick, was selected to fulfill the following functions:

a. grade the mismatch,

b. react chemically with both the ceramic and the metal layer, and

c. be stable through a wide temperature range.

In Figure 3b the grading effect of the intermediate layer is shown diagrammatically. The conditions of preparation of the film are adjusted so that the material at the ceramic surface is an oxide of a metal similar in lattice parameter and chemical characteristics to the base ceramic. The film material at the outermost surface of the metal layer has a lattice parameter and chemical characteristics similar to the metal layer. The intermediate material provides the transition between the oxide and the metal.

Several bonds of this type were investigated and are discussed in Section 2.2.4.4 below.

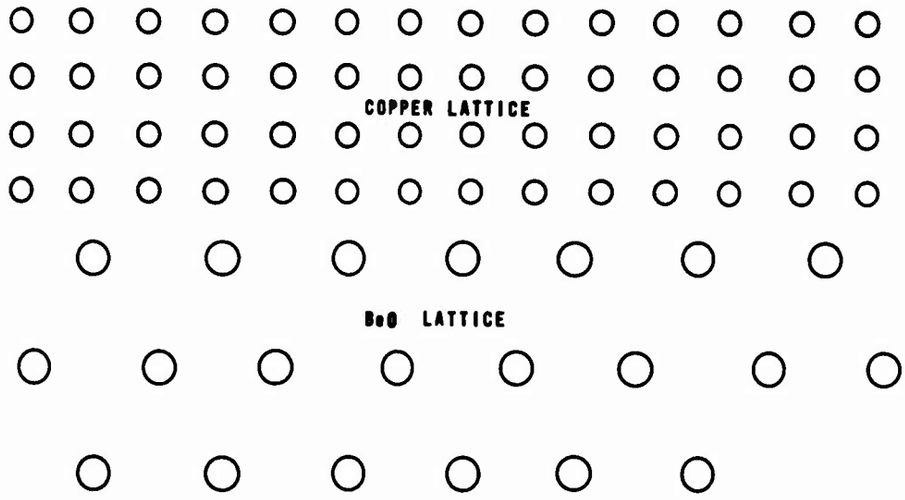

a. No Graded Bonding Structure

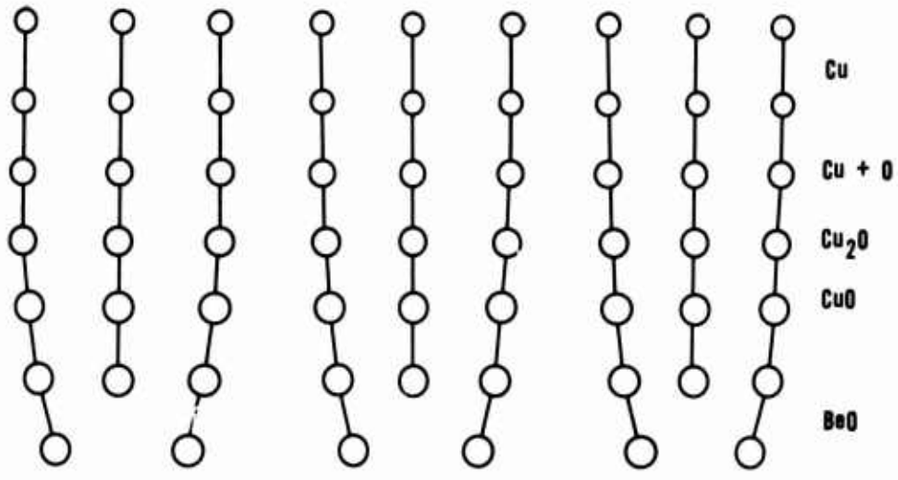

b. Bonding Structure of Graded Copper Oxides

Figure 3. Copper Film on Beryllia Substrate

2.2.4.4 Bonding Experiments

a. Graded Bond - (BeO + CuO + Cu_2O + Cu)

It was felt that a graded bond could be obtained if the copper was initially evaporated in a partial pressure of oxygen of approximately 10^{-1} Torr. Then, by gradually decreasing the partial pressure of oxygen (by gradually increasing the pumping rate), the evaporated film would become more and more copper-rich until finally, at 10^{-5} Torr, the deposits would be of pure copper.

Results were poor, and no specimen passed the adherence test. By conducting a series of isolated tests, it was found that the formation of the first oxide layer was cupric oxide (CuO) and that this oxide was extremely non-adherent. This approach was therefore discontinued.

b. Graded Bond - (BeO + Cu_2O + Cu_xO_y + Cu)

During these experiments, copper was evaporated in a poor vacuum (approximately 2.5×10^{-2} Torr) to form the Cu_2O layer. (The pressure level is very important here since higher pressures (4.0×10^{-2} or above) will produce a non-adherent CuO film.) After approximately 200 Å of Cu_2O was formed, the temperature of the copper structure was lowered to room temperature and the pressure decreased to 1×10^{-5} Torr of Hg. Pure copper was then evaporated until an approximately 10,000 Å layer was formed. A photomicrograph of this type of bond is shown in Figure 4.

After plating the specimen with 0.0025 inch of copper, the bond was tested in the usual fashion. The bonds obtained were very adherent and passed the adhesive test. However after firing in a hydrogen atmosphere the film was easily removed.

c. Graded Bond (BeO + TiO_2 + Cu)

During these experiments titanium was evaporated at a pressure of 0.01 micron of Hg. Due to the relatively slow rate of oxidation, it was necessary to bake the 200 Å layer of Ti in air at 400°C for 2 hours. Copper was then evaporated to the substrate until the required thickness for plating was obtained.

A very poor bond resulted which was easily stripped when subjected to the adhesive test.

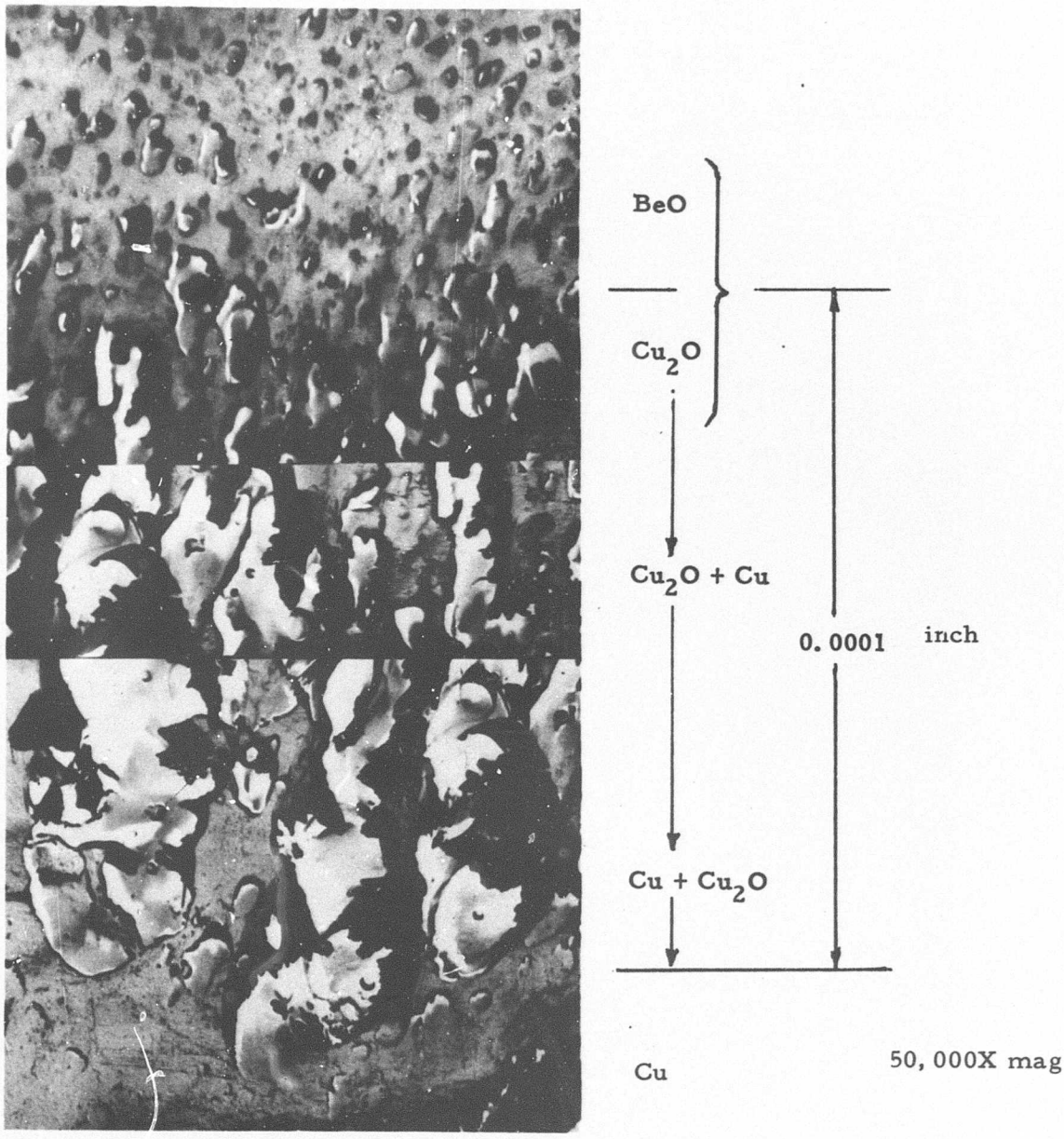

Figure 4. Photomicrograph of Copper-Beryllia Bond (50, 000 Mag.)

d. Graded Bond ($BeO + Al_2O_3 + Cu$)

Pure aluminum was evaporated at a pressure of 0.01 micron of Hg until a 200 Å film was realized. The test sample was then fired in air at 500°C for 2 hours to ensure formation of the oxide. Copper was then evaporated to the oxide layer in the usual manner at 10^{-5} Torr, until the 1-ohm resistive coating was obtained. The substrate was kept at 425°C during evaporation.

A very highly adherent bond was obtained. However, after a high temperature firing in hydrogen at 850°C, this bond was also easily removed.

2.2.4.5 Protective Layer on Finished Line

Since the high temperature firing in hydrogen appeared to be the limiting factor in our attempts to obtain a satisfactory bond, it was felt that the introduction of a protective film might prevent the hydrogen from reacting with the intermediate oxide layer.

Silicon monoxide (SiO) was chosen as the initial candidate because of its success as a protective film in the mirror making industry. There is some doubt as to the actual composition of the siliceous film and so it is designated SiO_x.

A 200 Å silicon monoxide film was evaporated over the copper oxide (Cu_2O) bonding system and then fired in hydrogen at 860°C. Results were excellent in that the bond remained strongly adherent.

The purpose of the thin silicon monoxide layer is to prevent the reduction of Cu_2O to Cu during subsequent hydrogen firings. This film is evaporated after the etching operation.

2.2.4.6 Hydrogen Firing

Hydrogen firing of the finished photodeposited circuits was required since the ceramics were designed to be brazed into the copper cylinder with eutectic silver solder in a hydrogen atmosphere. This process was later changed as reported in Section 2.2.10 of this report. The ceramic cylinders were brazed into the copper cylinder prior to photodepositing the delay line on the ceramic substrate. There was no need for the bond to be exposed to a hydrogen firing in this latter process.

The bond used for the construction of slow-wave structures as used in the first test vehicles (A1 through A5) was graded copper bond. ($BeO + CO_2 + CO_x\ O_y + Cu$). No protective layers were used on these lines.

2.2.4.7 Final Copper-Copper Oxide Graded Bond

Scrap analysis of test vehicles A1 and A3 revealed failure of the bond after limited tube operation (20 to 30 hours). Prior work on the CuO-Cu bond systems had shown that the adherence was good after repeated cycling at 600°C. However the earlier test pieces were not exposed to the photo-etching process. The following checks were made to isolate the exact cause of the lifting:

a. evaporating CuO-Cu onto the beryllia substrate and checking adherence both before and after a 600°C bakeout in a vacuum of 10^{-5} torr;

b. evaporating CuO-Cu onto the beryllia substrate and copper plating to the required thickness. Adherence was checked both before and after the 600°C bakeout. This determined the effects of the plating bath; and

c. evaporating CuO-Cu onto the beryllia substrate, copper plating, polishing and photo-etching the delay line. Again the adherence was checked both before and after the 600°C bakeout in a vacuum of 10^{-5} torr. This determined the effects of the photo-etching solution.

All stages of the bond formation withstood the cycling, and adherence was satisfactory after 12 hours at temperature. Failure occurred after the photo-etching. Upon a closer investigation into the photo-etching process, evidence was discovered that the etching reagent was attacking the bond region. The following approaches were taken in order to overcome this adherence problem:

a. Development of an etching reagent that would dissolve copper but not copper oxide

It was quite apparent after initial experimentation that any etching reagent that would dissolve copper would also dissolve the copper oxide. This approach was therefore abandoned.

b. Elimination of the etching process through direct evaporation using a masking technique

The deposition of the slow-wave structure directly onto the BeO substrate posed two major problems:

1. positioning of the shield (negative) during evaporation, and
2. copper supply during evaporation.

This process required new fixturing and a special mechanism to supply copper (the evaporating source), since a single tungsten boat filled with copper would not be sufficient for a 0.003-inch thick coating. This approach was delayed until the results of the other approaches were evaluated.

c. Electroplating the slow-wave structure up to the required thickness after etching the CuO and first layer of copper with a moderate reagent

Initial results on flat samples worked out very well with good definition evident in the corners and on the tips of the fingers. However attempts to fabricate a circular slow wave structure were unsuccessful because of the bridging of the copper plate. This approach was therefore abandoned.

d. Development of a chemical reaction bond between the BeO and the CuO by high temperature heat treating

A thin film of CuO was deposited onto the BeO cylinder by vacuum evaporation and then fired in air at 1100°C for 1 hour. The reaction was very severe with the depth of the reacted area measuring approximately 0.060 inch. Since the penetration obviously was too deep, other tests were run, each time lowering the temperature until a point was reached where one half of the 0.0005-inch film of CuO reacted with the BeO, thus leaving the remaining 0.0002-inch film as CuO. At this point, the part was fired in a reducing atmosphere to reduce the unreacted CuO film to copper. Initial attempts to accomplish this failed after the reducing operation, since the remaining film was nonconductive, although it did possess a copper color. A thicker CuO layer was therefore administered in an attempt to rectify this problem. However, the thicker layer flaked off after the reduction firing.

Finally, after many experimental runs, the following process proved successful:

1. Evaporate a thin film of Cu_2O onto the inside diameter of the BeO substrate.
2. Air fire at 1000°C for 1 hour.
3. Fire part in a reducing atmosphere at 850°C for 1 hour.
4. Evaporate a thin film of Cu_2O onto the reduced layer.
5. Fire in a reducing atmosphere for 850°C for 1 hour.

Two circular lines were fabricated in this manner. Both proved to have excellent adherence both before and after heat cycling. However, because of steps 1 and 2, the BeO cylinder in this case is not brazed into a finished anode assembly prior to the bonding operation. Instead it is treated separately during the initial phases of the bonding process and then utilizes the normal brazing cycle to complete the

reducing phase. In brief, the ID of the BeO cylinder is coated with a thin film of Cu_2O by vacuum evaporation, air fired to promote a reaction with the ceramic substrate, fired in a reducing atmosphere, coated with Cu_2O again in similar manner, placed in the anode brazing fixture, and fired again. This brazing operation accomplishes two things. It brazes the BeO cylinder to the copper support structure and it reduces the Cu_2O film to pure copper. The bond is now complete and the assembly is ready for the final stages of fabrication which consist of plating the ID of the BeO cylinder to the required thickness and photo-etching the delay line.

2.2.4.8 Development of the Titanium Oxide-Copper Bond

Although the above system functioned adequately, there existed many parameters that were quite difficult to control; the major ones were:

a. pressure during oxide evaporation,
b. thickness of the copper oxide-to-copper transition region, and
c. rate of pressure change through this transition region.

Another factor making the CuO-Cu bond system less attractive is related to possible thermal decomposition of the oxide. If we can assume that the tube will not be required to operate at an anode temperature greater than 500°C, then it is extremely unlikely that decomposition of $CuO \rightarrow Cu + O$ will occur. However, although it is difficult to establish the actual operating temperature of the anode, theoretical considerations can predict transients that would cause local temperatures to exceed 500°C and, in turn, would cause decomposition of the oxide.

Such an occurrence may cause failure of the bond but, more importantly, it is very likely to cause deterioration of the cathode emission. For these reasons an alternative bonding procedure was developed. The basis of the development was similar to the CuO-Cu philosophy except that two improvements were sought:

a. the bonding procedure should not be hypercritical in sensitivity to parameter variations, and

b. any oxide used as a lattice match between the beryllia substrate and the copper layer should be thermally stable to high temperature.

Earlier work had shown that several refractory metals in a state of partial oxidation could be used as bonding reagents between a ceramic substrate and a metallic film. Several of these oxides, (e.g., molybdenum oxide and tungsten oxide), are impractical from the point of view of thermal stability. Titanium oxide seems the most logical choice since the oxide is very stable to high temperatures and is also known to adhere firmly to a ceramic substrate.

Experiments were carried out on sample pieces of BeO in the following manner:

Two evaporation sources were set up at an equidistant point from the beryllia substrate. Titanium was evaporated until approximately 1000 Å had been deposited on the beryllia. Due to the residual gas pressure in the bell jar system, a certain degree of oxidation of the titanium occurred. While the titanium was still evaporating, the copper source was activated. The overlap of the two evaporating species was maintained for approximately 2 minutes. The titanium source was then turned off and the copper continued until the required thickness had built up on the substrate. Bonds prepared in this way have proved highly successful and were used in the later work.

The use of slow-wave structures utilizing this bond has been evaluated and the life test of test vehicles A-6 through A-8 confirm that this bond will not deteriorate under prolonged tube operation. This bond technique is detailed in the final process specification for the manufacture of circular slow-wave structures given in Sectior 2. 2. 10 of this report.

2. 2. 5 Development of the Initial Manufacturing Technique (Ref: Appendix A, Section IB1b(2)(a)(e))

2. 2. 5. 1 Establishment of the Photo-Etch Facility (Ref: Appendix A, Section Ib1b(2)(b))

To develop the basic techniques described in Section 2. 2. 3 and 2. 2. 4 into a feasible manufacturing process, a photo-etch facility was established. A description of the items of equipment is included in Appendix C of this report. The technique itself is presented in step-by-step detail for both linear and circular slow-wave structure construction, together with variations in the process developed throughout the life of the program.

2. 2. 5. 2 Development of the Manufacturing Process

a. Substrate Material

1. Linear Slow-Wave Structures

As described in Section 2. 2. 3. 1, the initial linear slow-wave structures were done on Stycast substrate because beryllia was unavailable. However, since beryllia had been chosen as the most desirable material, this was used on all subsequent linear slow-wave structures.

2. Circular Slow-Wave Structures

For production of circular slow-wave structures, the starting material was a 99% purity, 95% density beryllia cylinder of approximately 1. 800 in. inside diameter and 0. 325 in. length, with a 0. 100 in. wall. The inner surface was ground to a smooth (15 microinch) finish and there were two holes through the cylinder wall, accurately sized and spaced to orient the mask used in producing the slow-wave design on the inner surface. Drawing A624367 Rev. 5, included as Figure G-3 in Appendix G, shows the

design of the substrate. The design of the slow-wave structure used with this cylindrical part is identical in configuration and dimensions to that employed for the linear C-band line, and the same master negative was used as a starting point for developing this line internally on the cylindrical substrate.

b. Pre-Inspection Cleaning

The beryllia cylinders and linear substrates were cleaned according to Raytheon Process Specification 638703 (see Section 2. 5. 7). In fact, there is a special facility set up at Raytheon that receives all incoming BeO parts and cleans them in accordance with the referenced specification. The chemical cleaning process, identical for both types of structure, consists of vapor degrease, a cyanide bath, an additional water rinse, an acetone rinse, and a final quick dry with dry clean nitrogen gas.

c. Visual Inspection and Dimension Check

The strip or cylinder was critically inspected under 15X magnification with a stereo microscope for gross contamination that might have survived chemical cleaning, as, for example, particles of lint or other solid material.

In addition the beryllia cylinders received a 100% inspection on all the specified dimensions. A visual inspection was also conducted to insure against pits and discoloration.

d. Post Inspection Cleaning

Since the beryllia cylinder is handled during inspection, and since there is apt to be a considerable time lapse between steps, another cleaning operation similar to b. above is performed prior to the next step.

e. Braze to Supporting Structure

This step has occurred at various times in the process depending on the evaporation process used. In the final process evolved however, the braze to the supporting structure is carried out at this point. The braze is carried out using eutectic silver copper solder in a belt furnace with a hydrogen atmosphere.

After brazing, the assembly is leak-detected and mechanically inspected.

f. Post Braze Cleaning

After brazing, the structure is ultrasonically cleaned in a solvent to assure proper cleaning of possible areas of loose particles prior to vacuum evaporation.

g. Vacuum Bakeout

The incoming ceramics were chemically cleaned in an ultrasonic water and wetting agent, both followed by an ultrasonic alcohol rinse. The ceramic was then dried and fired at 800°C in vacuum for 2 hours.

h. Ion Bombardment

After vacuum bakeout the ceramics were placed in the vacuum bell jar ready for vacuum evaporation. Before vacuum evaporation started the heaters for warming the substrate to 450°C were turned on and the ceramic allowed to bake at this temperature in a 10^{-2} Torr vacuum for 2 hours.

The pressure was then raised to 10^{-3} Torr by the admission of argon and the ceramic region made the cathode of a 1500v diode. The glow discharge was kept on for 30 minutes effectively providing a final clean-up of the ceramic surface.

The vacuum evaporation technique was then started.

i. Vacuum Evaporation of Delay Line Foundation

1. Linear Slow-Wave Structure

In a vacuum bell jar operation a layer of pure copper was deposited on the substrate surface by vacuum evaporation in a sequence as detailed below:

The substrate was positioned in the bell jar at a distance of approximately 10 inches from the copper source, which was heated in a tungsten boat. The pressure inside the bell jar was lowered to 0.01 microns of Hg and the copper heated to 1150°C. A protective shield was positioned directly over the copper source to collect any impurities that might be introduced during the first few minutes of evaporation. The shield was then removed and evaporation continued for approximately 3-1/2 hours until a resistance of 1 ohm was measured across the substrate. This low resistance figure indicated that sufficient build-up of copper had been obtained to ensure successful subsequent electroplating. The current passing through the copper source was then cut off and the heat reduced to room temperature. The substrate was left in the bell jar for approximately 2-1/2 hours and allowed to cool to room temperature, after which it was removed and was ready for plating.

2. Circular Slow-Wave Structures

During the life of the programs there have been several modifications to the vacuum evaporation processes used on the circular slow-wave structures. These are discussed in detail below.

(a) Graded Copper-Copper Oxide Bond

During this investigation there were three main variables that were considered to be important in obtaining a satisfactory bond: the partial pressure at which the oxide was formed, the temperature at which the substrate was held during deposition, and the factor of ionized or un-ionized oxygen gas during the deposition. In addition, some of the structures were electroplated to the required copper thickness while others were evaporated tofull thickness. The following are the actual numerical values of the variables investigated.

1. Partial pressure of oxygen: 1×10^{-2}, 3×10^{-2}, 5×10^{-2}, 7.5×10^{-2}, 1×10^{-1}, 1.25×10^{-1}, and 1.5×10^{-1} Torr.

2. Temperature of substrate: room temperature, 325°C, 350°C, 375°C, 425°C, and 480°C.

3. Ionization at 2 kv potential when applicable.

The most successful bonds were obtained under the following conditions: partial pressure 5×10^{-2} Torr, temperature of substrate 375°C, no ionization. The procedure was as follows:

The ceramic was rotated around its mirror axis by means of a three fingered jig that clamped onto the O.D. of the cylinder. Rotational speed was 20 revolutions per minute. For the conditions where the substrate was to be heated, a cylindrical heater surrounded the ceramic around the O.D. The evaporation source was a tungsten boat containing copper which was positioned at the axis of rotation. In all the experiments the copper source was held at 1100°C. The copper oxide was evaporated for 15 minutes. At this point the bell jar was pumped down to a hard vacuum while the evaporation continued. Some ceramics were then evaporated for a further 10 minutes to provide a copper layer of approximately 0.0001 in., cooled, and held for electroplating to full copper thickness.

The electroplated copper in general had rather poor surface finishes and a polishing was required to provide the surface necessary for the photoetching procedure.

Several of the ceramics were evaporated to the full copper thickness and these gave much better surface finishes than the electroplated cylinders.

For the electroplated series the procedure is as follows:

The copper electroplating is carried out in an acid copper-sulfate solution having the following composition:

H_2SO_4 (Sp. G. 1.84) - 11 oz

$CuSO_4 \cdot 5H_2O$ - 30 oz

Water (distilled) - to make one gallon.

The ring is suspended in the electrolyte in a horizontal position and a 1/4-inch diameter OFHC copper rod is held so that it runs through the center of the ring. This becomes the anode and the ring itself becomes the cathode. Cathode and anode are connected to a periodic polarity reversal unit which, in turn, is fed from a dc power supply. The reversal unit is arranged to forward plate for 1 minute and reverse plate for 15 seconds in a periodic repetitive sequence. This method gives a smoother plate than would otherwise be obtained. The plating conditions are as follows:

Bath temperature	- Room temperature
Current level	- 0.01 to 0.10 amperes
Current density	- 10 amperes/square foot
Approximate time to give 3-mil plate thickness	- 5 hours

In practice, the piece is plated in the forward direction for 7 minutes before turning on the periodic reversal unit. This is necessary to provide a sufficient base for the subsequent plate. Figure 5 shows a diagram of the plating process.

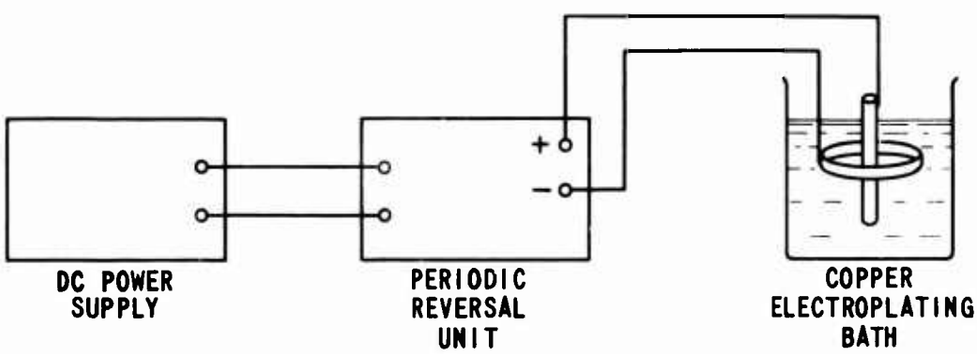

644-223

Figure 5. Copper Plating Set-Up

(b) High Temperature Copper Oxide Bond

The previously described technique, although moderately successful, did have problems of bond failure. The failures were thought to be due to the difficulty in close control of the variables in the process. * At the same time, the following techniques were also investigated.

(c) TiO-Ti-Cu Bond

The final bonding procedure was based on the use of TiO grading out to Ti as the bond mechanism. A full description of the process is given in Section 2.2.4.8. This bonding mechanism was the most successful of the various methods used during this program. Although the number of units manufactured by this method was limited, it is interesting to note that no bond failures were observed. The copper was evaporated to full thickness in each of the devices made by this method. The process was far less critical in operating parameters than the previously described processes and is, therefore, the best candidate for a production process.

j. Inspection

Following plating, the piece was again critically inspected for plating defects and for cleanliness.

k. Polishing

After the vacuum evaporation it was found that a clearer pattern could be obtained if the surface of the copper film were hand-polished with 4/0 carborundum paper.

---

* In particular the effectiveness of the bond between the BeO and the copper oxide, after exposure to elevated temperatures, was in question. It is apparent that BeO and copper oxide, when reacted at 1250°C, will form a eutectic system. One might expect a lesser degree of reaction, but still adequate to form a bond at lower temperatures.

Copper oxide was evaporated onto the surface of the ceramic in the same manner as in the previous process. In this case, however, the copper oxide was evaporated for a period of 30 minutes to provide approximately 0.005 in. of copper oxide. These layers were then fired in air at 900°, 100° and 1100°C. As expected, reaction with the BeO was proportionate to increasing temperature. The main problem was that the reaction with the BeO was not uniform; certain areas reacted far more vigorously than others. This variation was greater than that obtained by the temperature variations.

The next stage of the process was to reduce the remaining copper oxide to copper by firing in hydrogen at 850°C for 30 minutes. This process was then followed by electroplating, in the manner already described, to the required thickness of copper. The process was not altogether satisfactory. The bond strength was very high, but the areas that had overacted with the BeO would not plate very well and copper adherence was poor.

l. Inspection

After polishing the ID was checked and a visual inspection for surface defects was performed.

m. Cleaning

Next, the structure was cleaned again with moistened White Dot, followed by a thorough washing in cold water.

n. Plug Input and Output Holes

During the Photoresist coating operation, the resist fluid will fill the input and output holes in the cylinder unless they are plugged. This represents a gross amount of liquid, and, during the subsequent drying it will bubble back out of the holes and interfer with the formation of a smooth, uniform coating. To prevent this, the holes were plugged. This was accomplished by the use of a molded rubber taper pin. The end of the pin was threaded through the hole, grasped on the other side, stretched, and pulled through a side. It was stretched and pulled through a short distance and released. At this point, the ends on the other side were clipped close, leaving the plug tightly in place in the hole.

o. Photoresist Coating and Spin Dry

1. Linear Slow-Wave Structures

In the linear slow-wave structure, a minimum amount of 1-to-1 solution of Kodak Thin Film Resist (KTFR) was flowed over the plated surface of the strip, which was then secured to the turntable of a plate-whirler and rotated at approximately 250 rpm to obtain a uniform coating approximately 0.0005 inch thick. Rotation was continued for 7 minutes, sufficient to "set" the resist so that it appeared dry, both visually and tactually.

2. Circulator Slow-Wave Structures

Originally, an elaborate device for spinning the photo resist to achieve a uniform coating was contemplated. Trials soon demonstrated that a very simple method of spreading a small pool of resist by slow rotation of the cylinder gave perfectly satisfactory results. This method is described in detail in Section 2.2.5.5.

p. Slow Dry

In both linear and circular slow-wave structure work, the piece was then transferred to a chamber ventilated with dry nitrogen gas for 16 hours of slow drying. This was to ensure a gradual and thorough elimination of residual solvents from the resist film. Both the spin-drying and the subsequent dry-box treatment were carried out in non-actinic illumination, provided by a separate set of room lights equipped with yellow Kodagraph filters to which the photoresist is insensitive.

q. Oven Bake

To ensure complete elimination of residual solvent, the piece was baked in an air oven at 75°C for 10 minutes. This procedure applied to both types of slow-wave structures.

r. Exposure

1. Linear Slow-Wave Structure

After removal from the bake oven, a photographic mask in the form of a high-resolution photographic glass plate was positioned in contact with the resist-coated ceramic strip, so that the 2nd and the 81st fingers of the transparency image were positioned over the feed-through holes in the strip, and temporarily secured with scotch tape. The strip and the transparency thus oriented were placed in the print frame of the platemaking machine; a vacuum was drawn; and arc lamp exposure was provided for 6 minutes.

2. Circular Slow-Wave Structure

(a) Quartz Negative

The original concept for producing a delay line pattern on the photoresist-covered, copper-coated cylindrical ceramic surface, was to use a thin quartz ring that would have the required pattern on its outer surface. This ring was to be split and would be expanded to fit the ID of the cylinder snugly.

A split quartz ring was made and efforts were made to produce the required pattern on its outer surface. The image used in these attempts was a flexible photomask of the common 7 mil Estar base type. Efforts to produce a good quality image on the quartz ring were disappointing, and it was soon appreciated that even if satisfactory results were obtained, the image would be another generation removed from the master negative from which the flexible photomask was made. This approach was then abandoned.

(b) Flexible Negative with Quartz Back-up Ring

The next approach was to use the flexible film itself as the contact printing photomask, and to use the clear quartz ring as a means of applying pressure to hold the film tightly against the photoresist surface. This was attempted by mechanically wedging apart the split ends of the quartz ring to expand it to fit the ID of the cylinder tightly. This was only partly successful, as it was found that the printing pressure tended to be irregular and erratic, producing imperfect images, sharp in some places and fuzzy in others. A method that would hold the photomask film solidly and uniformly against the photoresist surface, and that would not interfere with the transmission of the printing illumination was needed, and an investigation was started to find a more effective method of supporting the flexible negative.

(c) Flexible Negative with Pneumatic Back-Up Device

A solution was found in a pneumatic pressure device consisting of ring-shaped transparent balloon, through the center of which the exposing light could be passed, and which would force the photomask against the cylinder surface with a uniform pressure. This device and its use is now described in detail.

(1) Negative Positioning

The negative consists of a flexible 7-mil-thick strip of Estar-base film made from a high-resolution glass plate master negative. The strip of film is trimmed to an overall width matching that of the beryllia cylinder, with the slow-wave pattern centered within this width, and the collector end is trimmed to allow the first finger of the line to be positioned over the output hole.

The negative is now placed, emulsion-side down, against the resist-coated inner surface of the cylinder and manually positioned so that the input and output holes are accurately aligned with the corresponding fingers of the transparency pattern. This is accomplished visually using a 15-power binocular microscope, and is possible because the photoresist is essentially transparent. The negative is secured in position with small pieces of transparent pressure-sensitive tape at each end of the strip. Figure 6 shows the cylinder with the negative in position.

(2) Negative-to-Cylinder Pressure Jig

An improved method of contact-printing the photographic image of the slow-wave structure onto the photoresist has been developed. As explained in subparagraph (1) above, this used a regular film-base photographic transparency instead of a semi-rigid quartz mask. One fundamental advantage gained by this change is that the mask is one generation less removed from the master negative. Another basic improvement has been in the method of achieving negative-to-resist contact pressure. To make a suitable photographic contact print of the slow-wave pattern onto the photoresist coating it is necessary to bring the flexible negative into intimate contact with the photoresist coating by the application of uniform pressure. A pneumatic pressure device has been devised to accomplish this.

This device, shown in the sketch of Figure 7, and in the photographs of Figures 8 and 9, consists of a polyethylene sleeve turned back upon itself and secured to the outside of an aluminum plug having a central longitudinal hole and a suitable air channel. An important aspect of the design of this device is that the diameter of the sleeve is made slightly smaller than the inside diameter of the cylinder. Thus the cylinder may be readily slipped over the sleeve without bringing any strain on the transparency, which is accurately positioned against the photoresist-coated surface of the cylinder. The sleeve can now be inflated, bringing a wrinkle-free uniform pressure against the transparency and forcing it tightly against the cylinder. A hole through the block that supports the polyethylene sleeve permits a miniature tubular ultraviolet fluorescent lamp to be passed through, with electrical connections to the lamp being made in conventional fashion.

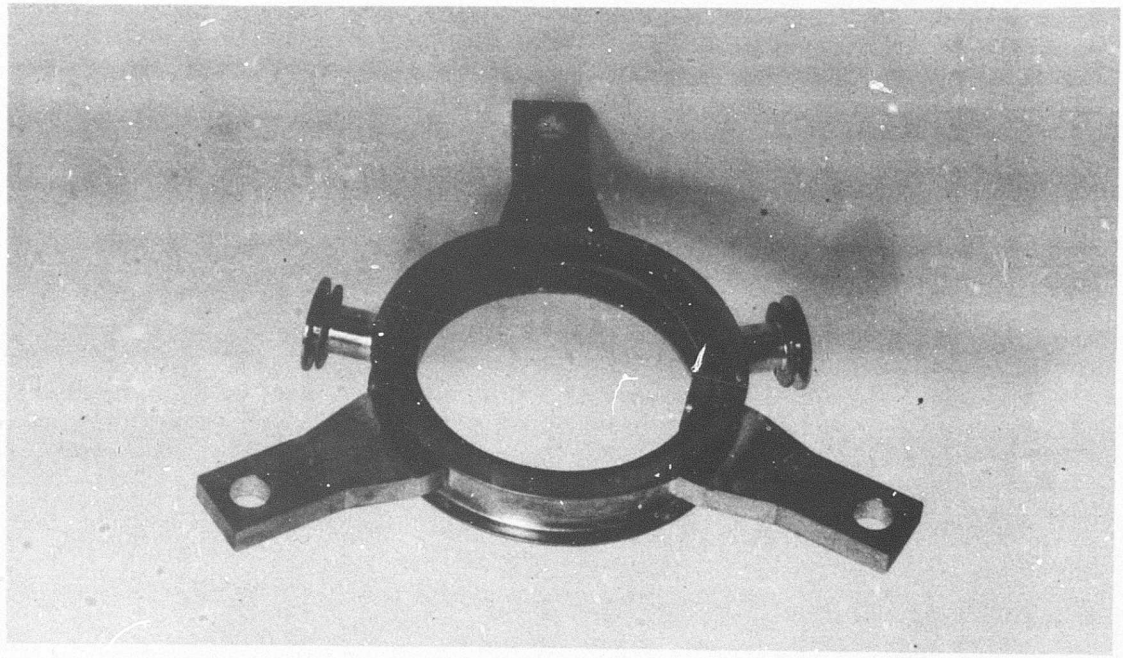

66 29522

Figure 6. Cylinder with Negative in Position

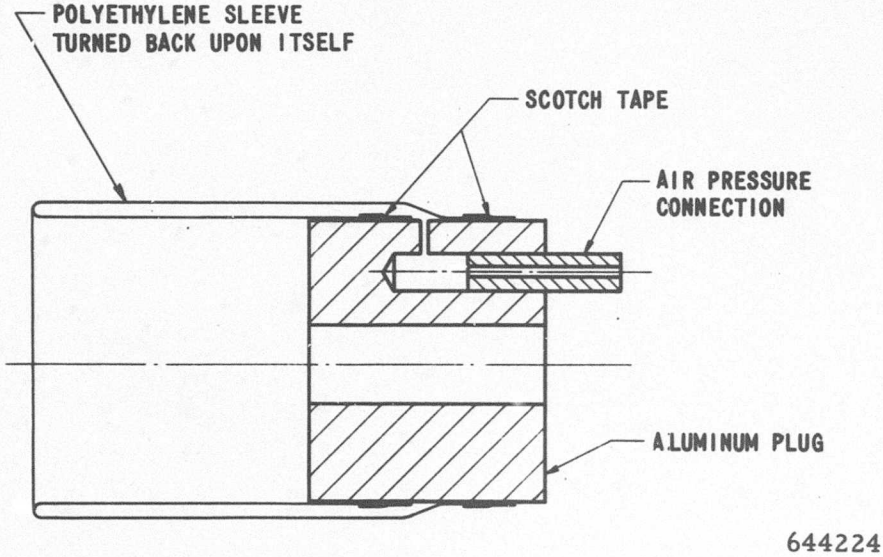

644224

Figure 7. Exposure Device, Diagram

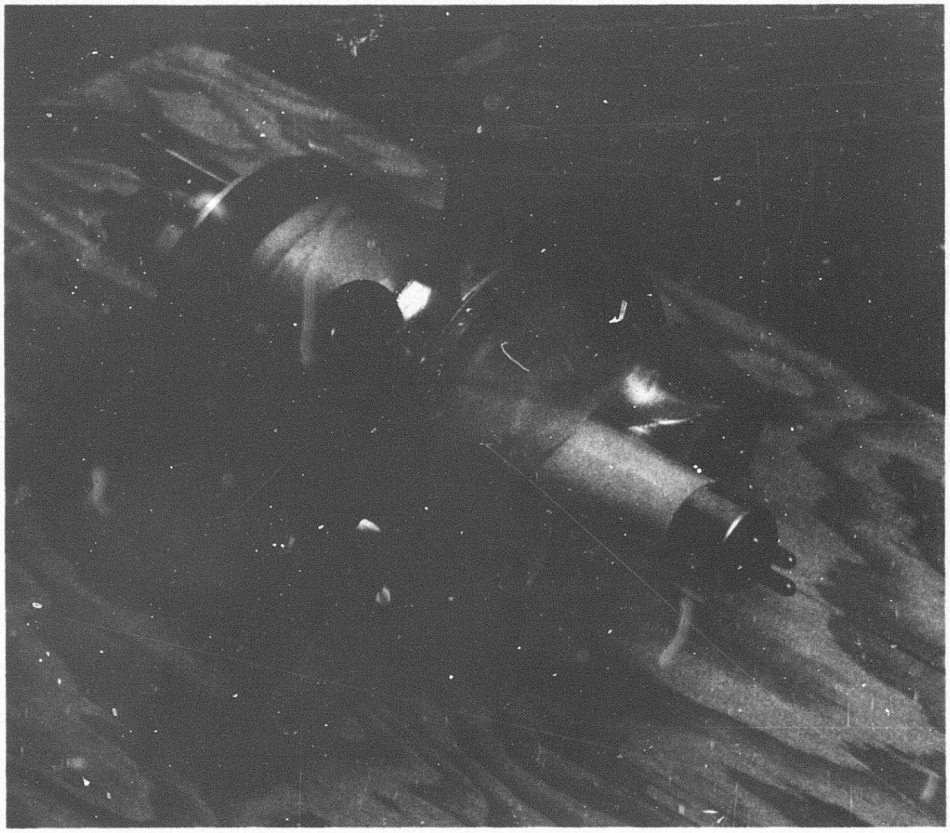

66-29524

Figure 8. View with Slow-Wave Structure in Place, but before Sleeve Inflation or Completion of Electrical Connections

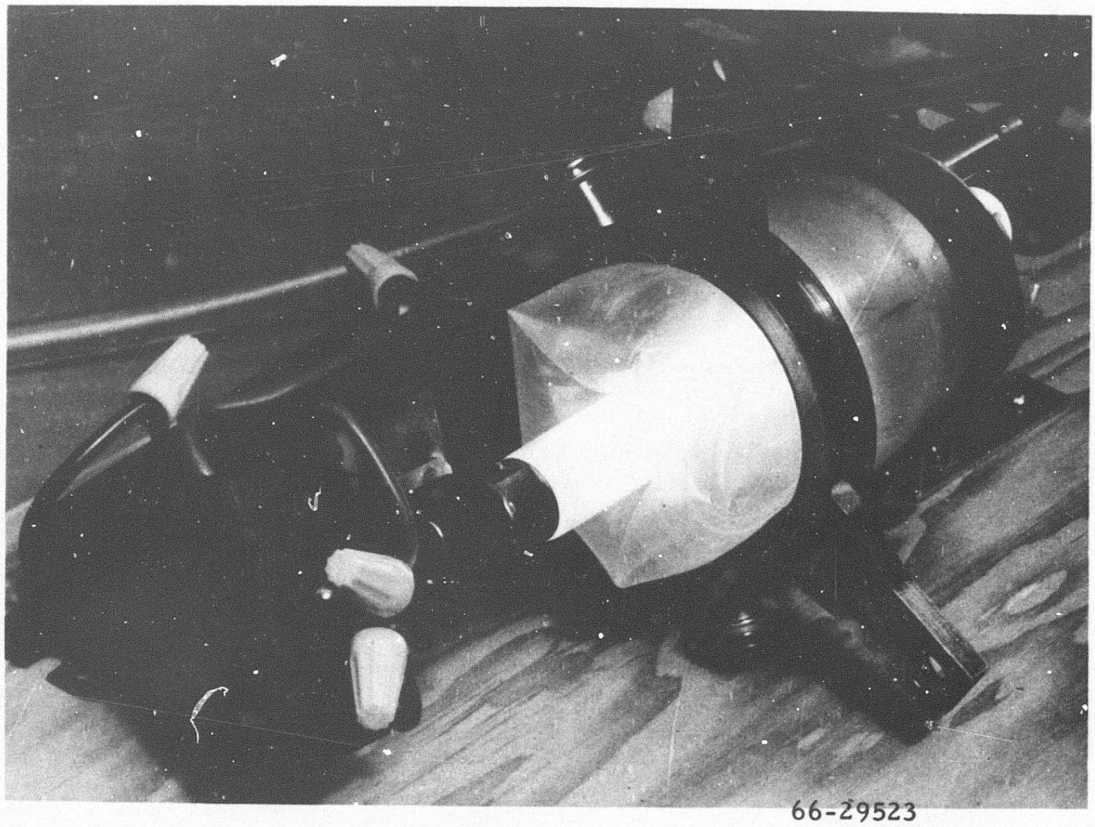

Figure 9. View with Slow-Wave Structure Assembly in Place and Polyethylene Sleeve

For use, the photoresist-coated beryllia cylinder, with the negative strip secured accurately in place, is slipped carefully over the deflated sleeve which is then inflated to 5 psi pressure. Electrical connections are made to the ends of the fluorescent tube, and the device is now ready for use.

(3) Exposing

Exposure is effected by long wavelength ultraviolet light from the black-light fluorescent lamp described in the preceding section. Using a model UV-21 light, the exposure time is 6 minutes. Both the polyethylene sleeve and the pressure-sensitive tape used to secure the negative strip on the beryllia cylinder are sufficiently transparent to the ultraviolet light that they provide no interference with exposure.

After completion of the exposure interval, the light is turned off; the air pressure is released; the connections to the lamp are taken off; the cylinder is removed from the pressure device; and the transparency is removed from the cylinder. The photoresist is now ready for development.

s. Development

The photoresist is developed by complete immersion of the cylinder in a container of photoresist developer. This dissolves the resist in the regions that have received no light, but leaves it intact where exposure has occurred. A short wash in running water leaves the pattern cleanly defined but rather faint because of the transparent nature of the resist medium. Dye is used to color the developed image and will disclose any defects in the resist pattern.

t. Post-Bake

At this point, the photoresist image is quite fragile. It is hardened, toughened and made resistant to subsequent etching by baking in an air-oven at 50°C for 15 minutes.

u. Masking

Before etching the delay line pattern on the BeO cylinder inside surface, all parts of the surface where the copper was to be left intact were protected from the etchant by hand painting with an acid resist masking material. In early work the delay line was produced on the BeO cylinder which was later mounted in the copper supporting structure after completion of etching. Masking then presented no problem. Later when it was required to form the delay line after the BeO cylinder had been brazed into the support structure, the latter had to be masked to prevent attack by the etchant. Initially this was accomplished by painting the entire support structure with the same acid resistant paint as previously used. This proved undesirable because of the difficulty of completely removing the paint from the cracks and crevices after completion of the etching. Subsequently other maskouts were tried, including a plastic material called thermocote, but none proved

very satisfactory. Finally a mechanical masking jig was constructed that performed very satisfactorily. This is described in Section 2. 2. 5. 5.

v. Etching

Etching of the pattern is carried out in a ferric chloride solution at a temperature of 75° C to 80° C, and is performed by complete immersion in a tray, using constant agitation. The etch time is approximately 3 minutes for a 2-1/2 mil copper thickness.

w. Strip Resist

After completion of etching, the residual photoresist is removed by treatment with a proprietary paint stripper.

x. Post Etch Clean

After removal of the slow-wave structure from the etching solutions, both for copper and later for titanium, it was customary for it to be cleaned by rinsing in running tap water for a short interval. Subsequently, after residual resist removal, the assembly was again thoroughly rinsed. While this sort of treatment appeared to give a clean product, subsequent examination of test vehicles that had failed in hot test indicated the presence of residual chloride ion, which, in turn, suggested imperfect cleaning. As a result, subsequent structures were final cleaned by soaking in several changes of cold distilled water until the used water no longer showed a positive test for chloride ion when treated with silver nitrate reagent.

y. Output Connection

One of the most serious problems encountered during the program was the attachment of the center conductor of the coaxial output to the first finger of the delay line. Several methods were utilized for the duration of the program and are discussed below. The problem was further complicated by the fact that since the substrate material was beryllia, special facilities were required for reoperation of the BeO, thus requiring them to be returned to the vendor if such rework was required. In view of this the decision was made not to reoperate the ceramics.

The original structures were made by brazing a solid center conductor through the hole (0. 020 in. dia) in the ceramic prior to the vacuum evaporation process. The electrical connection was made by evaporate copper film. This approach, although workable, accentuated the cracking problem during the brazing cycle (see Section 2. 2. 8. 4. b).

The next approach was to use a eutectic mixture of gallium and copper which is pliable at room temperature, but hardens under moderate heat and will not remelt until a temperature in excess of 700° C is reached. This, however, proved unsatisfactory since the electron beam of the tube caused the material to vaporize over the delay line, resulting in failure of a tube.

The method finally used was that of electron beam welding. An investigation into the various designs of the joint is discussed in Section 2.5.3. A process specification of the welding process is given in Section 2.2.5.6.

2.2.5.3 Summary of the Photo-Deposition Process

A summary of the steps of the photodeposition process is given below and shown in block diagram form in Figure 10.

1. Cylinder Received
2. Pre-Inspection Cleaning
3. Inspection
4. Post Inspection Cleaning
5. Braze
6. Post Braze Cleaning
7. Vacuum Bakeout
8. Ion Bombardment Cleaning
9. Evaporation
10. Inspection
11. Polish
12. Clean
13. Plug Holes
14. Inspection
15. Resist Coating
16. Slow Dry
17. Oven Bake
18. Exposure
19. Development
20. Post Bake
21. Masking
22. Etching
23. Strip Resist
24. Post Etch Cleaning
25. Electron Beam Weld of Output Assembly

Process specifications for the more critical steps namely steps 7-9 and steps 11-23 and step 25 are given in Sections 2.2.5.4, 2.2.5.5, and 2.2.5.6.

2.2.5.4 Outline of Current Process for Producing a 3 to 4 Mil Thick Coating of Copper Bonded to the BeO Cylinder ID

Starting Point: - BeO cylinder brazed into the copper supporting structure and entire assembly chemically clean and dry.

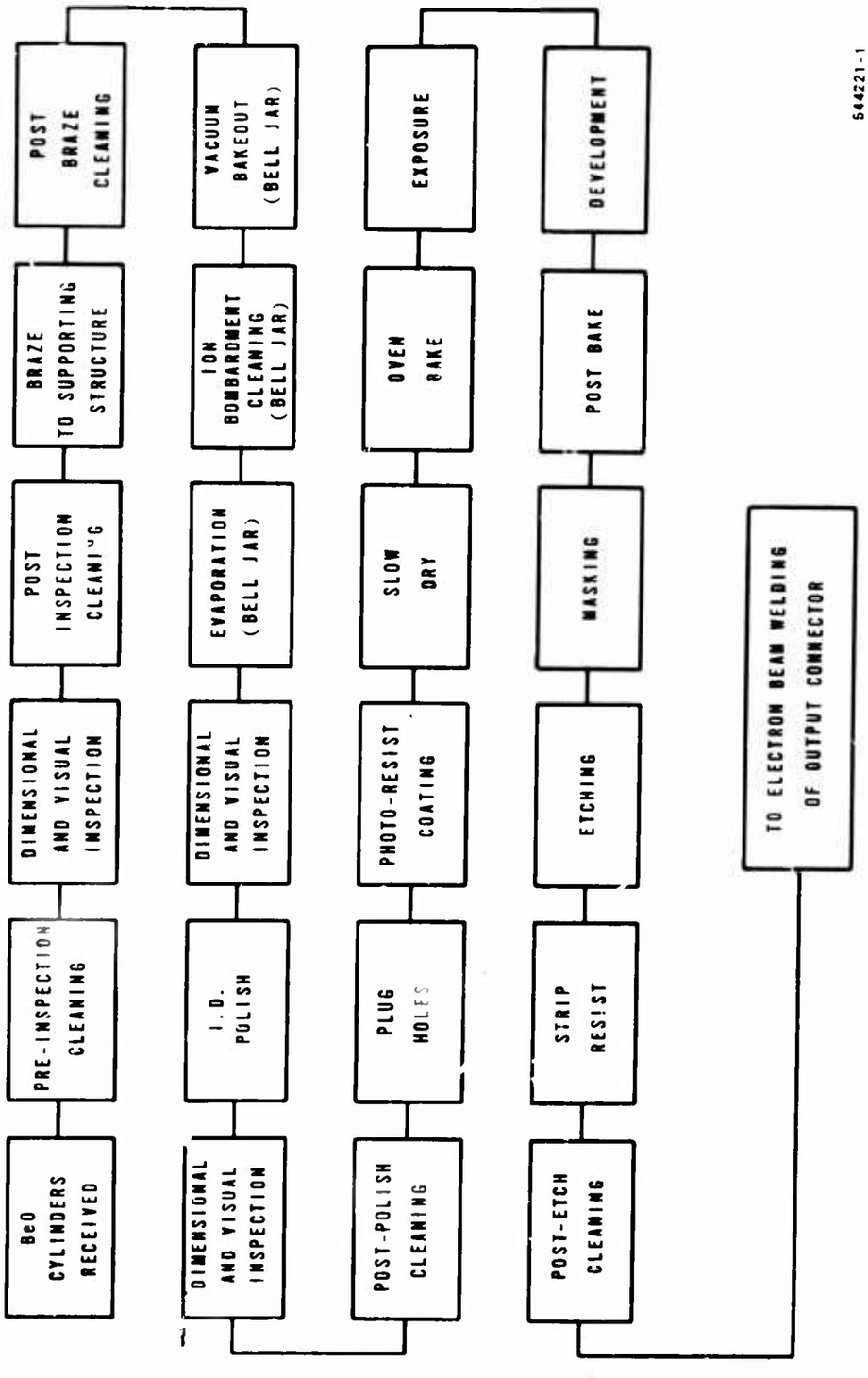

Figure 10. Fabrication of QK1329 Cylinder Slow-Wave Structure

Step	Summary
1.	Cylinder assembly installed in rotary fixture in vacuum bell jar and evacuated.
2.	Ion bombardment.
3.	Bakeout.
4.	Titanium evaporation.
5.	Titanium-copper evaporation.
6.	Copper evaporation.
7.	Cooling.

Details of current process for bonding a copper coating onto the BeO cylinder ID surface.

Step	Details
1.	The brazed cylinder assembly is installed in a rotary fixture in a vacuum bell jar and the jar pulled down to a pressure of 200 microns.
2.	The entire assembly is ion bombarded for a period of minutes at 1000 volts and 100 milliamps. During this interval pressure is gradually decreased from 200 microns to approximately 10 microns. At the end of this interval, the ion bombardment supply is turned off.
3.	The bell jar pressure is next reduced to 5×10^{-6}, the heating coil supplied with power and the temperature adjusted to 375° C. Vacuum bake-out is continued for 1/2 hour.
4.	With the heating coil left on, the cylinder rotating device is started, and titanium is evaporated from a titanium-wound stranded tungsten wire that passes through the axis of the cylinder assembly. Evaporation is at 1325° C and for a period of 1 minute.
5.	While still evaporating titanium, a copper evaporating source, consisting of copper in a tungsten boat (previously purified by boiling in vacuum for 3 minutes) and that is also physically supported near the axis of the cylinder, is turned on. When it reaches 1125° C the copper and titanium are evaporated together for 1 minute. The titanium source is then turned off, but the copper continued.

Step	Details
6.	Copper evaporation is continued at 1125°C for 1-1/2 hours at which time a 3 to 4 mil thickness of copper will have been deposited. After 5 minutes of copper evaporation the heating coil is turned off and the cylinder is allowed to slowly cool during the rest of the copper evaporation cycle.
7.	After the copper source and the cylinder assembly heater have been turned off at the end of the evaporation cycle, the equipment is allowed to cool for 2-1/2 hours before releasing the vacuum and opening the bell jar.

2.2.5.5 Outline of Current Process for Photo-Etched Delay Line

Starting Point: - BeO cylinder with 3-4 mil thick bonded copper ID coating.

Step	Summary
1.	Polish copper coating.
2.	Clean.
3.	Plug output holes.
4.	Clean surface around output holes.
5.	Resist coat.
6.	Register film strip photomask with output hole locations and temporarily fix in place.
7.	Place cylinder assembly over deflated pressure bag; install fluorescent tube and inflate bag.
8.	Expose patterns.
9.	Develop and dye image and oven dry.
10.	Inspect image and correct defects.
11.	Install in etching fixture and etch.
12.	Carry out any local etching where necessary.
13.	Etch titanium film previously under copper.
14.	Mechanically scrub pattern if necessary to throughly remove titanium coating.
15.	Strip residual photoresist.
16.	Remove from etching jig.
17.	Clear output holes.
18.	Clean thoroughly in cold deionized water until $AgNO_3$ test negative and dry.

Details of Current Process for Photo-Etched Delay Line

Starting Point: - BeO cylinder with 3 to 4 mils of copper bonded to ID surface and brazed on OD to copper support structure.

Step	Details
1.	As received from the evaporation operation the copper coating is smooth but matte in appearance. In order to obtain a sharp pattern it is necessary that the surface be as a fine a finish as can be obtained. The surface finish can be improved considerably by polishing with abrasive paper. This is done by hand using 4/0 carborundum paper, dry. Rubbing is continued until the surface is uniformly brightened. Measurements have shown that approximately 0.5 to 1.0 mil diameter is removed.
2.	The polished surface is cleaned by rubbing with slightly moistened White Dot, and then thoroughly washed in running water, quick dried with compressed air, and oven dried at 50°C for 15 minutes.
3.	To prevent photoresist fluid from running into the output holes and later bubbling out again during drying, the holes are plugged with wax. Twin rods of beeswax are formed and stuffed into the output holes with tweezers and smoothed off with a pointed X-acto knife blade. Excess wax is scraped from around each hole to make as nearly as possible a smooth continuous surface.
4.	The surface around each output hole where wax has been is cleaned quickly and locally with a small pad of tissue soaked in xylene.
5.	Resist coating is a hand operation using a Dynachem photoresist, full strength. The cylinder assembly is held vertically so that the axis of the cylinder is parallel to the table top, and so that the region of the surface opposite where the delay line will be, is down. Photoresist fluid from an eyedropper is squeezed to form a small pool about 0.5 inch long and the width of the BeO cylinder (0.325 inch). Surface tension forces will support a pool of from 6 to 10 drops. This is all the resist that is used to coat the cylinder. The resist fluid is distributed by very slowly rotating the cylinder on its axis so that the pool progressively moves along the surface. The time required to make one complete revolution is about 1 minute. It is important that the pool move slowly, uniformly and always in one direction. At the completion of one revolution the residual resist in the pool is soaked up with tissue and the cylinder hung in the same position in a 50°C ventilated oven for 7 hours.
6.	Under a 15X stereo microscope the film strip photomask is wrapped around the photoresist coated ID of the BeO cylinder and positioned so that the output hole comes in the center of the wide finger. This is practical because the output hole is clearly visible through the transparent photoresist, and the output fingers are the transparent portions of the photomask. The film strip is secured at each end with small pieces of pressure sensitive tape (Scotch tape).

Steps (cont'd)	Details (Cont'd)

7. The cylinder assembly with the photomask in place is slipped over the deflated polyethlene pressure sleeve, the black light fluorescent tube passed through the center of the sleeve and its support fixture and the sleeve inflated to a pressure of 5 lb per square inch. Electrical connections are made to the ends of the fluorescent tube and the device is ready for exposure.

8. Exposure is effected by long wavelength ultraviolet light from the black-light fluorescent lamp described in the preceding section. Using a model UV-21 light, the exposure time is 6 minutes. Both the polyethylene sleeve and the pressure-sensitive tape used to secure the negative strip on the beryllia cylinder are sufficiently transparent to the ultraviolet light that they provide no interference with exposure.

   After completion of the exposure interval, the light is turned off; the air pressure is released; the connections to the lamp are taken off; the cylinder is removed from the pressure device; and the transparency is removed from the cylinder. The photoresist is now ready for development.

9. The photoresist is developed by complete immersion of the cylinder in a container of photoresist developer. This dissolves the resist in the regions that have received no light, but leaves it intact where exposure has occurred. A short wash in running water leaves the pattern cleanly defined but rather faint because of the transparent nature of the resist medium. Dye is used to color the developed image and will disclose any defects in the resist pattern.

   At this point, the photoresist image is quite fragile. It is hardened, toughened and made resistant to subsequent etching by baking in an air-oven at 50° C for 15 minutes.

10. The interdigital finger image is inspected critically using a 15X stereo microscope and all defects in the pattern are corrected. These will usually be of two types, - (A) resist present where it should not be; this is corrected by cutting and scrapping with a fine pointed knife. (B) resist missing in areas that should be protected; this is corrected by painting, using a very fine artists brush and Worrow acid resistant paint type 145-3V suitably thinned with isophone.

11. An etching fixture is used to cover all of the parts of cylinder assembly that must be protected during etching. This fixture consists of two circular micarta plates that are suitably milled out to accept the cylinder assembly. O-rings seal the assembly at the edges of the BeO cylinder, and a rubber gasket seals the two micarta plates where they meet at their outer diameter. The

Steps (cont'd) Details (Cont'd)

whole assembly is held tightly together with gasketed nuts and bolts. When installed as described, the only exposed portion of the cylinder assembly is the surface to be etched.

Etching is carried out in a Pyrex dish using a ferric chloride etchant at a temperature of 75-80°C. The fixture is totally immersed in the etching solution which is agitated throughout the etch period. Etching is allowed to proceed over an approximate 3 minute interval, the fixture being turned over every 30 seconds to promote uniformity of etch action. The etched pattern is inspected every 30 seconds and the fixture removed from the etch bath when microscopic examination indicates that the fingers are sharply defined.

12. Occassionally some areas require further etching and this is accomplished locally by squirting etchant over the region with an eyedropper.

13. At the conclusion of the copper etch operation, the background of pattern is dark gray or black in color, indicating the titanium coating deposited under the copper. This coating, in the spaces between the fingers, is either removed completely or loosened by immersing the etching fixture in 10% hydrofluoric acid and water solution at 60°C for 30 seconds. If completely removed, the clear white color of the BeO substrate will show between the fingers.

14. If a gray color persists, the line is slightly scrubbed with White Dot powder using a bristle tooth brush. This will completely remove the titanium coating and bring out the white BeO color.

15. The residual photoresist is removed by swabbing briefly with a proprietary resist stripper, followed by a running water rinse.

16. The etching jig is disassembled and the cylinder assembly removed.

17. The output holes in the BeO cylinder previously plugged with beeswax are cleared by running a small drill through them. This drill is held in a cut-down pin vise and the operation is performed by hand under a microscope.

18. The cylinder assembly is finally cleaned thoroughly by soaking in several changes of deionized water until the rinse water no longer shows a positive test for chloride ion using silver nitrate reagent. The assembly is finally quick dried with compressed air, oven dried at 50°C for 15 minutes, and sealed in a polyethylene bag.

2.2.5.6 Process Specification for Electron Beam Welding of Copper Connectors and Collector on Slow-Wave Structures

1.0 Scope

To specify the equipment, materials and procedure to be used in electron beam welding copper connectors and collector on the slow-wave structure program.

2.0 Applicable Documents

None

3.0 Requirements

3.1 Materials - The materials to be used in this process are as follows:

a. Copper wire 0.018 in. dia. with a 0.008 in. slot cut in it leaving two tabs 0.005 in. thick for welding to slow-wave structure delay line.

b. Copper collector plate 0.5 x 0.5 x 0.060 in.

3.2 Equipment - The equipment needed for this process is:

a. Model W1-2 Electron Beam Welder with Vacuum Chamber

b. 3 kW power supply

4.0 Procedure

4.1 Place copper connectors in position and bend the 0.005 in. copper tabs 90° and clamp tightly to wide copper finger on the delay line, making sure you have a good electrical connection between the two.

4.2 Mask the rest of the delay line by placing a thin stainless steel sheet over it and clamp it into place to prevent the line from getting any of the melted metal evaporated on it.

4.3 Place slow-wave structure into vacuum chamber ane evacuate to $\approx 4 \times 10^{-4}$ Torr.

4.4 Raise power supply to 70 kV and 2 ma and by using a foot pulse proceed to make weld watching for melt while foot pulsing. Each connector is done separately using the same method. Weld is made on both edges of tube to insure good electrical contact.

4.5 Collector is then put in place and ready for welding.

4.6 The delay line is then washed the same way as in Section (4.2).

4.7 Power supply is raised to 90 kV and 7 ma and, by using a circle generator making a 0.010 in. dia circle at a speed of 15 in./min, we proceed to weld collector in place. Both sides of collector are done the identical way.

2.2.5.7 Cleaning Beryllia (Process Specification 638703)

1.0 Purpose

To specify equipment, material and procedure for rinsing beryllia as received from vendors in order to remove any beryllia dust and/or packing contamination.

2.0 Equipment

2.1 Ultrasonic generator and transducer, 25-30 KO
2.2 Exhaust unit with absolute filter
2.3 Sink
2.4 Appropriate containers for solutions
2.5 Appropriate racks, etc. for parts
2.6 Nitrogen oven (110°C)

3.0 Material

3.1 Distilled water per P.S. No. 637286
3.2 Methanol, C.P.
3.3 Nitrogen, prepurified, filtered at point of use

4.0 Procedure

4.1 Place parts in appropriate container
4.2 Rinse parts ultrasonically in distilled water for 1 minute
4.3 Repeat 4.2 two (2) times using fresh water each time.
4.4 Rinse parts ultrasonically in Methanol for 1 minute
4.5 Repeat 4.4 two (2) times using fresh Methanol each time

NOTE: Discard water and Methanol by dumping down sink, do not reuse. Flush sink thoroughly with water.

4.6 Blow parts dry with nitrogen or dry in nitrogen oven at 110±5°C for 15 minutes
4.7 Store parts in clean containers which will pass atomizer test (P.S. 637264)

*All beryllia operations must be performed in separate area.

2.2.6 Design and Evaluation of Prototype Photodeposited Linear Slow-Wave Structures (Ref: Appendix A Section IB 1b(2)(c)(d))

2.2.6.1 Design of Linear C-Band Slow-Wave Structure

The parallel plate approximation for c/v_o vs λ gives approximate values sufficient for use in tube design:

$$\frac{c}{v_o} = \frac{\lambda}{2p} - \frac{\ell + p}{p} (M) \qquad (1)$$

where $(\frac{c}{v_o})$ = ratio of velocity of light to velocity of phase

ℓ = length of finger
p = pitch of line
M = dielectric loading factor

The dielectric loading factor is approximated as:

$$M \sqrt{\frac{\epsilon_r - 1}{2}} \qquad (2)$$

where ϵ_r = dielectric constant.

The first step in the design procedure was to establish experimentally the validity of equation (2). It was decided to make the initial measurements at L-band, since tooling was available to fabricate accurate linear lines at this frequency. Several lines were fabricated and (c/v) vs λ measurements were taken of the lines in air and on materials with a dielectric of 6, corresponding to a substrate of beryllia (BeO), and a dielectric of 9, corresponding to a substrate of alumina (Al_2O_3). The measurement technique is described in Appendix D and the resulting data is shown in Figure 11. It appears that the departure of the experimental points from the theoretical values is consistent in the three cases. Thus, since it is known from previous work that the difference between actual and calculated values for the unloaded line is small enough to allow the use of the parallel plane approximation in tube design, a design of a C-band SWS was evolved on the basis of Equations (1) and (2).

2.2.6.2 Evaluation of Linear Slow-Wave Structure

In the evaluation of a slow-wave structure or delay line in cold test, there are four measurements of significance in determining the suitability of the structure for use in a particular tube. They are:

a. c/v_o vs λ relationship
b. Coupling Impedance
c. Insertion Loss
d. Match to 50-ohm type-N output.

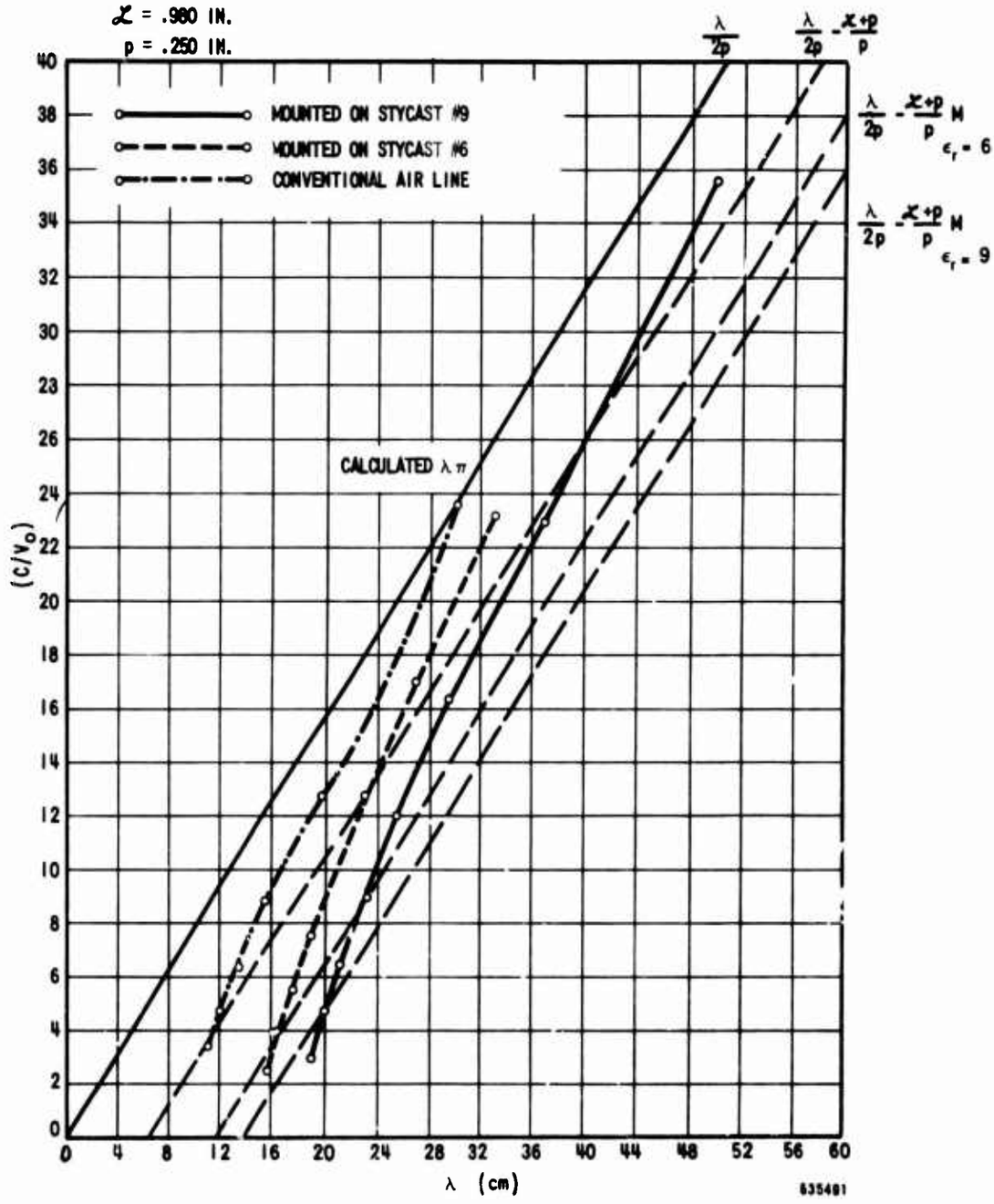

Figure 11. QK1329 Dispersion Curves

Prior to the receipt of the beryllia pieces, the line was photo-deposited on Stycast, and all initial measurements of the proposed C-band line were made using this material. The Stycast is readily machinable by conventional techniques, which further facilitated procurement of the special lengths and shapes required. The benefit is obvious since, if beryllia were used on the initial pieces, each operation would require grinding in a special facility.

a. c/v_o vs λ

The first measurements taken were the dispersion characteristics of the structure in the form of a delay ratio (c/v_o) vs wavelength (λ). The technique used for making the measurement was the resonance method, which is described in Appendix D. Figures 12 and 13 show the dispersion curve for the SWS on Stycast 6 and on beryllia, respectively. For comparison purposes, Figure 14 shows the dispersion curve for a conventional miniature C-band delay line. The departure of the experimental values from the theoretical values are of the same magnitude, indicating that the assumed dielectric loading factor was correct.

b. Coupling Impedance

The second measurement of interest, coupling impedance, was taken using the frequency perturbation method described in Appendix E. The coupling impedance, or degree of coupling between the rf wave and the electron beam, is actually a measure of the strength of the rf voltage field at the beam position. It is a function of the E field of the rf energy and its power and is generally expressed in ohms.

Since the starting current varies inversely with the coupling impedance this factor affects the number of pitches required; a tube with low coupling impedance requires more fingers to reduce the starting current to an adequate level.

Figure 15 is a plot of coupling impedance vs frequency for the C-band SWS on Stycast 6, the SWS on beryllia and also for a convertional miniature C-band delay line. Since the values are all of the same magnitude, the coupling impedance is considered satisfactory. The discrepancy in the first point was not understood at the time, but this point fell outside the design band.

c. Insertion Loss

The third factor of concern, measurement of insertion loss, requires a full length of line, whereas the dispersion and coupling impedance require only 20 pitches. In this measurement, the power loss must be divided into the losses from dissipation and reflection. The technique for doing this is described in Appendix F.

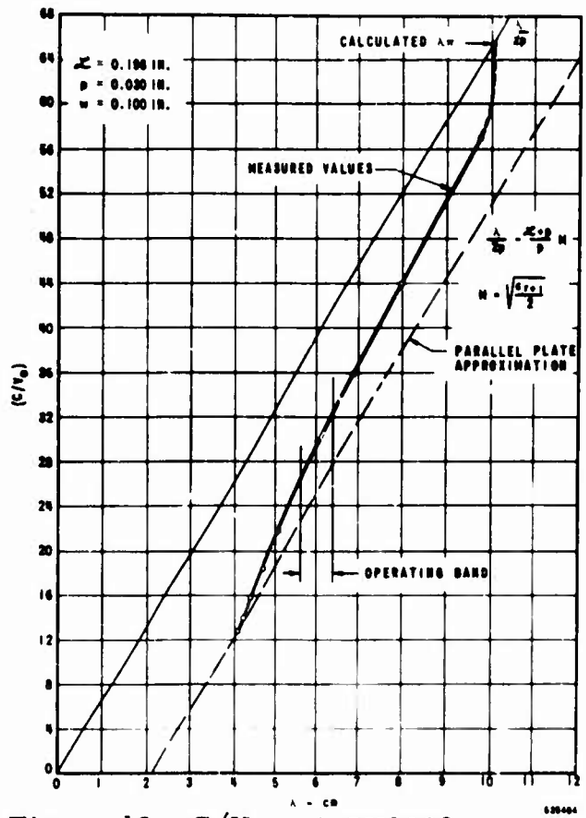

Figure 12. C/V_o vs λ QK1329
Line Mounted on Stycast No. 6

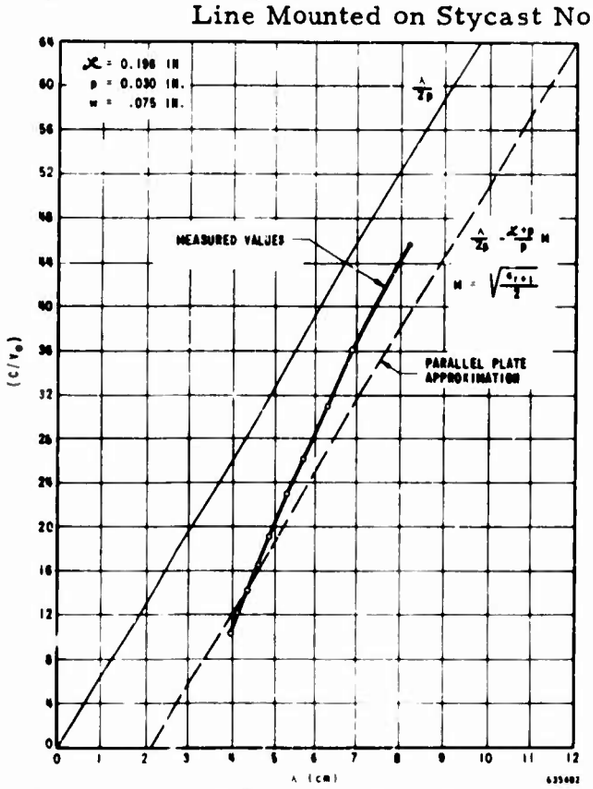

Figure 13. C/V vs λ QK1329
Beryllia Substrate

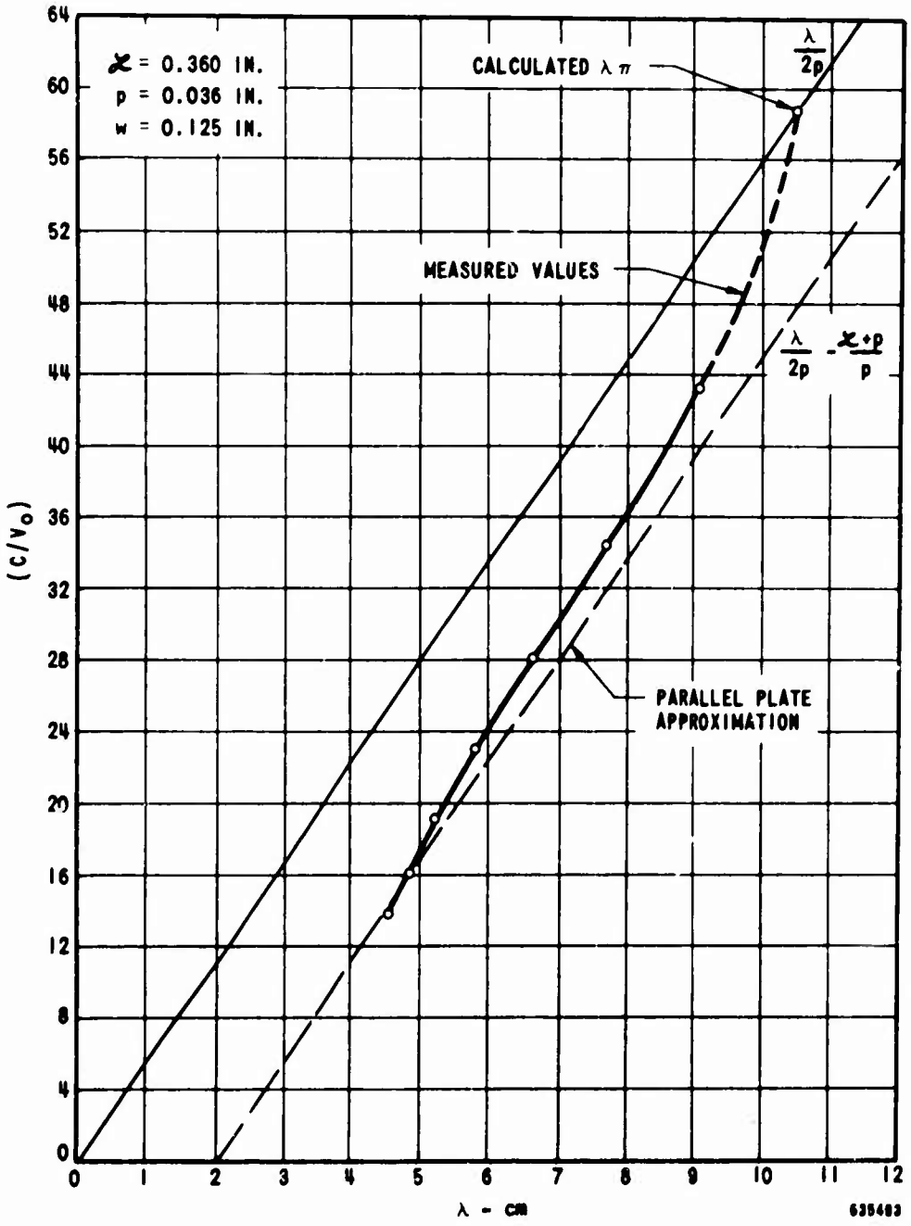

Figure 14. C/V_o vs λ QK1182

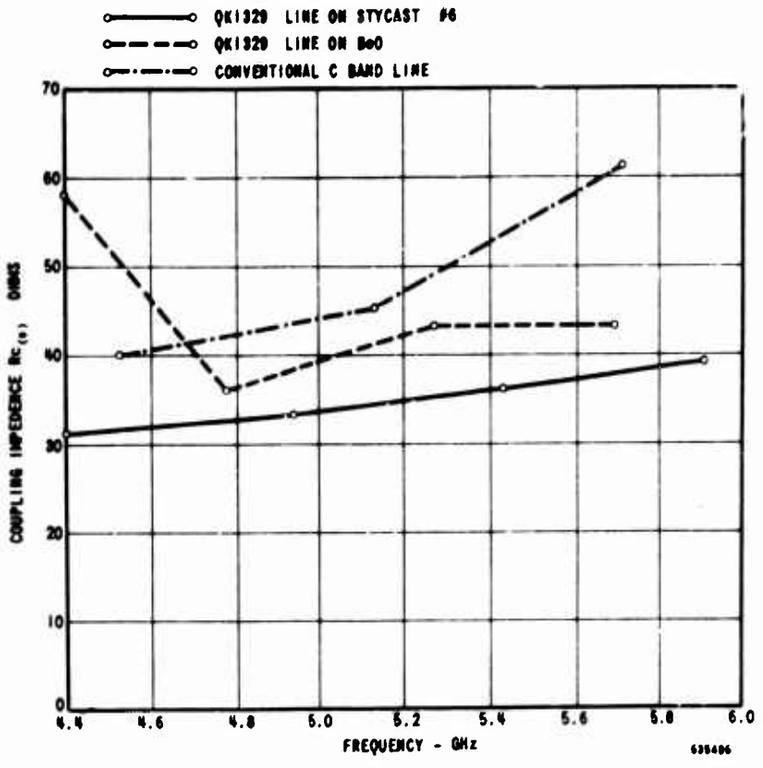

Figure 15. Coupling Impedance Measurements

Figure 16 shows the results of the measurements taken on a full-length line photodeposited on Stycast 6. The values obtained are approximately of the same magnitude as those obtained in the conventional X-band tubes. Conventional C-band tubes have a value in the order of 1.5 to 2.5 db. This means that although the present level of insertion loss is higher than the conventional tube, it is not high enough to seriously affect tube operation.

The additional insertion loss will tend to reduce tube efficiency somewhat, but, since most of the power in the MBWO is generated over the first third of the delay line, this reduction, based on experience with operation of conventional X-band tubes, should be less than 5%.

d. Matching of C-Band Linear SWS

The match to the linear line was achieved by utilizing a quarter-wave transformer between a 50-ohm coaxial type-N output and the delay line. While the quarter-wave transformer is usually considered a narrow-band device, it is sufficiently wide-banded for this application.

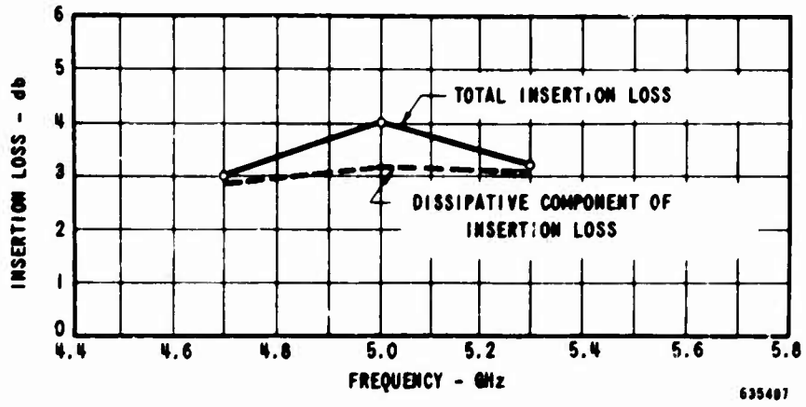

Figure 16. Insertion Loss Measurements Taken on QK1329 Delay Line Photocopies on Stycast No. 6

The initial cold test work was done on a substrate of Stycast 6, rather than beryllia, since it could be machined by conventional techniques. Once the initial configuration of the substrate was determined, linear beryllia strips were ordered from a vendor. This cold test model is shown in Figure 17 while Figure 18 shows the percentage voltage reflection vs frequency.

Full-length line beryllia pieces were designed, ordered, and procured. The rf match obtained is shown in Figure 19; the total insertion loss is shown in Figure 20. The output used in these measurements is a 50-ohm coaxial type using a quarter-wave transformer to couple to the delay line. The line is terminated by a 50-ohm external termination. The test data were certified by the Quality Control Engineering Department as correct.

This completed the evaluation of the linear slow-wave structures at C-band.

2.2.6.3 Linear K-Band Slow-Wave Structure (Ref: Appendix A, Section IB1b(2)(d))

a. Ku-Band Design and Fabrication

The Ku-band line was designed by the same parallel plate approximation method used in designing the C-band delay line.

The design of the slow-wave structure for Ku-band (described by Drawing No. A-632-311-Revision 0 included as Figure G-1 in Appendix G) consists of 101 fingers, each 0.0708 in. long, 0.0053 in. wide and spaced 0.0054 in. apart. The overall length of the line is approximately 1 inch and connectors to either end of the line are made by extending end fingers and terminating each in a pad 0.030 inch in diameter.

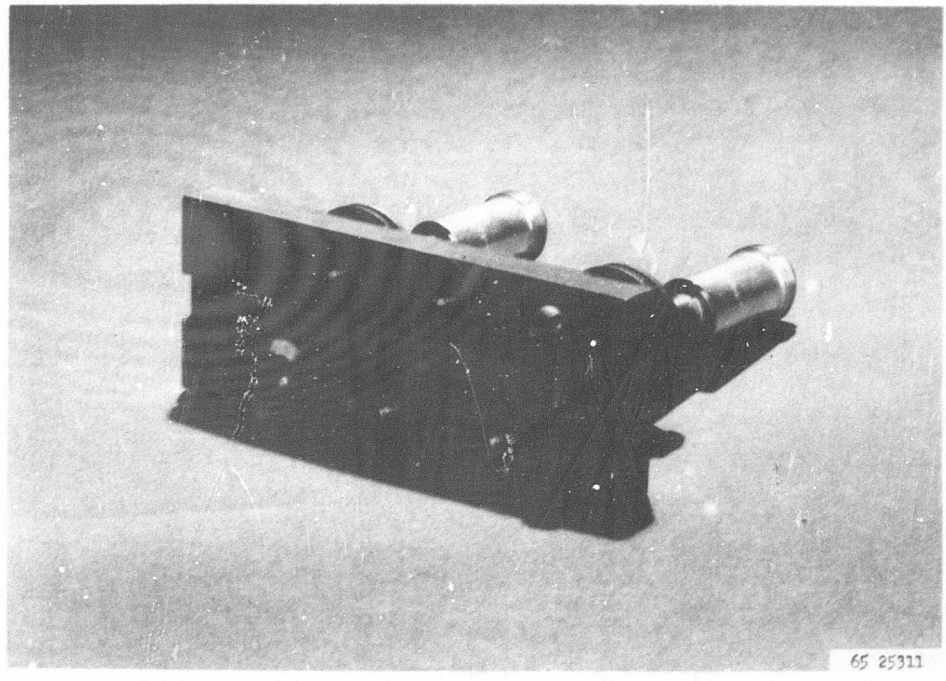

Figure 17. Cold Test Model

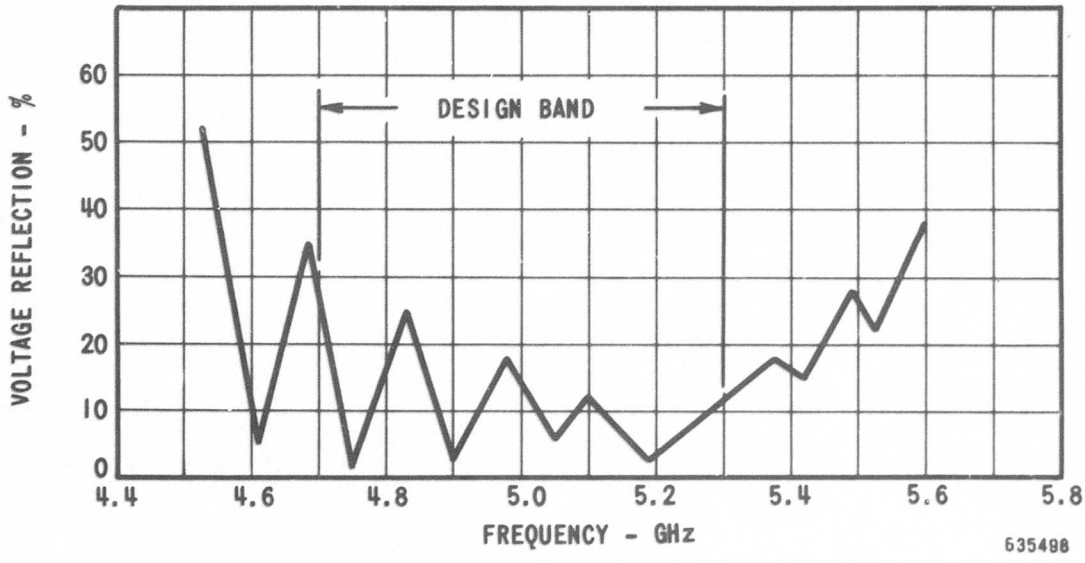

Figure 18. Cold Test Match Linear C-Band Slow-Wave Structure on Stycast Substrate Line Terminated in 50 ohms Coaxial Matched Load

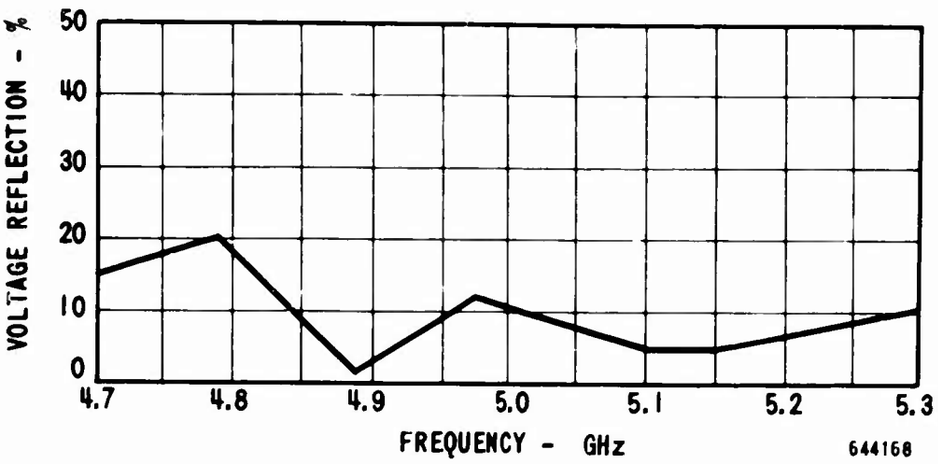

RF Match

Figure 19. Linear C-Band SWS on Beryllia Substrate

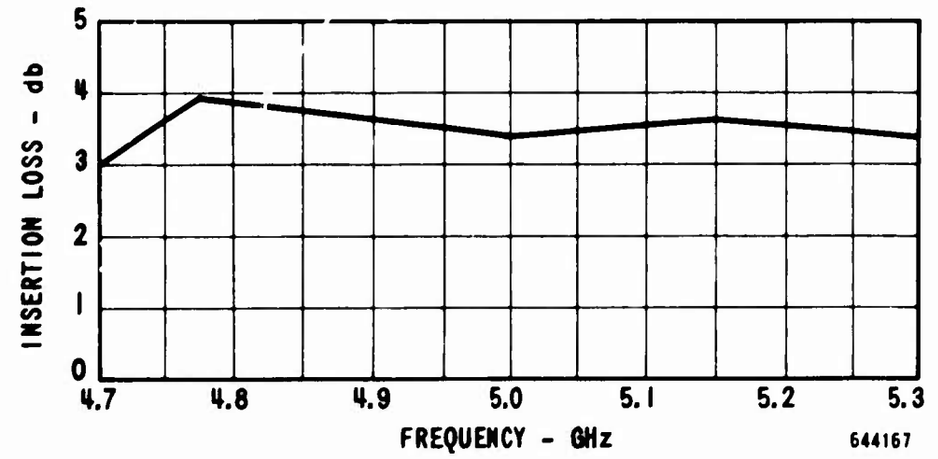

Insertion Loss

Figure 20. Linear C-Band SWS on Beryllia Substrate

The substrate on which the line is to be formed consists of a strip of beryllia 0.050 in. thick, 0.150 in. wide and 1.320 in. long. Accurately positioned holes corresponding to the input and output pads are provided. The piece is described by Drawing No. A-632-313 Revision 0, included as Figure G-2 in Appendix G. This material was obtained from the National Beryllia Company.

Sample slow-wave structures have been made by coating with copper by vacuum deposition, following the procedures for linear C-band slow-wave structures. The copper thus deposited was further built up with electroplating to a thickness of approximately 0.001 inch. As removed from the electroplating solution, the copper was somewhat grainy; it was polished mechanically to a bright finish using 4/0 abrasive paper.

After thorough cleaning, the strip was photoresist-coated by spinning, and processed through drying in the usual manner. The negative transparency was positioned against the strip, emulsion to copper, using a binocular microscope, and the pad images on the negative were indexed on the holes in the beryllia strip. The strip and the negative were temporarily secured together using adhesive tape and then transferred to the vacuum printing frame on a plate maker for a 6-minute exposure. After removal, the strip and the negative were separated, and the former was processed through development washing and drying in the usual manner.

Etching was carried out in the same ferric chloride solution used for the C-band slow-wave structures.

Measurements of the finger width and spacing of a typically photo-etched line have been made with a toolmaker's microscope. Not all of the fingers were measured, but several fingers and space at each end at the center were sampled as indicated by Table II; small errors in the finger widths were noted.

Table II

Finger and Space Width Measurements
Ku-Band Slow-Wave Structure

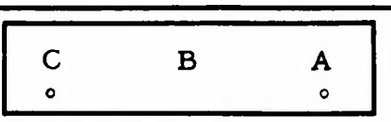

REGION A		REGION B		REGION C	
Finger Width	Space Width	Finger Width	Space Width	Finger Width	Space Width
3.2 mils	7.4 mils	3.2 mils	6.9 mils	3.3 mils	7.5 mils
3.3	7.3	3.9	7.0	3.2	7.0
3.3	7.5	3.5	7.1	3.7	7.3
3.2	7.2	3.6	7.4	3.3	7.6
				3.2	7.5
				3.3	7.4
				3.1	

The discrepancy between the design finger width of 0.0054 in. and the actual width of approximately 0.0033 in. is due to undercutting during the etching process, for which corrections could be made on the photographic master. However, since the electrical characteristics of the line are determined by the length and the pitch, changing the master at the time was felt to be unnecessary.

The effect of such errors in the interdigital delay line have been studied by M.C. Pease.* In the normal interdigital line three types of errors are encountered: small periodic errors, misregister, and random error. In the photodeposited delay line only the latter is significant. Since there is no error in pitch there will be no change in the phase of the rf wave, and the error will result in an increase in VSWR. Pease quotes an RMS error of 1% resulting in a VSWR of 1.2. The average error noted is of this order of magnitude, although the maximum does exceed this value. However, in a tube with a well-matched output, changes in VSWR of this magnitude could not markedly affect tube performance.

b. K-Band RF Match

A K-band linear line mounted on beryllia was fabricated using the photodeposition process described, and initial rf match was obtained utilizing a type-N coaxial output and termination. A quarter-wave transformer was used to transform from the 50-ohm line to the delay line. A cold test curve is shown in Figure 21. (Additional data and a delay ratio curve are presented in Section 2.4.4.2.)

Actually, at this frequency, waveguide rather than coaxial outputs are recommended, but an extensive program to develop a waveguide-to-delay-line rf match seemed unwarranted, therefore, the choice of type-N outputs was made. The objective of the program was to show the feasibility of fabricating a photodeposited line capable of operation over a 10% band centered around 14,000 MHz, and it was felt that the use of these outputs would more than adequately serve the purpose.

The results of using the type N Outputs and the associated type N to waveguide transitions necessary to make the measurements, is to raise the VSWR across the whole band. However the presence of a pass band indicates that operation of the slow-wave structure over these frequencies is feasible.

2.2.7 Evaluation of Circular Slow-Wave Structures
(Ref: Appendix A; Section IB1b(2)(f))

2.2.7.1 Bond

Several of the circular slow-wave structures were subjected to the simulated tube operating environment and withstood repeated application of the adhesion tests.

* The Effect of Tolerance on Interdigital Line - M.C. Pease, Crossed-Field Microwave Devices, Okress Vol. I. Chapter 2 Section 5. Academic Press 1961.

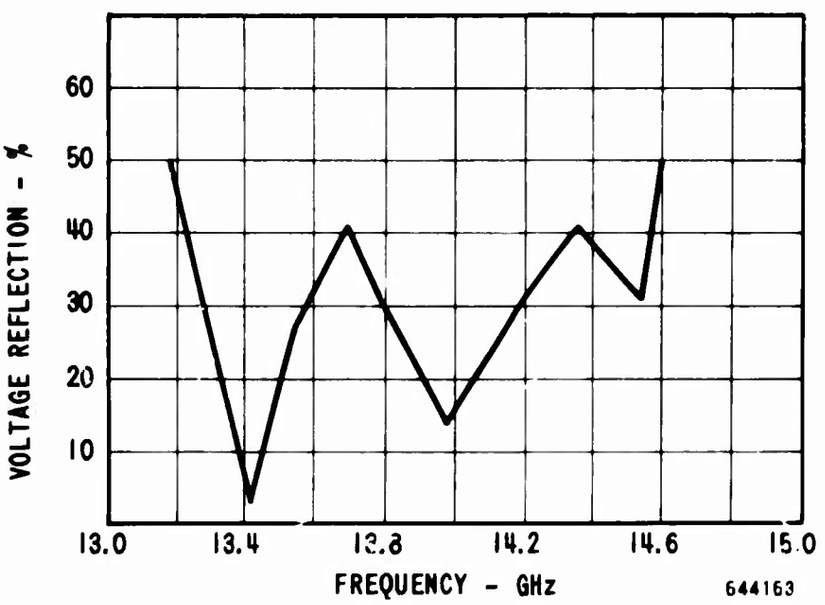

FIGURE 21. QK1329 K-Band Linear Line Cold Test Curve

2.2.7.2 Electrical Evaluation

The typical voltage standing-wave ratio obtained on one of these structures is shown in Figure 22. All structures used in actual test vehicles were also measured for insertion loss. The results were identical with the linear work reported, the value being between +2 and +5 db.

2.2.7.3 Mechanical Evaluation

One of the circular slow-wave structures manufactured by the previously described technique was evaluated. Table III gives the method and results obtained.

Table III.

Environmental Certified Test Data

The following is the text of Memo #RJS-66-1 dated 11 January 1966 concerning environmental testing of the QK1329 slow-wave structure.

Purpose

To determine if the bond between the line and the cylinder would meet the vibration requirements of the latest BWO Exhibit 'C' Specifications.

Results

There was no evidence of separation between the line and the cylinder wall. This test was performed on December 28, 1965.

Procedure

The structure was secured to the C-10 vibration test system and vibrated in each of three (3) mutually perpendicular planes. The vibration frequencies were 55 to 2000 cps at an acceleration of 20 g's. The vibration sweep time was 20 minutes per plane.

Detailed Discussion

During the vibration test a strobe-light was focused on the assembly. A close observation was made to determine if there were any resonances that would cause the line to break bond from the cylinder. There were no such resonances observed in any of the three planes.

The slow-wave structure was checked before and after vibration by engineering. This assembly exhibited no evidence of failure from the vibration tests.

Equipment Used:

C-10 Vibration Test System
Chadwick - Helmuth Slip Sinc System

Signed: R. J. Stearns, Environmental Technican
G.F. Dearborn, Sr. Environmental Engineer

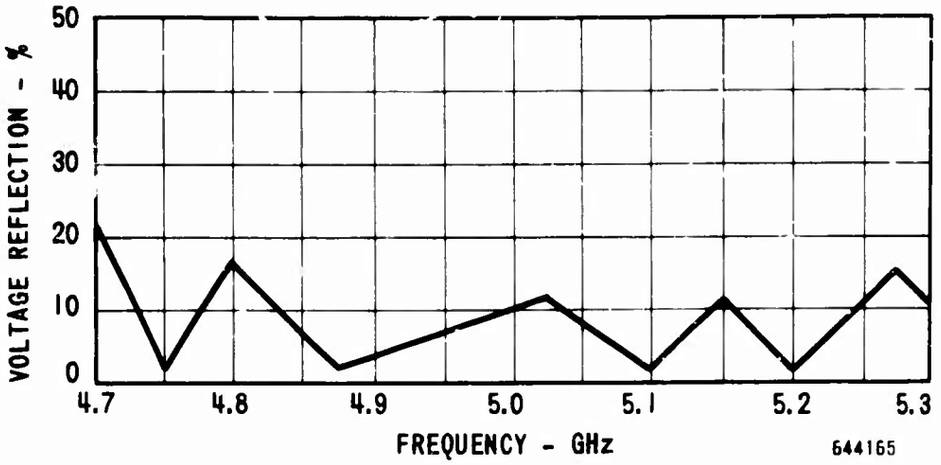

RF Match

Figure 22. Circular C-Band SWS on Beryllia Oxide Substrate

2.2.8 Design and Development of a Test Vehicle for the Ceramic-Mounted C-Band Slow-Wave Structures (Ref: Appendix A; Section IB1b(3))

2.2.8.1 Review of the Design of Ceramic-Mounted Slow-Wave Structures (Ref: Appendix A; Section IB1b(3)(a))

A review of the literature available was made at the start of the program. Raytheon review of this literature indicated that our basic design was sound. The greatest problem appeared to be the phenomena of "sputtering" discussed below. The literature reviewed is given in Table IV below.

Table IV

Literature Review

1. C.S.F. Final Report contract 445.1285 WR1235 July 1964.
2. C.S.F. Final Report contract 445.1285 WR1145 January 1964.
3. J. Arnaud & F. Diamond, International Congress on Microwave Tubes p. 300, 1960.
4. C. Lyon & R. Gerber, 6th International Congress on Microwave and Optical Generation and Amplification, p. 219, London, 1966.
5. C. Lyon & W. Sobotka, 7th National Conference on Tube Techniques
6. W. Sobotka, 5th International Congress on Microwave Tubes, Paris 1964.
7. N.R. Welten & A. B. Laponsky, Report, 18th Annual Conference Physical Electronics, March 1958, page 79 & 87.

2.2.8.2 Sputtering

The review indicated that, in the operation of crossed-field devices with ceramic-mounted delay lines, shorting of the delay line due to sputtering occurs after a few hours of operation.

It is generally accepted that the cause of this phenomenon is due to the impact onto the metallic sole member of ions of sufficient energy to cause sputtering of the surface atoms from the sole onto the slow-wave structure.

Since this can only occur in the presence of ionizable gases within the tube, it was obvious that an effort should be made to obtain extremely high vacuum in the tube at pinch-off. High-temperature bakeout during the outgassing phase was desired and it was toward this end that the high-temperature bond of the slow-wave structure to the ceramic was developed.

A study was made of the known sputtering yields for elemental metals. The spectrum of sputtering yield is bracketed by the heavy, low-melting-point, metals, having the highest sputtering yields and the refractory metals, having the lowest. The lowest yield is exhibited by tantalum. From the practical point of view these differences in sputtering yield make only small differences in tube performance; the highest sputtering yield materials would cause shorting of the slow-wave structure in a matter of minutes; the lowest yield materials, in a matter of a few hours. Obviously, therefore, materials with orders of magnitude lower sputtering yields are required. Such characteristics are provided by metal oxide refractory ceramics. Ideally, a sole could be fabricated from alumina or beryllia; these materials would give rise to an extremely low sputtering rate. Additionally, any sputtered material would not adversely affect the oxide material.

Although desirable from the sputtering yield point of view, the use of ceramic soles is not a practical solution because the sole discs have to be electrically conductive ceramics. These materials are ceramic matrices with interconnected pores throughout the bulk material; the pores are filled with an electrical conductor. It is apparent from experiences with these types of material that the final sputtering yield would be similar to that of the conductive material. The overall reduction would essentially be due to the reduction in total surface area of conductive material at the sole surface.

Also considered was the use of ceramic shields or guard wings, but these suffer from the problem of charge build-up.

The final approach considered was the use of extremely thin metal-oxide films deposited onto the surfaces of the sole.

These films consist of vacuum-evaporated alumina of approximately 100 Å thickness. It was hoped that the film would be sufficiently thick and coherent to prevent the sputtering characteristics of the oxide and at the same time be sufficiently thin to allow drain-off of any electrical charge by electron tunneling through the oxide to the metallic part of the sole.

2.2.8.3 Electron Bombardment of the Dielectric Material of the Photocopied Delay Line in an M-BWO

During normal operation of an M-BWO, there will be electron collection on the delay line and, therefore, some electron bombardment of a dielectric substrate in the case of the photocopied line. It was believed that the processes associated with this bombardment probably would not cause any deleterious effect under normal operating conditions and could be completely avoided, if necessary, by the use of a thin anisotropic conducting film on the dielectric. It was found and confirmed by the life test conducted on this program that the anisotropic film was not required.

Figure 23 is a sketch of the geometry at the surface of the delay line.

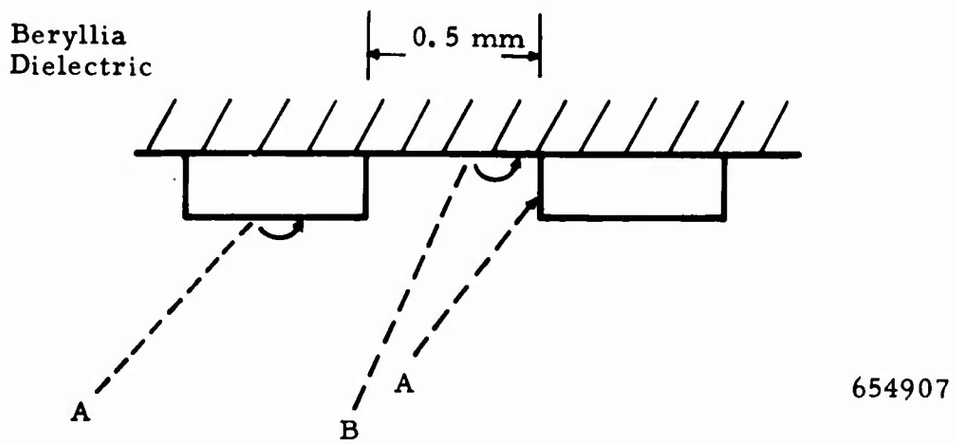

Figure 23. Delay Line Surface

Ideally electrons are collected on the delay line only after yielding considerable energy to the rf fields. At worst, the bombardment energies will equal the anode potential < 2 kV. The current density could be high, ~0.1A/cm^2. The electron collection exists predominantly in a region of moderate rf field. The finite thickness of the metal elements shields the dielectron to some extent, perhaps reducing the current density by a factor of 2 or 3.

The bombardment energies are relatively small < 2 Kev and, therefore, we can conclude that (a) no radiation damage will ensue (this requires ~50 Kev or more) and (b) the resulting effects are surface effects. The electron penetration depths at most are a few hundred Angstroms.

It was believed that the net results of the electron bombardment would be an equilibrium flow of electrons to the metal delay line by means of several mechanisms including the following:

a. ionic conductivity enhanced by increased temperature,

b. significant electron-beam-induced conductivity

c. migration of secondaries to the metal fingers – the secondaries with a typical emission energy of 10 ev will have a trajectory hop along the surface of perhaps 0.1 mm min. diameter, which indicates that, within 2 or 3 hops, an electron could migrate from the dielectric surface to the metal member, and

d. conduction in sputtered thin films – this will be small and will not be detected by the rf fields presumably until a critical thickness of the order of 150 Å is reached.

Associated with the bombardment will be cathodoluminescence, but this has no deleterious effects for this case.

As far as rf loss mechanisms are concerned, the conditions for significant multipactor are not believed present. The enhanced conductivity may lead to a detectable loss that then should be far below that caused by sputtered films – which remains, at present, the principal problem.

It was assumed that no exotic contaminants were present on the dielectric surface which could lead to spiral reactions that alter the chemical nature of the dielectric.

A thin film of alumina (≈ 100Å) was used on test vehicles constructed during this program; no difficulty or adverse tube performance was detected. The life test results reported in a later section of this report indicate that the life of crossed-field devices with ceramic-mounted delay lines can be greatly prolonged by using such films. Although use of an alumina film does increase the possibility of secondary emission from the sale, in this case the energy levels are not considered sufficient to cause significant secondary emission.

2.2.8.4 Design of Test Vehicle (Ref: Appendix A; Section IB1b(3)(b))

a. Electrical Design

The test vehicle for the evaluation of the slow-wave structure was a C-band M- type BWO.

The design parameters were as shown in Table V.

Table V. Test Vehicle Electrical Design Parameters

Parameter	Limits
Frequency	4,00 - 5300 MHz
Delay Line Dimensions	
Pitch	0.030 in.
Length	0.198 in.
Thickness	0.002 - [illegible] 003 in.
Number of Fingers	80
Anode Voltage	1900 v
Anode Current	175 mA maximum
Sole Voltage	650 - 1300 V
Sole Current	+5 to -10 ma
Grid Voltage	200 - 500 V
Grid Current	± 2.0 Ma maximum
Accelerator Voltage	1500 V nominal
Accelerator Current	+2.0 Ma maximum
Power Output	50 W minimum

The test vehicle features a Beam Miser, an external attenuator, 50-ohm type-N coaxial output connector and is conduction-cooled through centrally located mounting lugs. If packaged, the tube would be 4 in. in diameter and would weigh approximately 3.5 lb.

A cross ection of the test vehicle is shown in Figure 24.

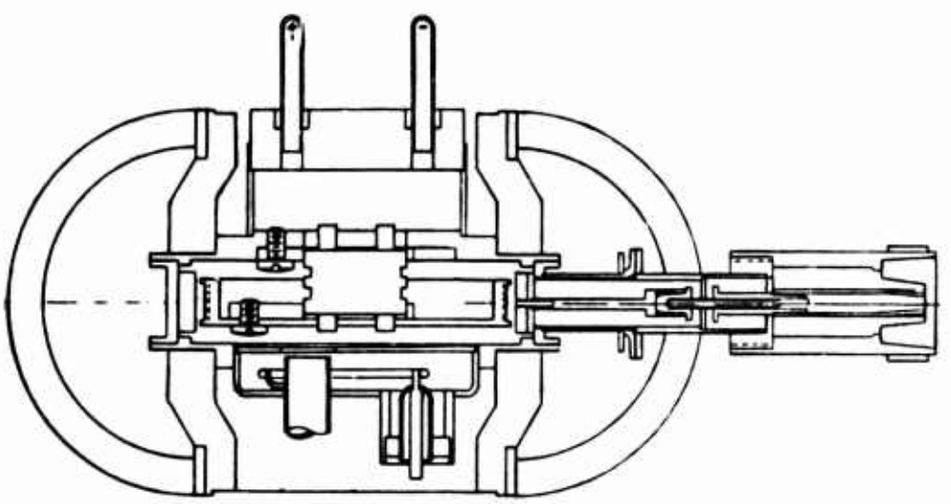

654908

Figure 24. Cross Section of Test Vehicle for Evaluation of Slow-Wave Structure (C-Band M-Type BWO)

A problem was encountered in the design and positioning of the electron gun. In a tube with a conventional delay line, the area of the cylinder adjacent to the electron gun is relieved to allow sufficient clearance between the anode wall and the gun elements in general – the accelerator in particular.

Relieving the ceramic did not seem to be advisable in the design of the test vehicle, due to stress of the ceramic cylinder to copper cylinder braze. Two other alternatives were considered, namely: lowering the entire gun structure with respect to the interaction space, or redesigning the electron gun elements, reducing them in size to maintain more normal spacing with respect to the interaction space. The first alternative, the lower gun, was selected for the first test vehicle.

b. Mechanical Design

1. Cylinder Braze - When the initial design of the C-band short-wave structure was evolved, the design of the cylinder was a matter of concern, since a relatively thin-walled ceramic cylinder would have to be brazed to the ID of a copper cylinder. It was recognized that the stresses in the ceramic after such a braze might be sufficient to cause a fracture of the ceramic.

Since beryllia pieces were not available at the time, alumina cylinders were fabricated, and test brazes were made. The assemblies were thermal-cycled several times with no failures. Since the published data showed that the allowable stresses in beryllia were only slightly less than those of alumina, it was felt that the same results would be obtained with beryllia assemblies.

However, experience with beryllia cylinders later proved that this was not true. The first beryllia cylinders received were cast 80% dense bodies, rather than the specified 99% dense bodies. Thus, when the first cylinders cracked after thermal cycling, the failure was attributed to the fact that the strength of the cast body is considerably less than the pressed body. However, when the same type of failure occurred after receipt of the dense beryllia, it became apparent that the difference in strength between the beryllia and alumina was greater than expected, and that a modification of the brazed joint was required.

The failure, actually a crack in the ceramic, always occurred during thermal-cycling after the initial braze, not during the braze itself, meaning that the failure was due to stresses set up by the differential in thermal expansion between the copper and the ceramic. The stresses involved are both radial and tangential, both of which place the ceramic in tension, the weaker mode. The solution to this problem, therefore, would have to reduce both of these stresses. Since the delay line occupies an arc less than 180°C, the brazing area was limited to just the area of the delay line. This would markedly reduce the radial stresses. Were the anode diameter such that the active line would occupy a greater portion of the circumference, it would be necessary to thicken the ceramic substrate to provide sufficient strength to withstand the stresses involved.

The tangential stresses were reduced by machining orthogonal slots in the copper cylinder in the area of the braze as shown in Figure 25. This "waffle plate" effect allows the copper to yield under the stresses due to differential expansion, thus reducing stresses in the ceramic. Since this method was initiated, there have been no instances of cracked ceramics.

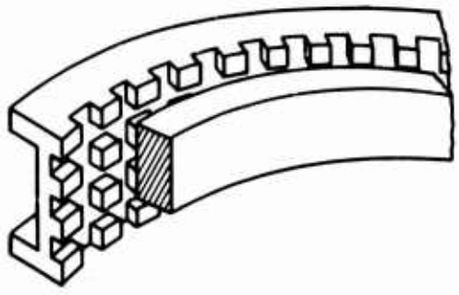

644166

Figure 25. Cylinder-Anode Braze

2. Porous Circular Beryllia Ceramic - The first lot of circular beryllia structures received were subject to a normal brazing cycle in a hydrogen atmosphere. During this brazing operation, several areas of heavy discoloration appeared on the surface of the beryllia cylinders. Further investigation showed that this discoloration extended throughout the entire thickness of the ceramic. This was concluded to be due to an impurity in the beryllia which reduced to a visible impurity during the hydrogen firing. An immediate check with the vendor indicated that the beryllia structures supplied had been machined from a cast rather than a hydrostatically pressed body, which meant that the density was in the order of 80% rather than the 99% specified.

Replacement cylinders of 99% density were obtained and, as might be expected, hydrogen-firing showed no effects of impurity absorption into the body. All subsequent work was carried out on high-density beryllia material.

2.2.9 Evaluation of Test Vehicles (Ref: Appendix A Section IB1b(3)(c))

Using the manufacturing technique described in Section 2.2.4 and the test vehicle design discussed in Section 2.2.8, circular C-band slow-wave structures were fabricated and evaluated in test vehicles.

These tests demonstrated that photodeposition of slow-wave structures was feasible for use in microwave tube manufacture. As a result, a design specification for linear C-band slow-wave structures was completed (as reported in Section 2.2.10), and a final processing technique was established (as reported in Section 2.2.11). Details of the evaluation are presented in Section 2.4.1.

2.2.10 Design Specification for the C-Band Slow-Wave Structures (Ref: Appendix A; Section IB1b(3)(d))

The specification for the C-band slow-wave structure is shown in Figure G-1 included in Appendix G of this report.

2.2.11 Conclusion Phase I

Section 2.2 of this report has described in detail the work done on Phase I of the contract. A basic technique was established and the development of a satisfactory bond was accomplished. Initial results indicate that the problem of sputtering has been minimized. The evaluation of the cold test and hot test results indicate that a photocopied slow-wave structure is adaptable to microwave tube operation. Design data and certified test data were submitted to the Air Force and the contractor obtained permission to initiate work on Phase II and III of the work statement.

2.3 Phase II (Ref: Appendix A; Section IB2)

The objective of Phase II of the general program concerned with the development of manufacturing methods for Improved Delay Lines, called for the development of a plan for an unbalanced pilot line to produce ceramic-mounted slow-wave structures made by vacuum evaporative, high temperature bonding, and photo-etching techniques.

The development of these techniques was the subject of Phase I of this program. In carrying out Phase II these techniques were expanded and modified as necessary to achieve the objective, i.e., establishing the capability of producing slow-wave structures at the rate of 10 per hour.

The proposed manufacturing facility has been designed to be entirely self-sufficient except for the manufacture of the ceramic cylinder substrates.

2.3.1 Breakdown of Final Process into Steps (Ref: Appendix A Section IB2b(a))

The operations involved in the development of a manufacturing process were those discussed in Section 2.2.11, organized into 25 distinct steps as follows:

Step	Description of Operation
1.	Beryllia cylinders received from vendor
2.	Pre-inspection cleaning
3.	Dimensional and visual inspection
4.	Pre-processing cleaning
5.	Braze to supporting structure
6.	Post-braze cleaning
7.	Ion bombardment
8.	Evaporation process
9.	Cooling to room temperature
10.	ID dimensional check
11.	ID surface polish
12.	ID dimensional final check
13.	Chemically clean prior to coating
14.	Plug input and output holes
15.	Photoresist-coat cylinder ID
16.	Dry and bake photoresist coating
17.	Position slow-wave structure flexible photographic negative with relation to the input and output holes
18.	Expose the negative and cylinder assembly to ultra-violet light
19.	Develop and dye the exposed photoresist image
20.	Touch-up developed photoresist image
21.	Post bake
22.	Mask
23.	Chemically etch the slow-wave structure pattern
24.	Strip the residual photoresist image
25.	Final clean cylinders
26.	Final inspection
27.	Ship to assembly area

Based on this list of steps, a block diagram showing the flow of materials during processing was prepared (see Figure 26. This diagram was then used as a basis for determining the best physical location of the various processing areas. These areas were laid out to provide a smooth flow of product from one area to the next, with a minimum of shuttling back and forth. Their physical layout or floor plan is shown in Figure 27.

2.3.2 Description of Equipment Required (Ref: Appendix A; Section Ib2b(b)(c)(d))

The following is a description of the processing equipment required to produce photo-etched slow wave structures on the interior surface of beryllia cylinders at a rate of 10 completed structures per hour. This equipment will be described step by step as was the processing in the preceding section. The estimated or actual cost of the tooling or equipment used is also given.

Step 1 - Beryllia Cylinders Received From Vendor

No processing equipment required.

Step 2 - Pre-inspection Cleaning

1	One gallon capacity ultrasonic cleaning machin	$ 1,000

Step 3 - Dimensional and Visual Equipment

2	1-inch micrometer	50
2	2-3 inch micrometer	100
2	Plug gages	50
2	Pin gages	25
1	Air gauge and accessories	400
1	Inmike	105
1	Toolmakers microscope	4,500
1	Pedestal dial indicator	75
1	Profilometer	2,000
1	Set gage blocks	1,200
1	Rotomicrometer	1,600
3	Binocular microscopes	1,800
1	Kocour Tester	600

Step 4 - Post Inspection Cleaning

1	Deetex vapor degreaser model 2D-500	550
6	100 gallon type 304 Stainless Steel Tanks with bottom drain, dara and legs	1,500

Step 5 - Braze to Supporting Structure

No additional equipment required.

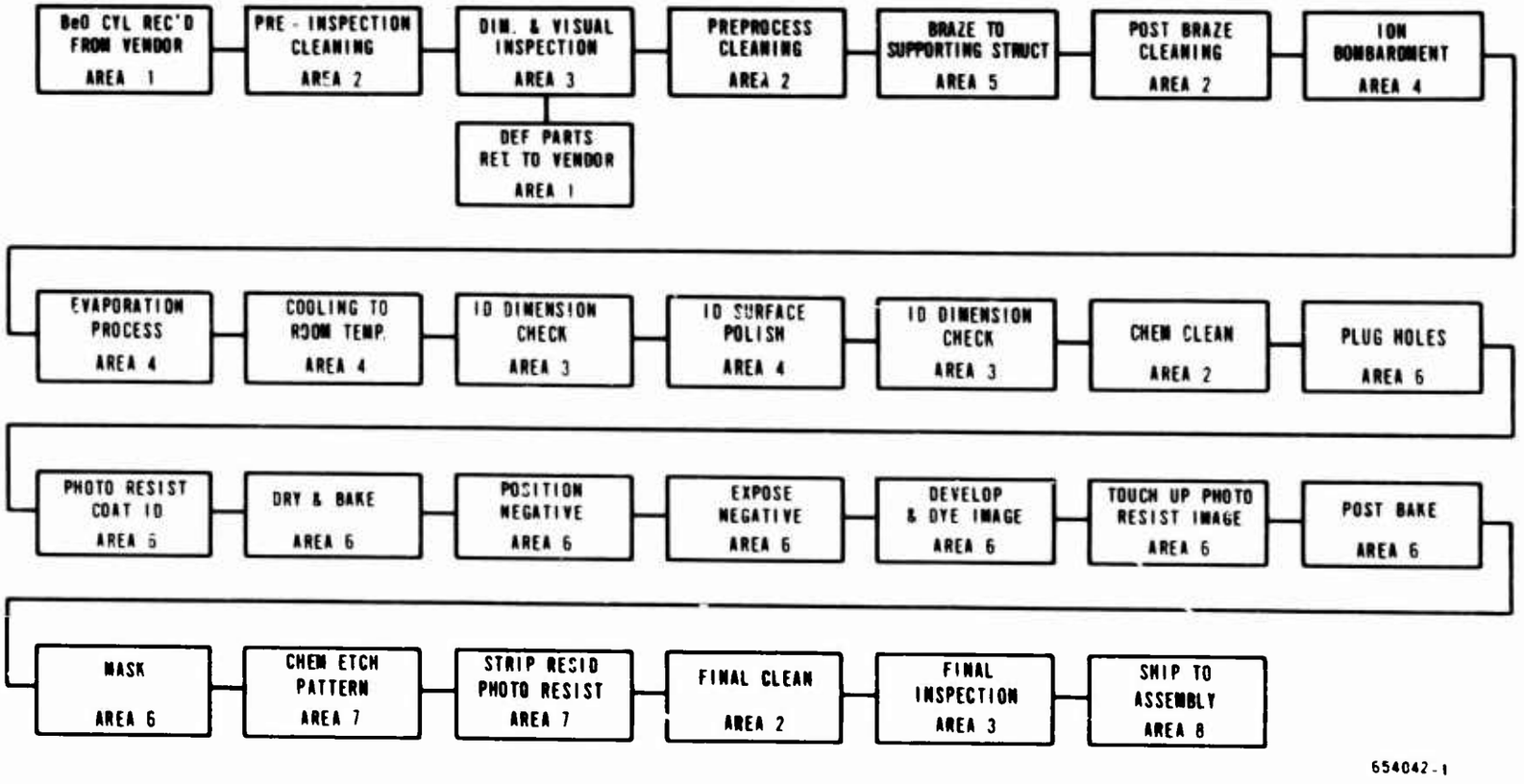

Figure 26. Flow of Material During Processing

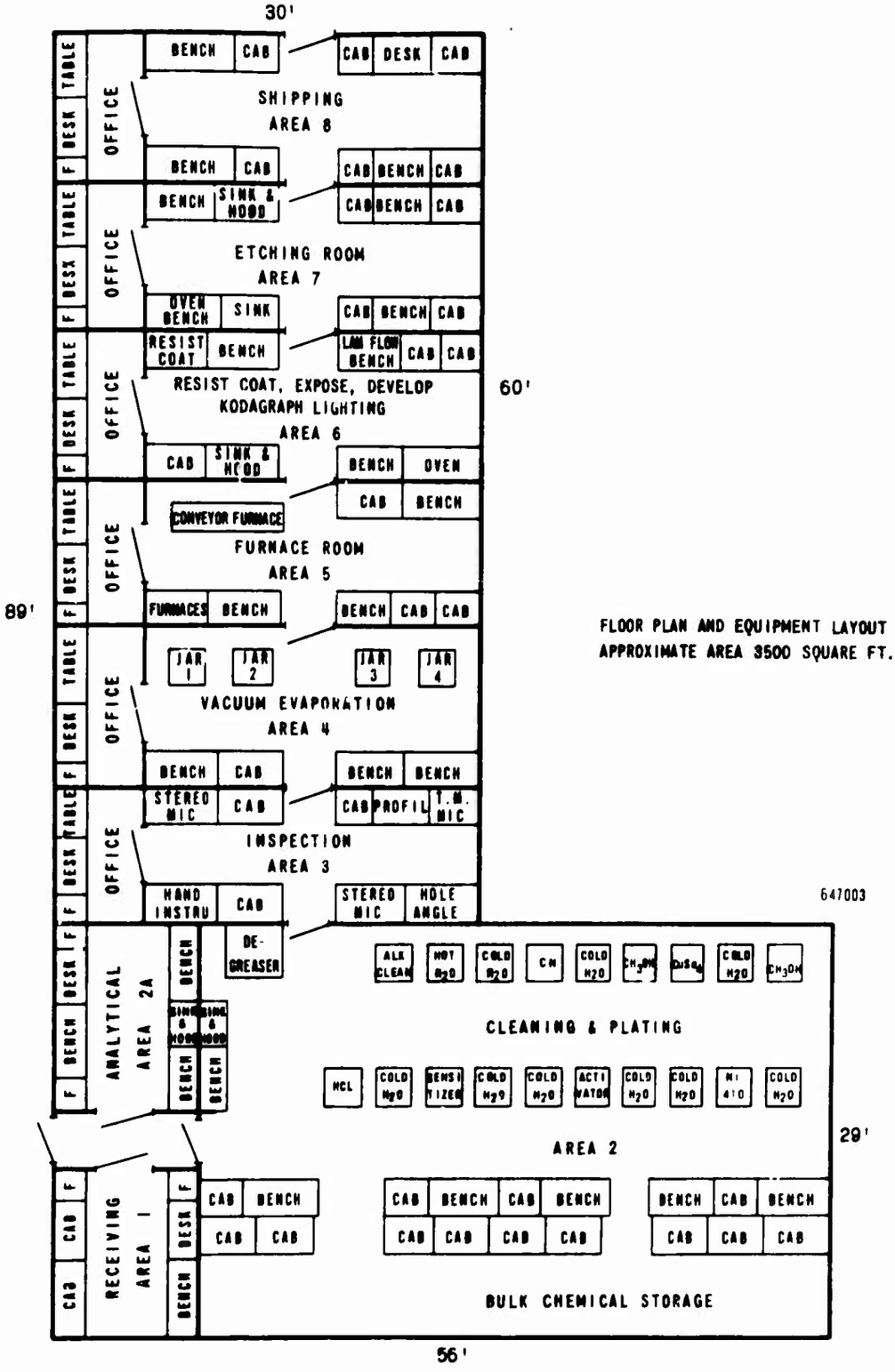

FLOOR PLAN AND EQUIPMENT LAYOUT
APPROXIMATE AREA 3500 SQUARE FT.

Figure 27. Slow-Wave Structure Manufacturing Facility

Step 6 - Post-Braze Cleaning

1	Sanogen Ultrasonic Cleaner	$ 600
6	100 gallon type 304 Stainless Steel Tanks with bottom drain, dara and legs	1,500

Step 7 - Vacuum Bakeout and Ion Bombardment

4	30-inch diameter vacuum bell jar stations complete with feed-through collar and necessary attachments	80,000
2	2000 volt - 400 ma power supplies	4,000
18	Low voltage ac power supplies, 15 volt, 200 ampere capacity	9,000

Step 8 - Evaporation Process

Same equipment as Step 7 is used.

Step 9 - Cooling to Room Temperature

Same equipment as Step 7 is used.

Step 10 - ID Dimensional Check

Measuring equipment described in Step 3 is used.

Step 11 - ID Surface Polish

2	Electrically driven polishing heads fitted with in-house designed and constructed chucks.	200

Step 12 - ID Dimensional Final Check

Measuring equipment described in Step 3 is used.

Step 13 - Chemically Clean Prior to Coating

Same equipment as Step 4 is used.

Step 14 - Plug Input and Output Holes

No special equipment is required to perform this operation.

Step 15 - Photoresist-Coat Cylinder ID

4	Specially designed and constructed motor driven rotators with cam-actuated stopping switches	1,000
1	Lamilar Flow Bench	1,200

Step 16 -	Dry and Bake Photoresist Coating	
1	Ventilated, thermostatically controlled electric oven. Blue M batch type 8 cu. ft	$ 500
Step 17 -	Position Slow-Wave Negative	
1	15x binocular microscope	600
Step 18 -	Expose Negative and Cylinder Assembly	
4	Specially designed and constructed pneumatic exposure device as described in Step 21 of procedure	900
Step 19 -	Develop and Dye Exposed Photoresist Image	
2	1 gallon capacity stainless steel tanks with removable covers	75
Step 20 -	Touch-up Developed Photoresist Image	
	Same equipment as Step 16 is used.	
Step 21 -	Post Bake - Same oven as Step 16 above	
Step 22 -	Mask	
	No special equipment required	
Step 23 -	Chemically Etch the Slow-Wave Pattern	
1	Chemcut Model 201 modified Spray Etching Machine, 9 gallon capacity	2, 500
Step 24 -	Strip the Residual Photoresist Image	
1	Stainless steel tank, 1 gallon capacity	38
Step 25 -	Final Clean Cylinders	
	Same equipment as Step 4 is used.	
Step 26 -	Final Inspection	
	Same equipment as Step 3 is used.	
Step 27 -	Ship to Assembly Area	
	No special equipment required.	

2.3.3 Recommended Production Rates (Ref: Appendix A; Section IB2b(b))

At many steps in the process there are operations where a large number of pieces can be handled and treated without difficulty and in a short time. Some of the operations, notably the vacuum deposition and electroplating steps, are either limited by the number of pieces that can be processed at a time, or by the length of time required to complete the operation.

The block diagram of Figure 28 gives the anticipated rates of production for each step in the process.

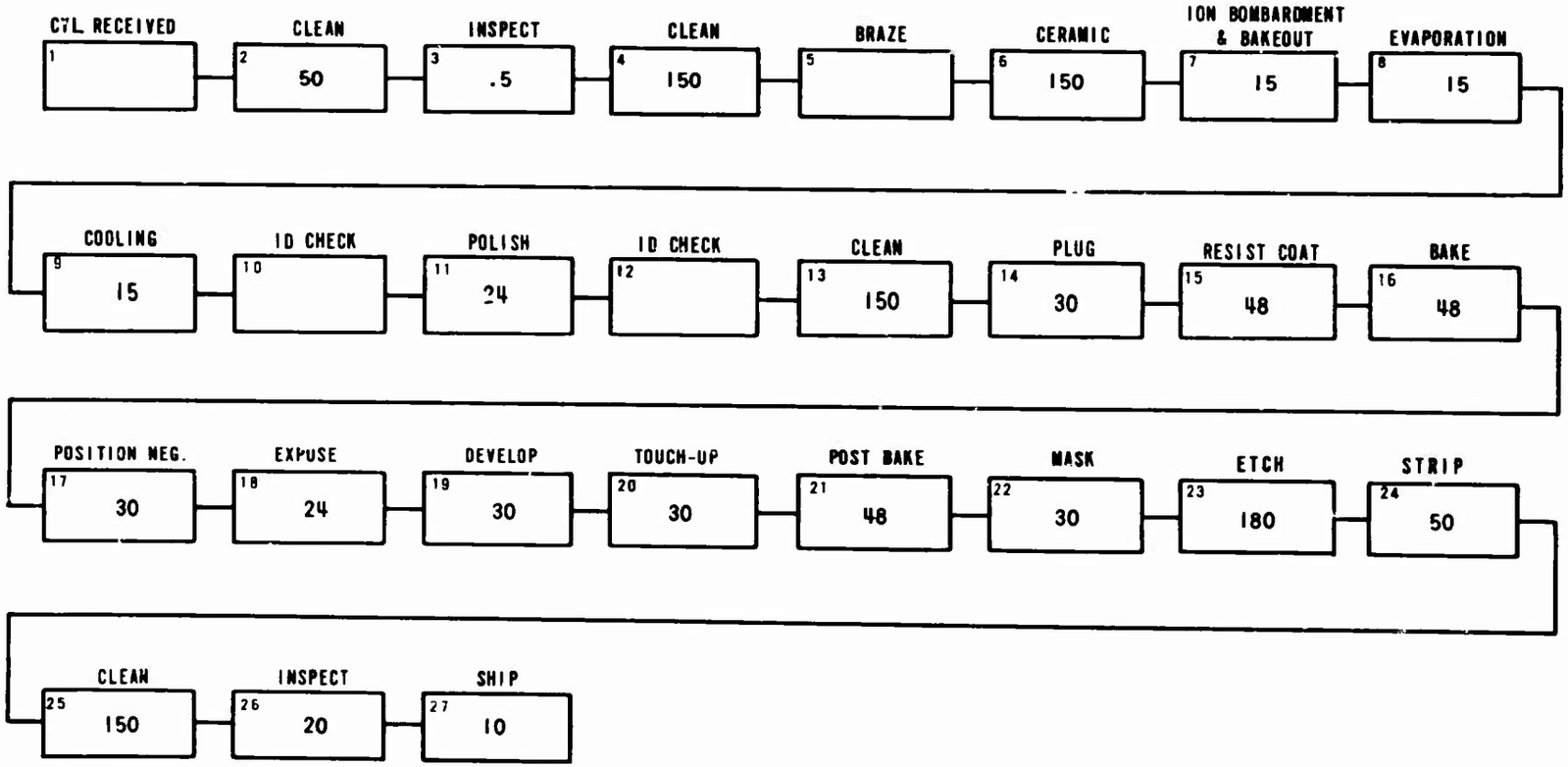

Figure 28. Anticipated Production Rates (Pieces Processed per Hour)

These rates are based on a number of factors, and to some extent are arbitrary, depending on the number of pieces it has been decided to handle in a batch. In order to explain, therefore, how the figures have been calculated, the following comments, presented step by step are given.

Step 2 - Cleaning

It is planned that the cylinders will be cleaned 25 at a time in a compartmentized wire mesh tray. The cleaning will consist of two washing cycles of 15 minutes each. This will be 30 minutes for the 25 pieces, or a 50 pieces/hour rate.

Step 3 - Inspection

This is a time-consuming process and cannot be on a 100% basis. As explained in the section under procedure, inspection will be based on a sampling plan as specified by the Quality Control Department. It is estimated that complete inspection of one cylinder will require 2 hours. This is a rate of 0.5 cylinders per hour.

Step 4 - Clean

As explained in the section on procedure, this will be a multi-tank line cleaning process. Ten minutes is estimated for traversing the line, with 25 pieces being handled at a time. This is a rate of 150 pieces per hour.

Step 5 - Braze to Supporting Structure

Since the braze is carried out in a continous belt furnace, the rate is governed by the number of brazing jigs available.

Step 6 - Post-Brazing Cleaning

Ten anode assemblies will be processed at one time. This process consists of positioning 10 assemblies on a fixture and running them through the post braze cleaning cycle as previously described.

Step 7 - Vacuum Bakeout and Ion Bombardment

Steps 7, 8, and 9 must be considered as one operation, since all are performed on one batch of six fixtures (four units/fixture) at a time. The total time required may be broken down as follows:

Step 7 (including pumpdown time)	25 minutes
Step 8	120 minutes
Step 9	25 minutes
Total Time Required	2 hours 50 minutes

Since two stations will be in operation, each providing for six fixtures holding four units per fixture (for a total of 24 hours per station) the total output will be 48 units during the 2 hours 50 minutes. This results in a rate of 15 units per hour.

During this operation six groups of four anode assemblies will be mounted in the vacuum chamber and baked out at 375° C. Following this the anodes will be exposed to ion bombardment for 10 minutes at a pressure of 200 microns.

Ten separate power supplies will provide the power to each of the five groups involving two sources apiece. Five additional power systems will supply the heat for the bakeout ovens. One more power supply will be required at each station to provide the power for the "glow discharge".

Each group will consist of four beryllia cylinders clamped together as shown in Figure 29.

Step 8 - Evaporation Process

See Step 7.

Step 9 - Cooling to Room Temperature

See Step 7.

Step 10 - ID Check

This check will be made on a statistical basis. No rate estimated.

Step 11 - Polish

As explained in the section on procedure, this operation will use a motor-driven polishing head with a quick-operating chuck that will hold the cylinder securely. The polishing time will be 5 minutes per cylinder and two machines will be used. This is a rate of 24 cylinders per hour.

Step 12 - ID Check

Same as Step 10.

Step 13 - Clean

Same as Step 4.

Step 14 - Plug Holes

This will be accomplished by the use of molded rubber tapered pins. Estimated time per hole is 1 minute; two holes per cylinder. This is 1 cylinder per 2 minutes, which is 30 cylinders per hour.

Step 15 - Resist Coat

A bank of 4 rotators will be used. Speed of rotation is 1 rpm. This means that the machines can be loaded one after another. By the time No. 4 has been loaded, No. 1 may be unloaded. Therefore, it is estimated that 4 cylinders can be coated every 5 minutes. This is a rate of 48 cylinders per hour.

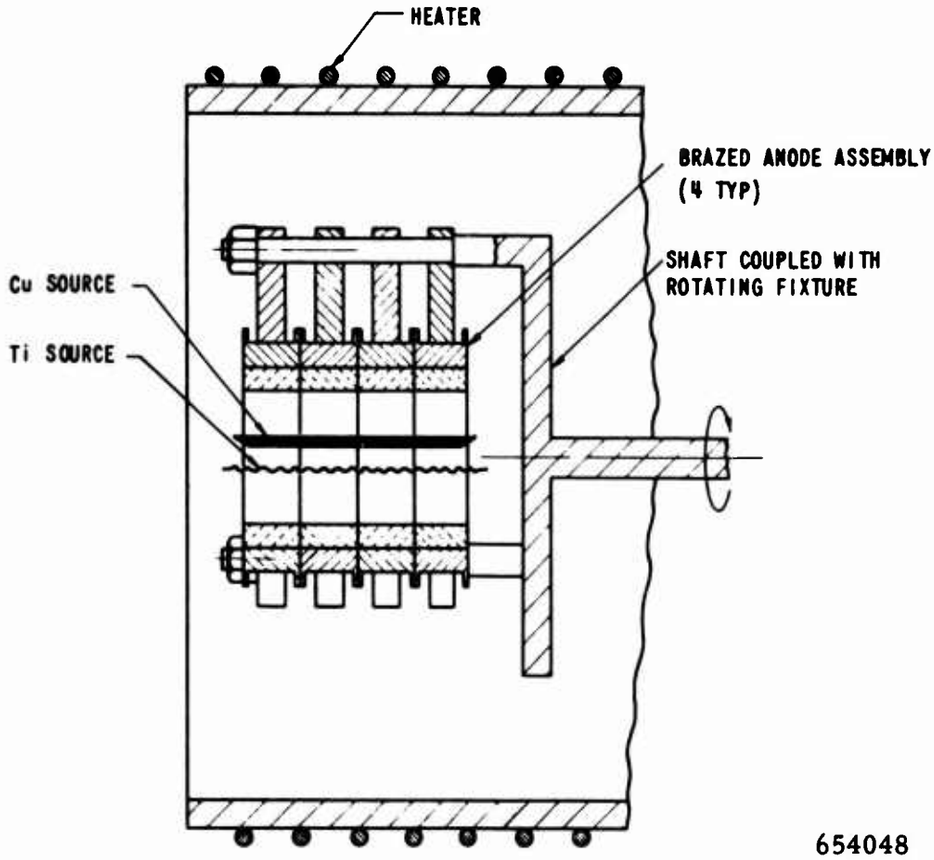

Figure 29. Evaporation Set-Up
(6 per vacuum station)

Step 16 - Bake

This is a batch oven drying process. All can be dried at once. Rate, therefore, is as above, 48 per hour.

Step 17 - Position Negative

This is a critical operation. It is doubtful if it can be jigged because of variations in the hole location. It is estimated that 2 minutes will be required to perform this operation. This is a rate of 30 pieces per hour.

Step 18 - Expose

This operation uses 4 exposure devices. These will be loaded and started one after another in sequence. The exposure time is 10 minutes. By the time the last unit is loaded it will be only a short wait until the first is complete. Effectively, then, 4 cylinders will be exposed every 10 minutes. This is a rate of 24 pieces per hour.

Step 19 - Develop

This is a short operation; 10 seconds in developer, 5 seconds in dye, 30 seconds in water rinse, and 15 seconds quick dry. This is a 1 minute total. To insure prime image quality, it is judged best to process one cylinder at a time. This will probably result in a rate of 30 pieces per hour.

Step 20 - Touch-Up

As explained in the procedure, image defects must be corrected. Because of the random nature of these defects, it is difficult to assign an average time for their repair. It is estimated that 2 minutes should be allowed per cylinder. This is a rate of 30 pieces per hour.

Step 21 - Post Bake

Same as Step 16.

Step 22 - Masking

Masking is a hand process estimated to take 5 min per cylinder.

Step 23 - Etch

It is estimated that 30 pieces can be etched at a time in a horizontal spray etch machine, and that a turn-around time of 10 minutes will be required. This is a rate of 180 pieces per hour.

Step 24 - Strip

This will be a batch-type operation that can handle a large quantity because it is noncritical. A stainless steel compartmented tray will be used to handle 25 cylinders at a time. The sequence will be a short soak of 1 minute in the photoresist stripper solution, followed by individual handling and thorough scrubbing of each piece to insure removal of the photoresist particles. The total cleaning time is estimated at 30 minutes for 25 pieces, or 50 pieces per hour.

Step 25 - Clean

This will be at the same rate as Step 4, 150 pieces per hour.

Step 26 - Inspection

This step performed by vendor.

This will be a visual inspection only, for obvious physical defects. It is estimated that 3 minutes will be required per cylinder on a 100% inspection basis. This is a rate of 20 pieces per hour.

Step 27 - Ship of Assembly

This final step will be accomplished at a rate of 10 pieces per hour.

2.3.4 Proposed Quality Assurance Program (Methods)
(Ref: Appendix A; Section IB2b(d))

2.3.4.1 Introduction

The inspection equipment used in the manufacture of the slow-wave structures on this program was detailed in Section 2.3.2 of this report. A quality control plan was established to insure compliance with the contractual and specification requirements of this program.

2.3.4.2 Purpose

The major objective of this QC plan is to minimize fabrication imperfections which may result in degradation of reliability from the design capability. This is accomplished through an extensive schedule of prime parts and assembly inspection, material control and traceability, and special tests to detect and eliminate potential failure modes resulting from manufacturing variations. The individual steps are described in Sections 2.2.11 and 2.3.3 of this report.

2.3.4.3 Quality Assurance Provisions

The QA activities detailed herein are performed by the organizational responsibilities indicated. The Tube Operation Quality Assurance Manager is responsible for audit and review to assure performance consistent with the provisions of this section:

Index to Quality Assurance Provisions

a. Drawing and Change Control
b. Measuring and Testing Equipment
c. Purchased Material Control
d. Raw Material Inspection
e. Tools and Parts Inspection
f. In-Process Inspection
g. Material Review
h. Failure Analysis
i. Special Processes

a. Drawings and Change Control

Drawings and specifications for materials, prime parts, assemblies, and processes are prepared and distributed by the Mechanical Design and Drafting Department. This department is responsible for maintenance of up-to-date specification books and for coordination of all initial issues and changes with the concerned activities.

During the Design and Development phases, temporary and/or permanent changes will be authorized by Engineering and reviewed by QC Engineering and Reliability. All such changes will channel through the Mechanical Design and Drafting Department which is the custodian of the master drawings and is responsible for change records. Controlled use of sepia reproducibles eliminates the need for marked prints, expedites changes, and provides the historical records necessary in a development program.

Prior to Production phase, complete final design specifications will have been resolved. These specifications are subject to Engineering Change Notice (ECN) control.

No drawing which is under ECN control shall be redrawn, retraced, added to, changed, corrected or otherwise revised unless such revision is authorized by an approved ECN. QC Engineering/Reliability must approve all ECN's prior to the drawing's becoming effective.

b. Measuring and Testing Equipment

Instrumentation Engineering is responsible for selection, maintenance, and adequacy review of all testing equipment. Quality Control is responsible for similar review of inspection equipment.

Equipment calibration is performed by the cognizant Quality Assurance Department (Standards Laboratory for test equipment, Precision for measuring equipment), utilizing Automatic Call-In in accordance with Gage Control Manual B-1 (Mechanical) and A-23, Procedure for the Calibration and Certification of Electrical Test Equipment.

Maintenance and repair of such equipment, as required, is performed by Quality Assurance Electronic Maintenance (electrical equipment) and Precision Inspection (mechanical equipment). After repairs, the equipment is recalibrated as necessary.

c. Purchases Material Control

The Purchasing Department is responsible for the preparation and issuance of purchase orders for the procurement of parts and material. Vendors are selected and purchase orders are issued issued in accordance with the Raytheon Corporate Purchasing Manual and with Power Tube Procedure "Purchase of Subcontracted Material". QA reviews all purchase orders and materials and effects necessary liaison with vendors.

The vendor section of QC Engineering reviews vendor performance as indicated by the Vendor Rating and inspection results on received material, and initiates, through Purchasing, corrective action liaison, as necessary.

New vendors, whose rating is not established, are surveyed, as required, to evaluate performance capability. Such surveys are coordinated by Purchasing, with participation by QA and other cognizant technical personnel.

d. Raw Material Inspection

All raw material is segregated and held in the Raw Material Storage area. Samples for mechanical inspection are delivered to the Inspection Department for the required inspection. The Inspection Department then cuts further samples and delivers these to the Metallurgical Laboratory where the required analysis is performed.

Both Mechanical and Metallurgical inspections are performed in accordance with the applicable Purchase Specification and QC Procedures.

If the material is acceptable, it is stamped, tagged, or otherwise documented and is placed in a storage area under a controlled inventory system.

Nonconforming material is subject to material review. (See paragraph 2. 3. 4. 3g below).

e. Tools and Parts

All completed prime parts and tools, whether purchased outside or fabricated within Power Tube, are inspected routinely by the Inspection Department using sampling plans specified in MIL-STD-105, or as otherwise specified in an Inspection Procedure.

QC Engineering specifies the method of inspection to be used. For a part to be acceptable, every characteristic of the part must be within the specified limits. Non-conformance parts are subjected to material review.

Inspection status is indicated by the use of tags, stamps, or other controlling documentation either directly on the part or on its container as applicable.

f. In-Process Inspection

Engineering and Quality Control jointly determined the points at which In-Process Inspection shall be performed. The basis for this determination includes consideration of the effect of passing defective material to the next step, the likelihood of detection and correction potential at further steps in the process, and other considerations.

During the Production phase, QC Engineering will prepare, issue, and maintain a formal Inspection Schedule with detailed inspection procedures for the points so determined.

As in the case of raw material and parts inspection, parts are identified as to status, and non-conforming material is subject to material review.

g. Material Review

Nonconforming parts, assemblies and other material are held by the Inspection Department in a segregated area pending review and disposition.

Project Engineering will review all non-conforming material and recommend disposition, i. e., scrap, rework or accept "as-is",

Final disposition of every non-conformance requires further review and approval by QC. Any non-conformance disposition to accept must be of such a nature that it will not affect performance, reliability or interchangeability of the end item and that it will not result in violation of any contractual requirements.

Acceptance of non-conforming material will require written notation as to why it is accepted.

The QC Engineer will be responsible for initiating corrective action investigations to prevent recurrence of discrepant material. He will assign items for corrective action to responsible departments (e. g., Purchasing, Engineering, Manufacturing, etc.). Responsible departments will comply with such requests within one week, or as otherwise specified.

h. Failure Analysis

Performance evaluation and scrap analysis of failures is a basic analytical technique used in the Microwave Tube Operation.

Every failure will be analyzed by Engineering to the extent necessary, and results will be reviewed with Quality Assurance Reliability Engineering to determine the cause of such failure and the nature of indicated corrective action, if any.

QC Engineering is responsible for coordination and follow-up to assure that indicated corrective action is implemented and effective.

i. Special Processes

Special processes such as cleaning, plating, brazing, coating, etc, are detailed by Engineering in the form of a process specification. These specifications are controlled and maintained by the Mechanical Design and Drafting Department. QC Engineering audits their use in the various areas.

2.3.5 Conclusions Phase II

Section 2.2.10 of this report forms a final process specification for the manufacture of C and Ku-band slow-wave structures. All lines manufactured for Phase III of this program were fabricated using these process and inspection procedures.

Methods of duplicating equipment so that the rate of 10 C-band slow-wave structures per hour were described in Section 2.3.3.

The equipment and cost of equipment have been detailed. in Section 2.3.2.

2.4 Phase III (Ref: Appendix A, Section IB3a)

2.4.1 Equipment (Ref: Appendix A, Section Ib3b1)

A minimum quantity of machinery and test equipment of the type described in Section 2.3.2 of the report was set up and slow-wave structures were manufactured.

2.4.2 Quality Control (Ref: Appendix A, Section IB3b2)

The quality control plan as described in Section 2.3.4 of this report was utilized for this phase of the work. Figures 30 and 31 are samples of the quality control documentation on the C-band slow-wave structure manufactured during this phase of the work.

2.4.3 Fabrication of Slow-Wave Structures (Ref: Appendix A, Section IB3b3)

A total of 36 circular C-band slow-wave structures and 5 K-band slow-wave structures were manufactured during this phase of the work.

2.4.3.1 Problems

Utilizing the manufacturing method described in Section 2.2.10 of this report, the following problems were encountered and resolved:

a. Bonding Problems

The first 12 slow-wave structures fabricated utilized the cupurous oxide bond described in Section 2.2.5.7 of this report. Although satisfactory bonds were obtained using this technique, and two slow-wave structures were utilized in test vehicles A-4 and A-5, the yield was extremely poor due to bond failures. The major reason for the poor yield was due to the difficulty in controlling the process used to achieve this type of bond. A TiO_x-Cu bond was developed and is described in detail in Section 2.2.5.8 of this report. There was no bond failure on the remainder of the slow-wave structures fabricated using this type of bond.

Cylinder No. 141 Date 6/9/67

Operation No.	Description of Operation	Inspection Points	Acc	Rej	Remarks
	Preinspection Cleaning of Beryllia Cylinder				
	Incoming Inspection	ID. 1.7998	✓		
	Post-Inspection Clean	Visual	✓		
	Copper Cylinder to Beryllia Cylinder Braze	Mechanical Leak Detector	✓		
	Cleaning	Visual	✓		
	Vacuum Bakeout - 375°C (Bell Jar)				V = 260v I = 6 amps 375°C 15 minutes
	Ion Bombardment Cleaning				V = 1000 Pressure 50 microns
	Evaporation Process				Titanium evaporation temperature of 1325°C 2 1/2 minutes titanium and copper evaporated 1 minute together, copper then evaporated for 1 1/2 hours to reach needed thickness
	Cooling to Room Temperature				
	ID Dimensional Inspection	Mechanical	✓		ID 1.7998
	ID Polish	Visual	✓		
	ID Dimensional Inspection	Mechanical	✓		ID 1.7954
	Cylinder Inspection	Visual Adherence	✓		
	Plug Holes	Visual	✓		
	Photo-Resist Coating	Visual	✓		
	Bakeout				Time 1 hour Temperature 46°C
	Negative Positioning				
	Negative-to-Cylinder Pressure Jig				
	Ultra-violet Light Exposure				Time 8 minutes
	Photo-Resist Development	Visual	✓		
	Post-Bake				Time 15 minutes Temperature 46°C
	Chemical Etch	Visual	✓		
	Resist Strip	Visual	✓		
	Final Process Inspection a. Line Quality b. Adherence	Visual Mechanical	✓		
	Clean	Visual	✓		
	Cylinder Output Assembly	Leak Detector Initial Cold Test	✓		
	Center Conductor Assembly	Visual Cold Test	✓		

Comments:

Figure 30 Quality Control Log - QK1329 - Cylinder No. 141

Cylinder No. 118 Date 5/25/67

Operation No.	Description of Operation	Inspection Points	Acc	Rej	Remarks
	Preinspection Cleaning of Beryllia Cylinder				
	Incoming Inspection	ID 1.7997	✓		
	Post-Inspection Clean	Visual	✓		
	Copper Cylinder to Beryllia Cylinder Braze	Mechanical Leak Detector	✓		
	Cleaning	Visual	✓		
	Vacuum Bakeout - 375°C (Bell Jar)				V = 260 I = 6 amps 375°C 15 minutes
	Ion Bombardment Cleaning				V = 1000 Pressure 50 microns
	Evaporation Process				Titanium evaporation temperature of 1325°C 2 1/2 minutes titanium and copper evaporated together for 1 minute, then copper was evaporated for 1 1/2 hours to reach needed thickness of 2 1/2 mils
	Cooling to Room Temperature				
	ID Dimensional Inspection	Mechanical	✓		ID 1.7997
	ID Polish	Visual	✓		
	ID Dimensional Inspection	Mechanical	✓		ID 1.7952
	Cylinder Inspection	Visual Adherence	✓		
	Plug Holes	Visual		✓	noticed crack in cylinder while plugging holes due to expansion
	Photo-Resist Coating	Visual			
	Bakeout				Time Temperature
	Negative Positioning				
	Negative-to-Cylinder Pressure Jig				
	Ultra-violet Light Exposure				Time
	Photo-Resist Development	Visual			
	Post-Bake				Time Temperature
	Chemical Etch	Visual			
	Resist Strip	Visual			
	Final Process Inspection a. Line Quality b. Adherence	Visual Mechanical			
	Clean	Visual			
	Cylinder Output Assembly	Leak Detector Initial Cold Test			
	Center Conductor Assembly	Visual Cold Test			

Comments:

Figure 31. Quality Control Log - QK1329 - Cylinder No. 118

b. Cracking of Beryllia Ceramic

The beryllia cylinders for this program were initially received from two vendors, National Beryllia and Consolidated Ceramics. During the manufacture of the slow-wave structures cracking was observed in the beryllia cylinders during the initial ceramic-to-copper braze and upon reheating at the photo-etch station. Investigation showed that only the National Beryllia cylinders were cracking. Both vendors were given identical specifications but it appears that the Consolidated Ceramics cylinders passed at greater tensile strength.

At this time all the remaining National Beryllia cylinders were scrapped and replacements were ordered from Consolidated Ceramics. No further evidence of cracking was observed.

c. Connection of the Output Center Conductor to the First Delay Line Finger

One of the most difficult problems encountered in this program was the connection of the center conductor of the output coaxial to the delay line. This problem and its solution is fully discussed under Section 2. 5 of this report dealing with the evaluation of test vehicles.

d. Output Ceramic Mismatch

The coaxial output and input of the tube have ceramic seals which provide a vacuum seal. Several of the first group of slow-wave structures manufactured during this phase of the work were found to have a high VSWR at cold test. Investigation of this problem revealed that the coaxial output ceramic seal was marginal in design. A new ceramic seal was developed and new parts were ordered. Subsequent slow-wave structures evaluated with this new design showed no trouble with high VSWR.

2. 4. 3. 2 Results

As a result of the above problems only 15 slow-wave structures were manufactured successfully and completely evaluated during the program. All design and processing changes have been incorporated in the final process specification given in Section 2. 2. 10 of this report.

2.4.4 Evaluation of Slow-Wave Structures (Ref: Appendix A, Section IB3b4)

2.4.4.1 Circular C-Band Slow-Wave Structures

Fifteen circular C-band slow-wave structures were electrically evaluated during the course of this program. The values of VSWR and insertion of 11 of these structures are given in Figures 32 through 42. Data on the other 4 structures are given in Sections 2.5.2 and 2.5.4, since these structures were used in Test Vehicles A-4, A-5, A-6 and A-8.

A value of 30% voltage reflection is generally considered as an acceptable level for use in a tube. While some of the structures shown exceed this value, it was felt that the data should be included for comparison purposes.

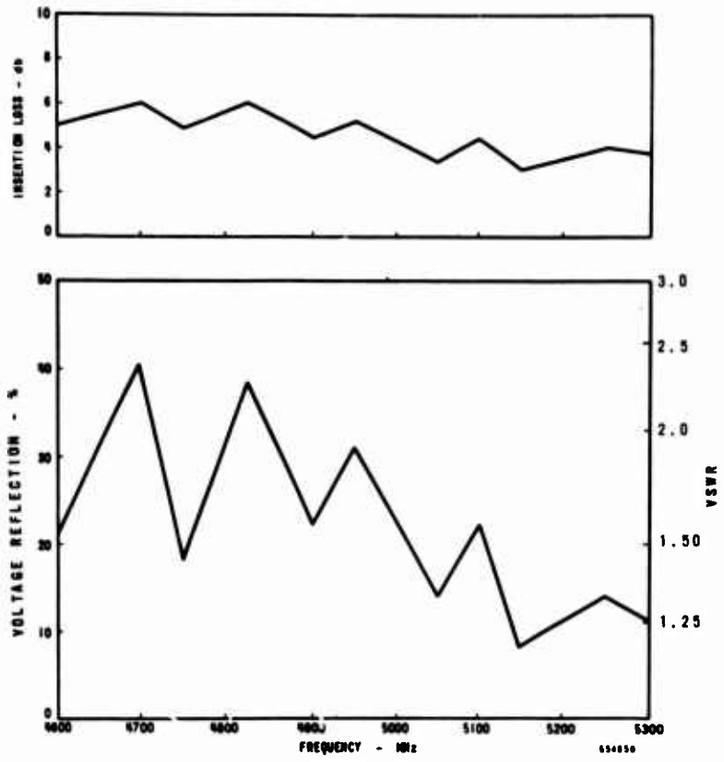

Figure 32. QK1329 Circular C-Band SWS Serial No. C-139 Insertion Loss and VSWR

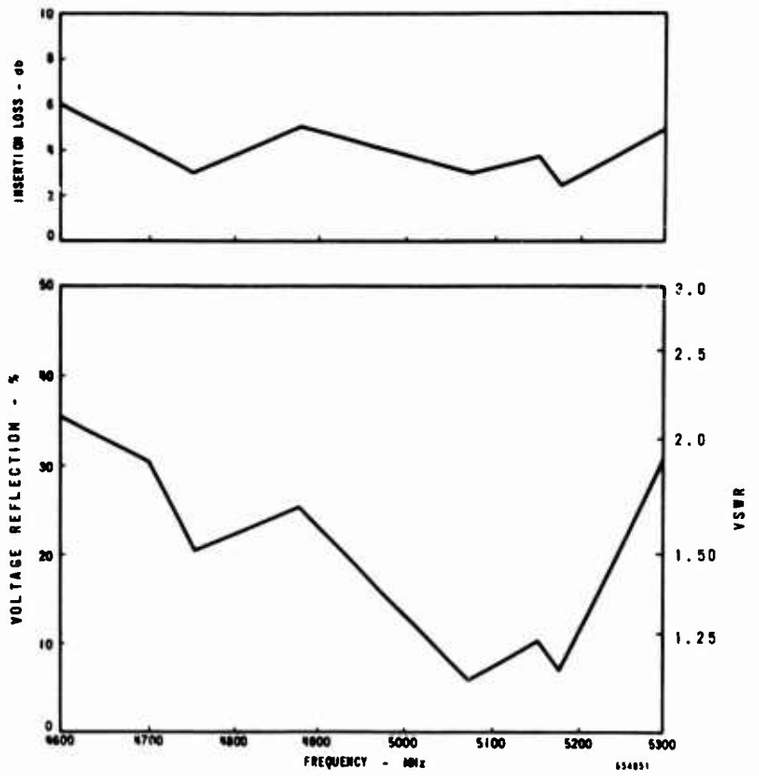

Figure 33. QK1329 Circular C-Band SWS Serial No. C-140 Insertion Loss and VSWR

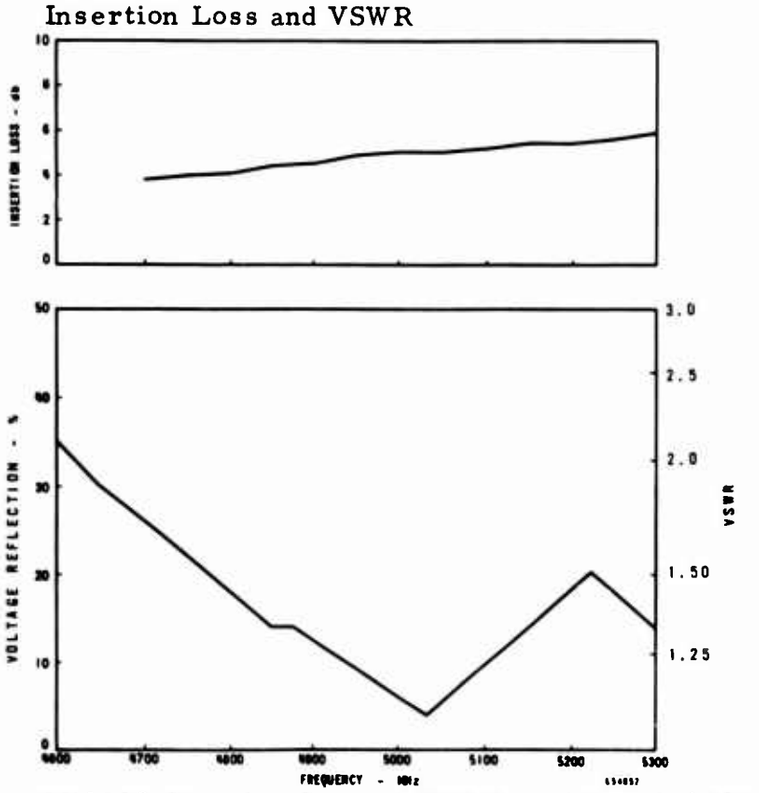

Figure 34. QK1329 Circular C-Band SWS Serial No. C-140R Insertion Loss and VSWR

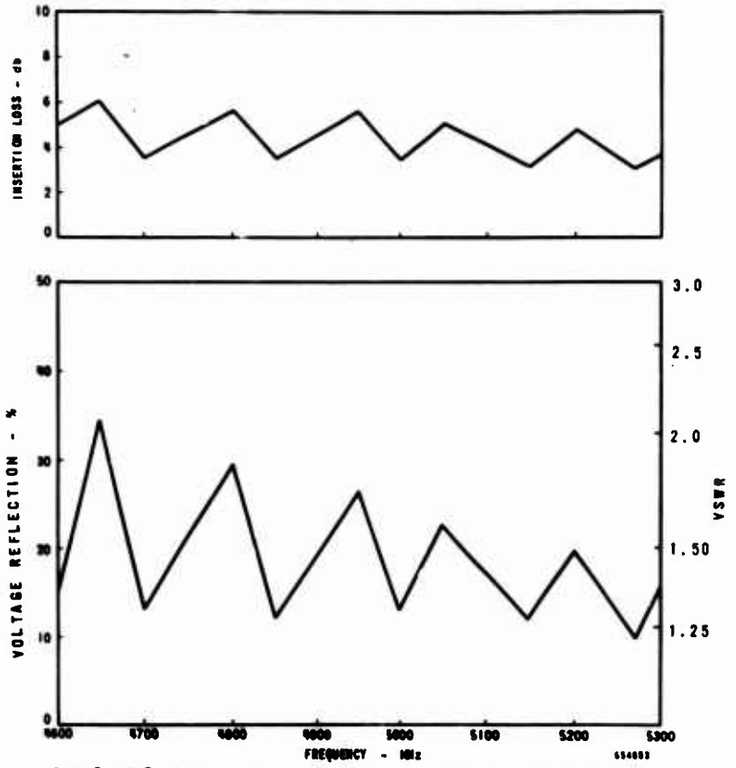

Figure 35. QK1329 Circular C-Band SWS Serial No. C-141 Insertion Loss and VSWR

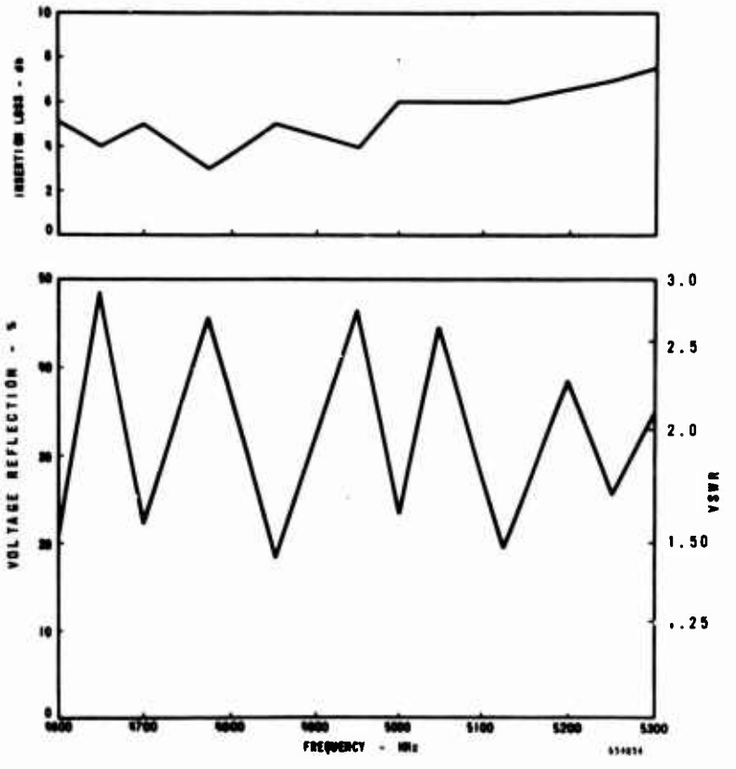

Figure 36. QK1329 Circular C-Band SWS Serial No. C-142 Insertion Loss and VSWR

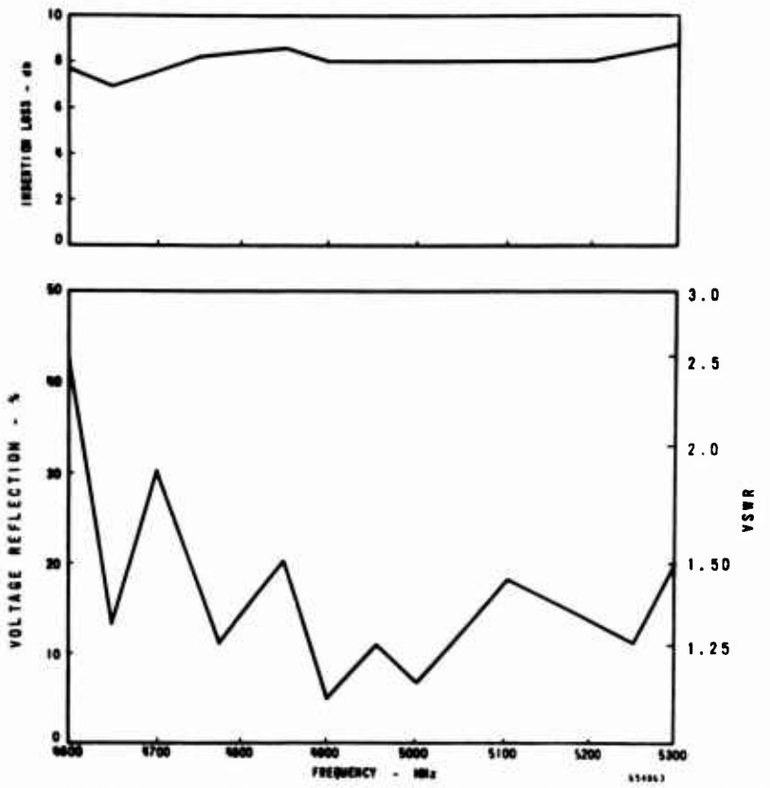

Figure 37. QK1329 Circular C-Band SWS Serial No. C-142R Insertion Loss and VSWR

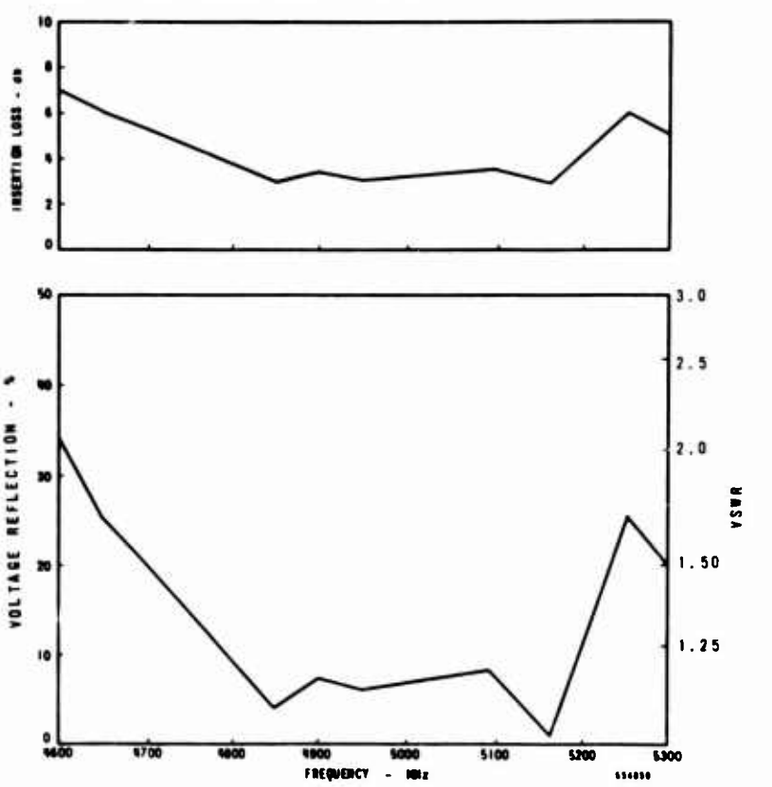

Figure 38. QK1329 Circular C-Band SWS Serial No. C-143 Insertion Loss and VSWR

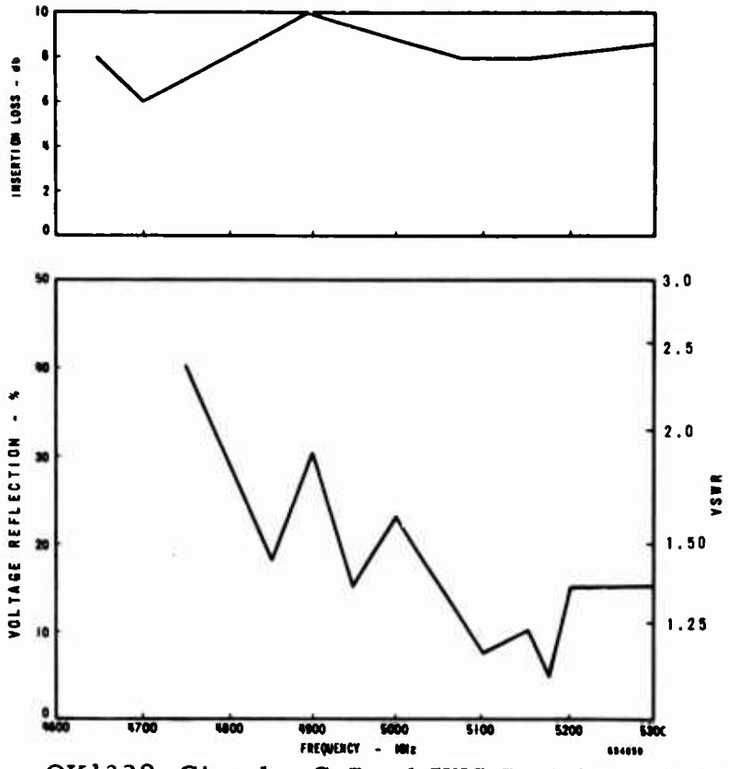

Figure 39. QK1329 Circular C-Band SWS Serial No. C-144 Insertion Loss and VSWR

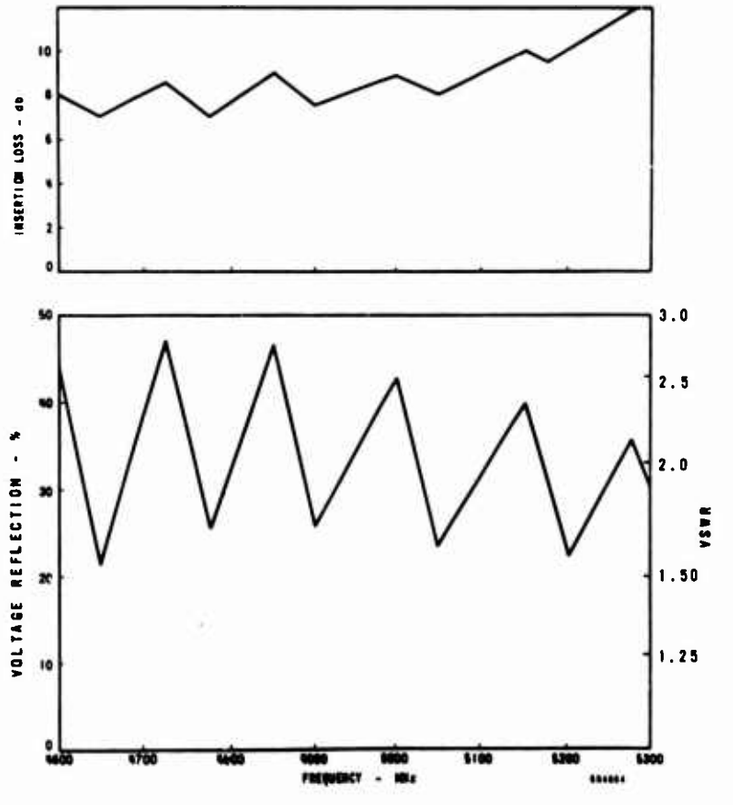

Figure 40. QK1329 Circular C-Band SWS Serial No. C-146 Insertion Loss and VSWR

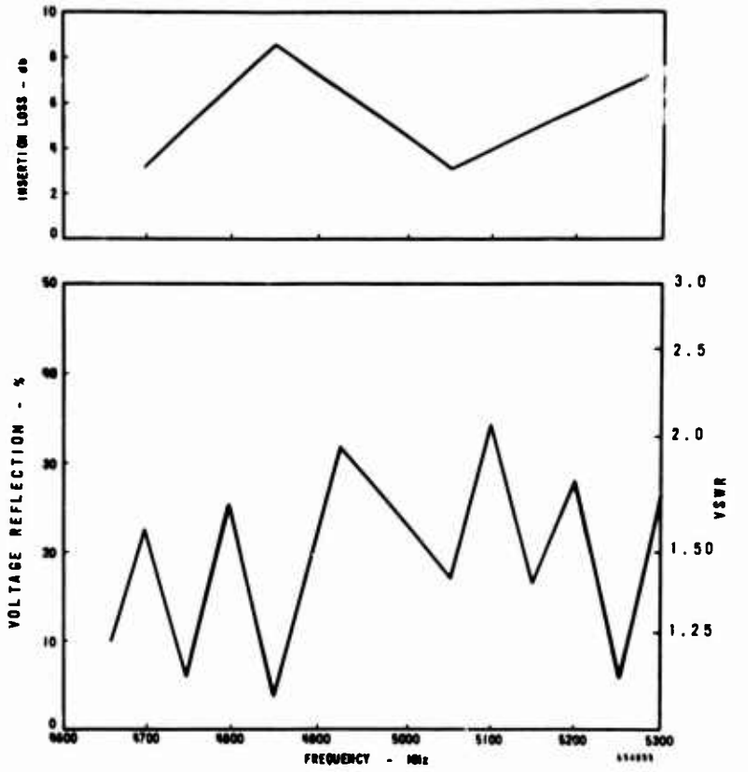

Figure 41. QK1329 Circular C-Band SWS Serial No. C-147R Insertion Loss and VSWR

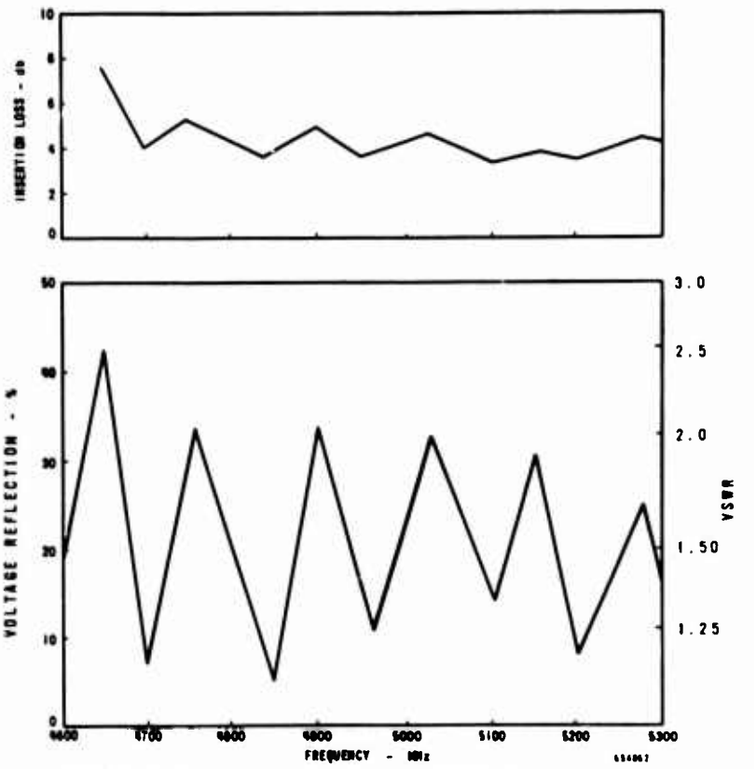

Figure 42. QK1329 Circular C-Band SWS Serial No. C-149R Insertion Loss and VSWR

2.4.4.2 K-Band Linear Slow-Wave Structures

To prove the feasibility of using the photocopy technique for manufacture of slow-wave structures at higher frequencies, an evaluation program was conducted of a structure designed to operate over a band around 14000 MHz.

The dimensions of the structure were as follows:

Finger length	0.0708 in.
Pitch	0.0107 in.
No. of pitches	100
Substrate of material	beryllia

Five of these lines were fabricated using the same technique and process as used on the circular C-band slow-wave structures; one of these lines is shown in Figure 43.

First a dispersion curve of the structure was taken by the resonance method using a segment of 30 pitches. The resulting curve is shown in Figure 44. It should be noted that the agreement with the theoretical values obtained by using the parallel plate approximation is within the range one would expect.

The problem of selecting the method for evaluation of the complete structure was one of presenting the final results in a manner that would be most meaningful and useful. It was decided that no useful purpose would be served by devoting the time and funding to develop an rf match in K-band waveguide to the slow-wave structure. It was decided instead to feed the rf through 50-ohm coaxial output, and through a quarter-wave transformer to the slow-wave structure. Although the rf match to the structure was poor, particularly since the commercially available coaxial to waveguide transitions necessary to adapt to the rf oscillator are quite poor in themselves, it was felt that measurements could be made by taking the insertion loss of the components of the system and subtracting these from the total system measurements.

This was applied to five different K- band lines and the results, shown in Figure 45, indicate that one could expect insertion losses of the order of 6 to 8 db. This is well within what one would expect for successful operation at the frequency.

The insertion loss measured was taken on a line of 100 pitches, which is probably more than would be needed for an actual operating tube. This, of course, is dependent upon the operating voltages and currents required.

While there will be an effect on tube efficiency, as estimate of the resultant decrease of efficiency is difficult without experimental data at this frequency, since most of the tube power is generated early in the delay line.

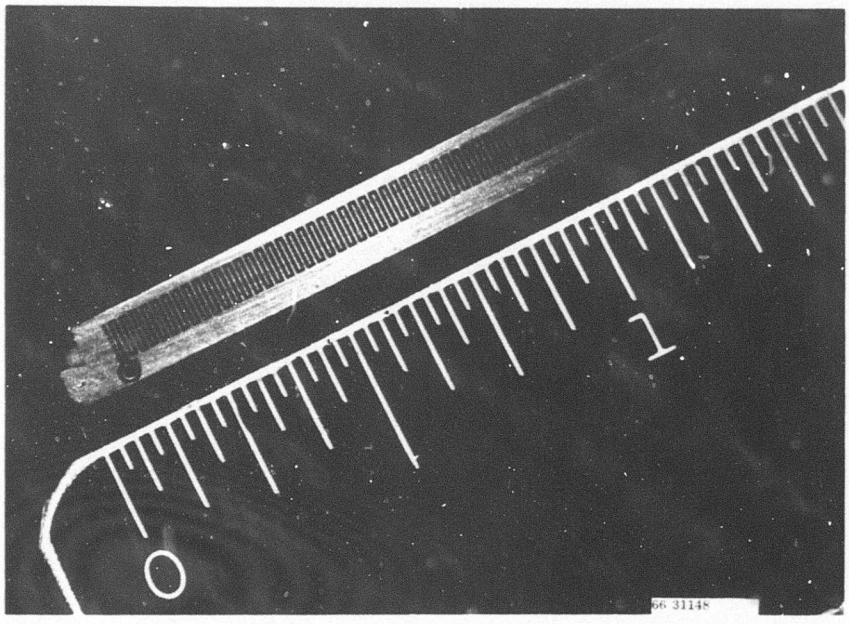

Figure 43. K-Band Linear Slow-Wave Structure

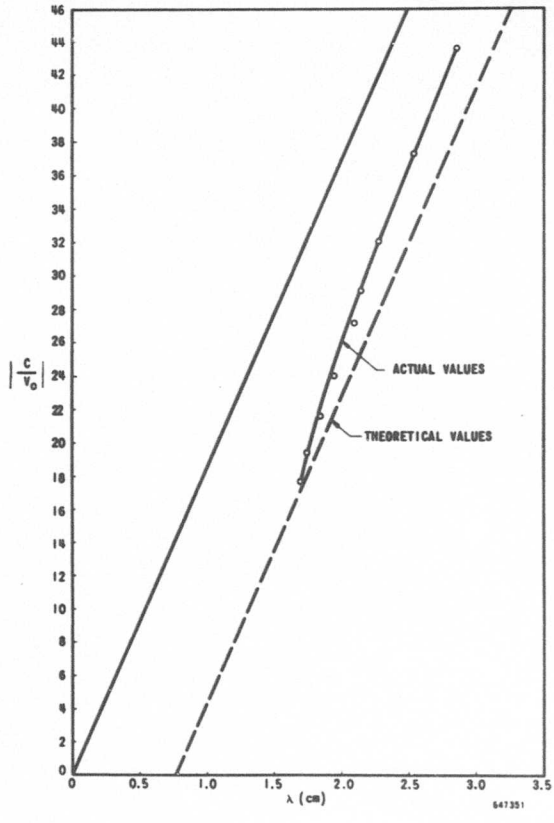

Figure 44. Dispersion Curve K-Band Linear SWS on Beryllia Substrate

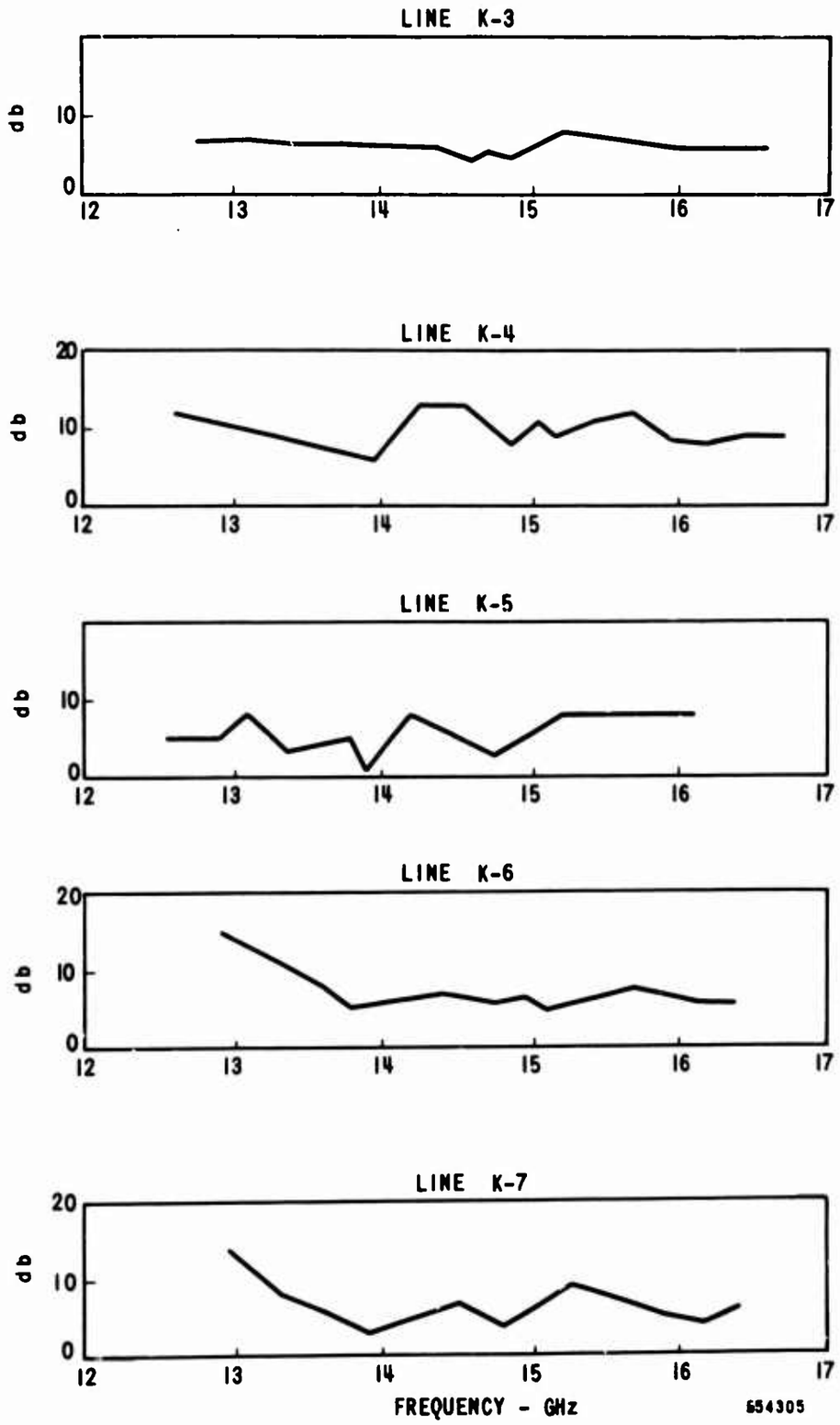

Figure 45. Insertion Loss Measurements on 5 K-Band SWS

2.4.4.3 Environmental Evaluation of C-Band Slow-Wave Structures

Six of the circular C-band slow-wave structures manufactured during this phase of the work were subjected to 20g vibration of the frequency range 50 to 2000 cycles. Examination and electrical spot test of these structures showed no adverse effects due to vibration or heat cycling.

2.5 Construction and Evaluation of Test Vehicles (Ref: Appendix A, Section IB3b(5)(6))

2.5.1 Early Test Vehicles

The first three test vehicles for circular C-band slow-wave structures were actually constructed during Phase I, using the initial manufacturing techniques described in Section 2.2.4. Detailed discussion of these evaluations was delayed until now to provide better report continuity.

2.5.1.1 Test Vehicle No. A-1

This tube was sealed in, but, during the cooling cycle after bakeout, a leak developed in the cylinder-to-output heliarc weld. The tube was removed from the pump; the leak was located; and the tube was baked out again. Again the leak appeared during the final stages of the cooling cycle, but it was small enough to repair without removing the tube from the pump. Cold test measurements indicated that the delay line had not been damaged by the repeated thermal cycling. Figure 46 is a plot of the VSWR of the seal-in.

Upon initial test the cathode proved to be inactive, probably attributable to the leak which occurred during bakeout. After several hours of aging, however, the cathode recovered sufficiently to allow anode currents of 70 to 80 mA to be obtained. Efforts to draw more current resulted in the appearance of current on the accelerator. The accelerator current caused gas in the tube, which in turn resulted in an internal arc, thus shutting down the power supply.

The tube was operated over the band with the limited anode current available with very encouraging results. Figure 47 shows a curve of power output vs frequency; the maximum anode current obtainable is noted for each test point. From the data, it would appear that, were the full beam current available, the tube would successfully meet the minimum power output requirement.

After approximately 24 hours of operation, the tube failed because of apparent excess arcing between the sole and anode. Analysis revealed that the first portion of the line had been destroyed over a distance of 10 to 15 pitches. At the time it was felt that local overheating of the delay line had caused the bond to fail, or that possibly the failure was due to the leak in the tube during bakeout, which is done in a reducing atmosphere and which had allowed the forming gas to reduce the oxide in the bond. The actual cause of failure was later determined to be the etchant attaching the CuO_x bond region. A further discussion of this is given in Section 2.2.5.7.

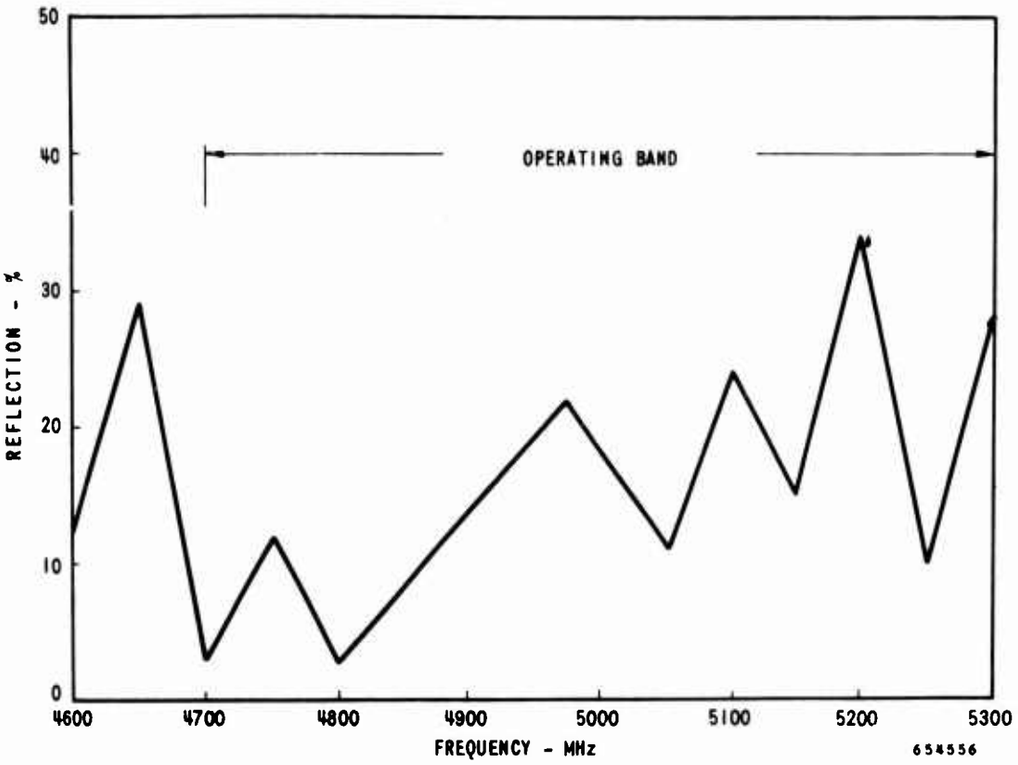

Figure 46. QKA1329 Test Vehicle No. A-1 VSWR

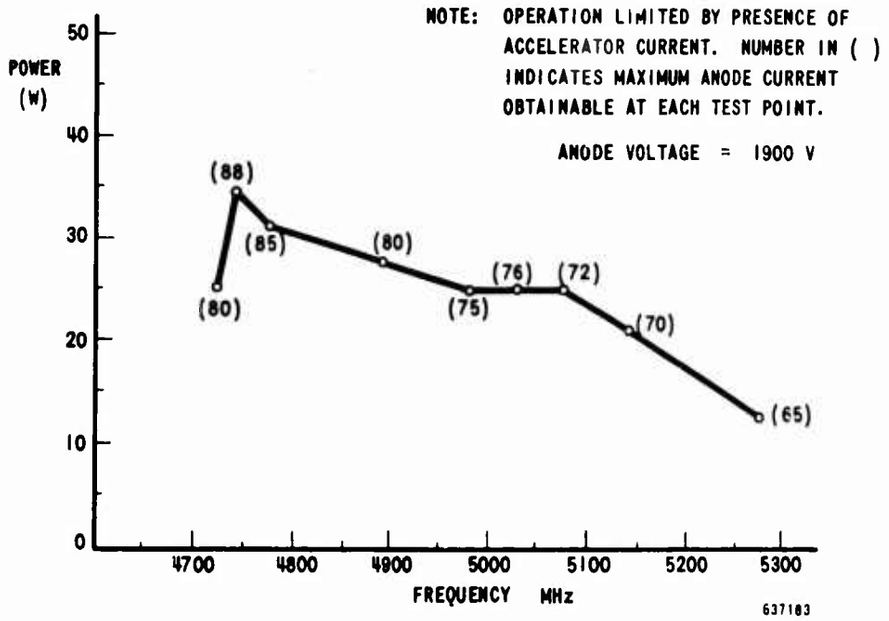

Figure 47. QKA1329 Test Vehicle No. A-1 Power vs Frequency Sole-Tuned Operation

Although failure of the bond caused the tube to fail prematurely, the results obtained were quite encouraging with regard to tube efficiency. Of particular importance is the absence of deleterious effects due to sputtering. Careful analysis of the delay line showed no visible evidence of any deposition on the delay line of copper from the sole, and the interference patterns due to the alumina coating on the sole were clearly visible, indicating that the film was still intact.

2.5.1.2 Test Vehicle No. A-2

This tube was constructed in an attempt to solve a problem in the electron gun in test vheicle no. A-1. In tube no. A-1, the cathode was set underflush to the sole element by 0.010 in because of space considerations in the electron gun area. In a conventional tube, the anode wall is relieved behind the electron gun to allow clearance for the accelerator positioning. In tube no. A-1 however, the anode backwall, whick is actually the ceramic substrate, could not be relieved because of strength requirements. To permit the required clearance, and to allow use of a conventional accelerator structure, the cathode in no. A-1 was positioned below the sole. It was felt that the optics could be matched by adjusting the grid voltage.

After operation of tube no. A-1 however, it was found that the beam actually intercepted the accelerator, causing excessive accelerator current. Since the calculations of the trojectories do not normally take into account the effect of the grid field, the calculations did not predict that this would happen.

Because of this, tube no. A-2 was built with the accelerator structure so modified that the cathode structure could be raised flush with the sole and grid, thus lessening the effect of the grid field on the beam trajectories. This eliminated the beam interception.

Figure 48 shows the VSWR and insertion loss of this seal-in.

The tube developed a leak during bakeout in the ceramic-to-metal seal in the input header. Attempts to repair the leak were unsuccessful and the tube was scrapped.

2.5.1.3 Test Vehicle No. A-3

This tube was sealed in with the same type of electron gun as used in tube no. A-2. The tube was processed normally with no unusual incidents. Because of the failure of the delay line in the first tube, it was decided that the initial testing of this tube would be done under pulsed conditions using a pulse width of 1 ms at a 10% duty cycle. Once the optimum operation was achieved under pulsed conditions, the tube would then be operated under the cw mode. Figure 49 shows the VSWR and insertion loss of this seal-in.

There was no evidence of accelerator current at peak currents up to 300 mA, so the gun modification appears to be satisfactory. The tube was prone to arcing, however, and had to be aged occasionally during operation. A performance curve taken under these conditions is shown in Figure 50.

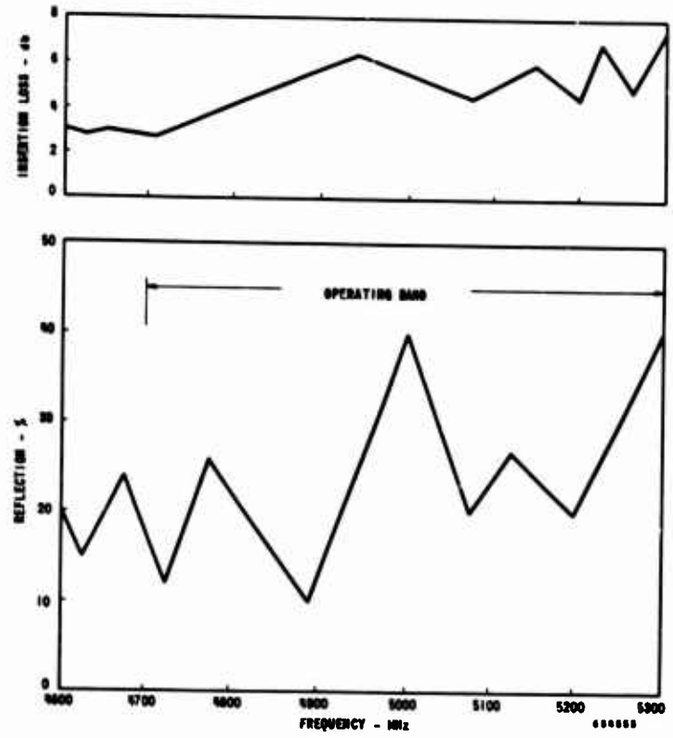

Figure 48. QKA1329 Test Vehicle No. A-2 Insertion Loss and VSWR

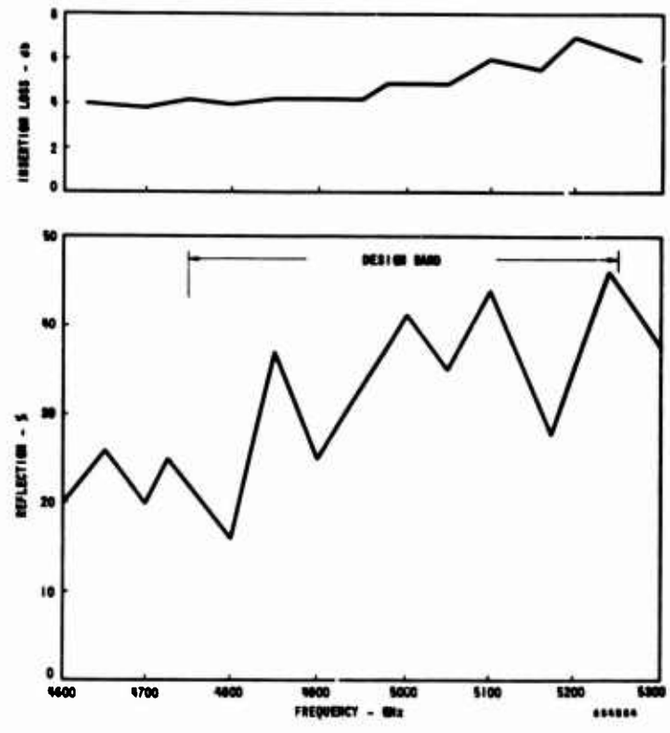

Figure 49. QKA1329 Test Vehicle No. A-3 Insertion Loss and VSWR

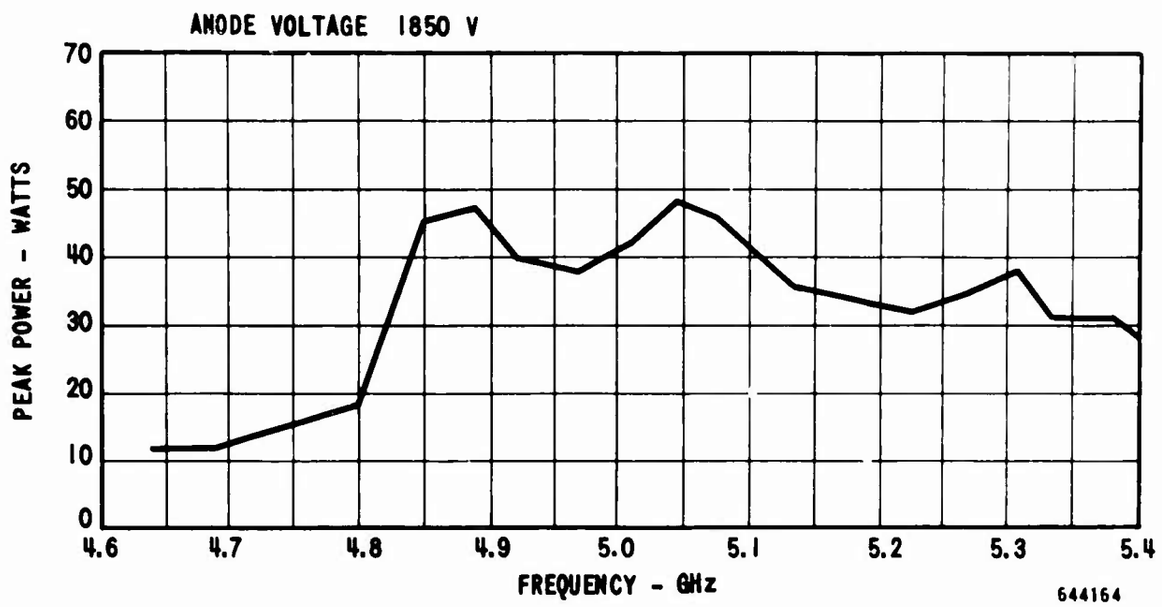

Figure 50. QK1329 Test Vehicle A-3 Power vs Frequency
Pulsed Operation 10% Duty Cycle

After approximately 30 hours of operation under pulsed conditions, the tube was operated under cw conditions. The tube showed a great tendency to arc and failed after 2 or 3 hours as a result of a sole-to-anode short circuit. Analysis showed that the bond had failed, causing the delay line to short to the sole.

It was deduced that arcing was probably caused by initial lifting of a portion of the line, with unusually heavy arcing the result.

This failure could not be attributed to a leak in the tube, and at this point, construction of tubes was halted pending a full investigation of the bond failure. This is discussed in detail in Section 2.2.4.7.

An analysis of the tube operation at this time, however, showed that the use of photodeposited short-wave structure in M-BWO's had great promise. Tube efficiency, particularly in the initial tube, was quite good. Sputtering to date has not presented any problems up to 24 hours of operation. The cause of the failure of the bond was determined and corrected and is not expected to cause problems in future tubes. The electron gun problem encountered in the first tube was corrected, and no evidence of accelerator current was encountered well above the rated operating current. The objectives of Phase I, i.e., the demonstration of the feasibility of the use of photodeposited slow-wave structure as a practical device in electron tubes, were essentially accomplished.

2.5.2 First Test Vehicle in Phase III

During this last phase of the work, seven test vehicles were constructed using the photodeposited slow-wave structures produced by the method described in Section 2.2.11. The first of these was designed QKA1329 serial no. A-4.

In the previous seal-ins (QKA1329 No. A-1, A-2 and A-3) the center conductor was brazed into the hole in the ceramic cylinder. However a great deal of difficulty was experienced in cracking of the ceramic cylinders during the initial braze or at subsequent processing operation. To avoid this problem, QKA1329 no. A-4 featured a gallium copper connection between the output center conductor and the first finger of the delay line.

The VSWR and insertion loss of the tube is shown in Figure 51.

This tube was processed and operated under pulse conditions at a 10% duty cycle and a pulse width of 1 millisecond for a period of 18 hours. A performance chart showing the operation obtained is included as Figure 52.

The tube failed after 18 hours of operation due to failures of both a connection between the rf coaxial output center conductor and the delay line, and also a similar point between the external attenuator and the slow-wave structure, which caused vaporization of the point material.

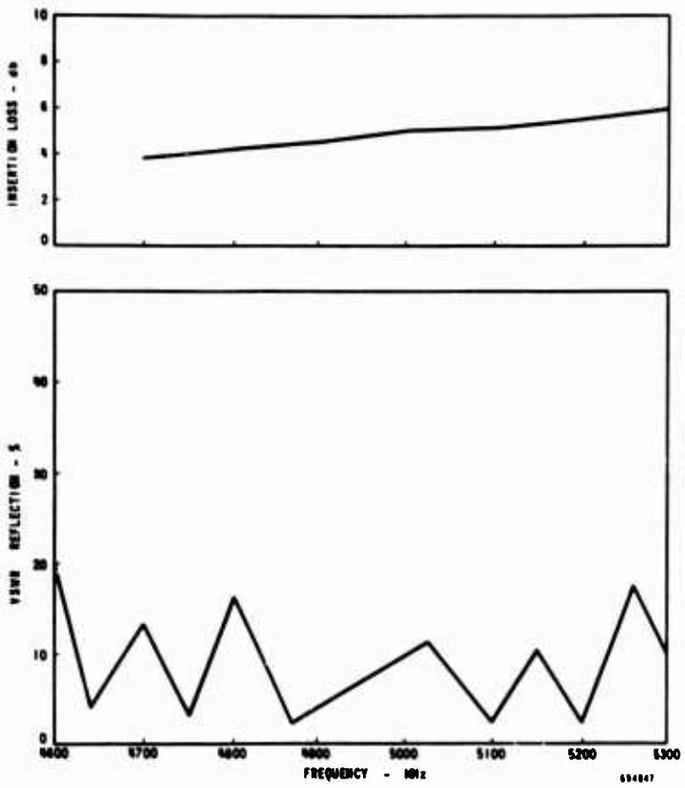

Figure 51. QK1329 Test Vehicle No. A-4 Circular C-Band SWS Serial No. C-108 Insertion Loss and VSWR

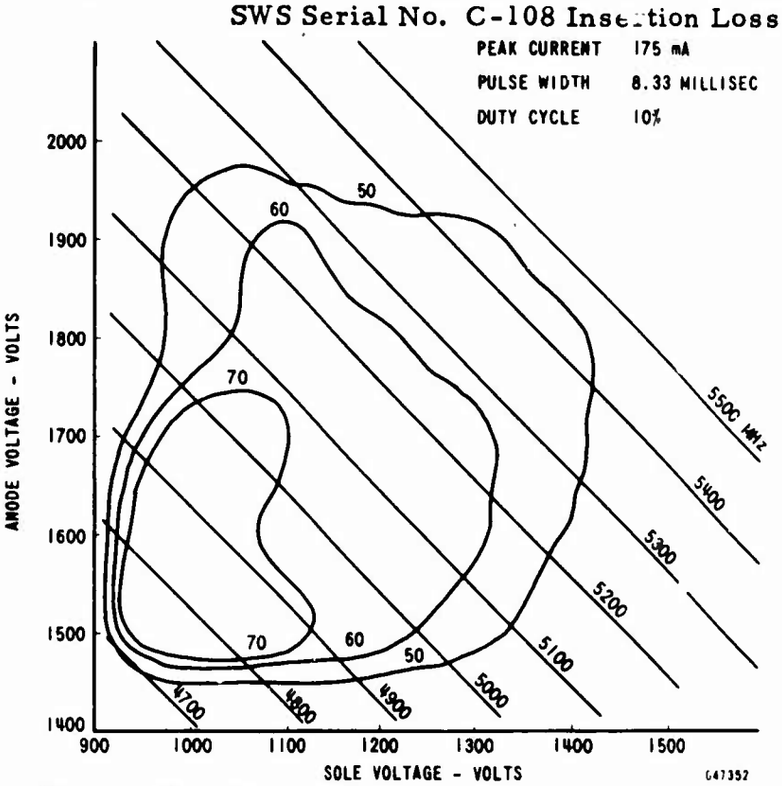

Figure 52. QKA1329 Serial No. A-4 Performance Chart Pulsed Operation

The first indication of failure was a slow decrease in the output power of the tube. The tube was cold tested and its characteristics were found to have changed considerably. Although the rf match was still good, the lack of ripple in the curve indicated the line was heavily attenuated. The external attenuator had no effect and was presumed to be open. There was no evidence of the arcing condition usually associated with a failure of the bond between the slow-wave structure and the ceramic substrate.

In an effort to remove whatever was attenuating the rf signal, a cw current of 200 mA was applied to the tube, for approximately 1 hour. When no change in the output power was noted, the test was terminated and the tube was scrap-analyzed.

Scrap analysis revealed that the gallium copper material used in connecting the center conductors to the first and last finger had melted at the attenuator connection and deposited over the delay line causing the high attenuation. The delay line itself was still intact and firmly bonded to the ceramic substrate.

2.5.3 Study of Output Connection

As a result of the failure of A-4 an investigation was undertaken in an attempt to improve the connection between the center conductor and first finger of the slow-wave structure.

2.5.3.1 Design of Output Finger

The first or output finger of the delay line is 0.015 in. wide; the diameter of the center conductor is 0.018 to 0.020 in. A new first finger design was evolved which did not adversely effect the VSWR or tube operation. The first finger was widened to 0.075 in. A sketch of the old and new output finger design is shown in Figure 53.

This wide finger design allowed for a more practical method of connecting the center conductor of the output coax.

2.5.3.2 Electron Beam Welding

The most practical method of connecting the output finger at this time was electron beam welding.

Simulated test assemblies were prepared and a number of sample welds were made and analyzed to determine the welding parameters and the best method.

Both copper and phosnic were used for center conductor of the coax.

Early experiments using the 0.015 in. output finger and various center conductors were extremely difficult to control and it was felt that the wider finger was the best solution.

Experimental center conductors were made with both a flattened end and a clipped end as shown in Figure 54.

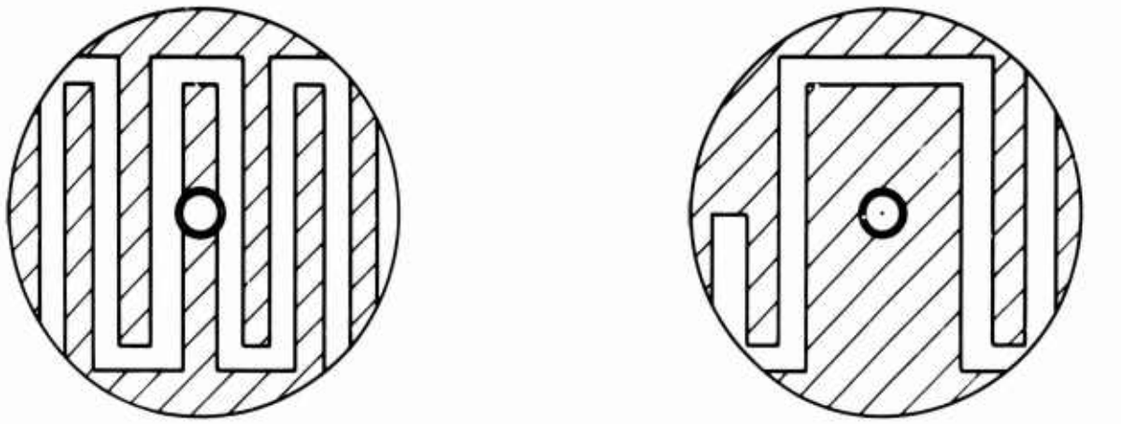

a. NARROW FINGER
TYPICAL ETCHED PATTERN

b. WIDE FINGER
TYPICAL ETCHED PATTERN

FIGURE 53. Output Finger Design

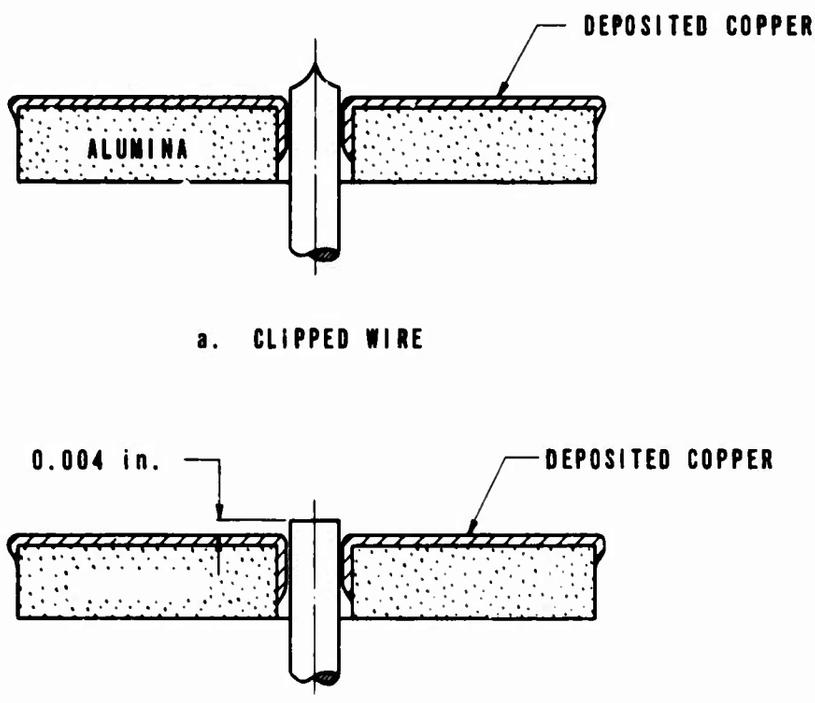

a. CLIPPED WIRE

b. FLATTENED WIRE

648951
SHEET 1

FIGURE 54. Center Conductor - Output Finger Design

Photographs of the wide finger experimental welds are shown in Figure 55.

The first weld made in an actual assembly required adjustment of the electron beam to a higher level; the weld on the wide finger was easily made and looked very good.

2.5.3.3 Split Wire Connection

In the last test vehicle sealed in as the program, tube no. A-10, the center conductor connection was fabricated in the following manner:

the 0.015 in. diameter copper wire is split and positioned as shown in Figure 56.

The tabs measure approximately 0.004 in. thereby providing a better weld situation than previously encountered (0.004 in. thick copper strip to 0.0025 in. metallized layer).

2.5.4 Later Test Vehicles in Phase III

2.5.4.1 QKA1329 No. A-5

Tube No. A-5 was sealed in and processed. The VSWR and insertion loss of this tube is shown in Figure 57. This was the first tube to feature electron beam welding of the input and output connection and the TiO_x-Cu bond described in Section 2.2.5.8 of this report.

During the construction of the tube, it was noted that a portion of the deposited film had lifted from the ceramic during the final cleaning operation. The portion lifted was well away from the active line, and was mechanically removed prior to construction of the tube.

After bakeout, during a routine resistance check between all elements, a low resistance was noted between the anode and the accelerator. This was removed by arcing the tube and the tube was set up for operation.

After a few minutes of oscillation under pulse conditions, the accelerator again shorted to the anode. The short was once more burned out, but again returned after a short period of operation.

Finally it was impossible to remove the short and the tube was opened for failure analysis. This showed that the copper film had lifted behind the accelerator, causing the short circuit to the anode. The delay line itself, however, was still intact.

It was felt that the mechanical stresses set up by physically cutting and removing the film from the damaged area were such that, even though the remaining edge appeared firmly bonded, it was not, and the thermal effects of bakeout and operation were sufficient to cause the film to peel back and short to the accelerator.

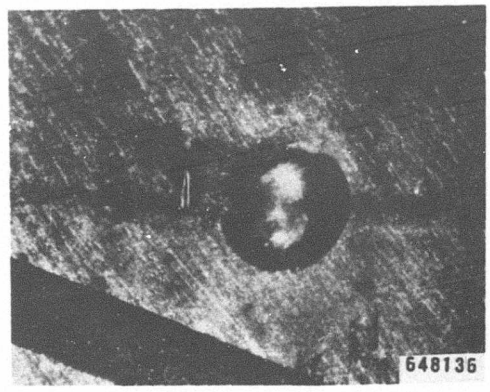

a. Wide Finger - Phosnic Wire Clipped

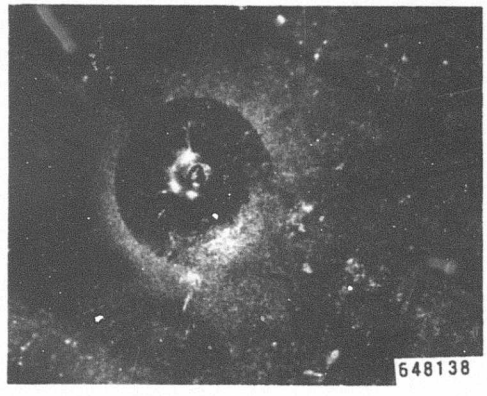

b. Wide Finger - Phosnic Wire (Gold Plated) Clipped

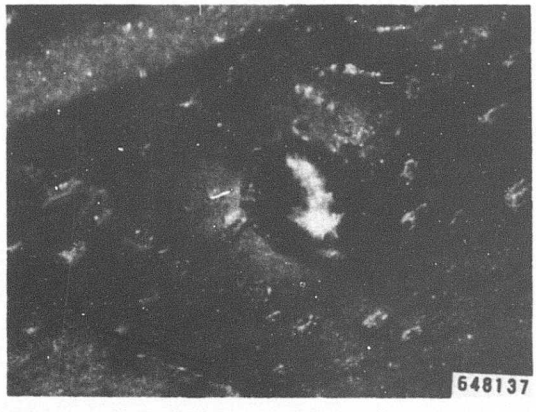

c. Wide Finger - OFHC Copper Wire Clipped

Figure 55. Experimental Welds - Output Finger

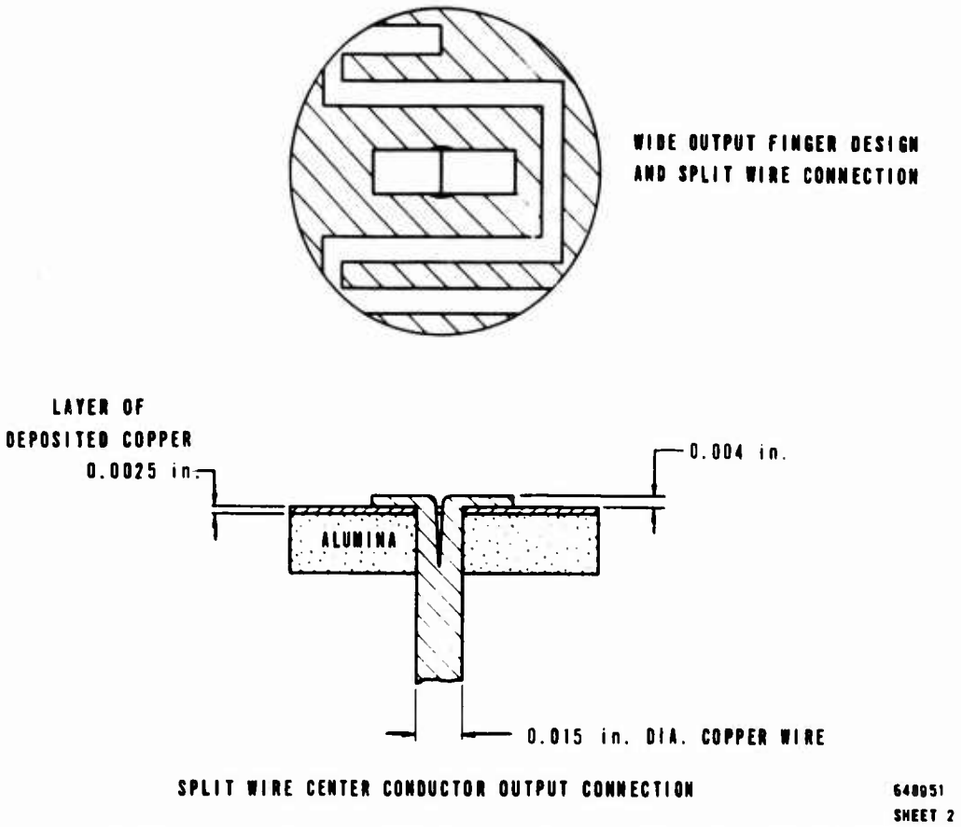

Figure 56. Center Conductor Connection for QKA1329 Test Vehicle No. A-10

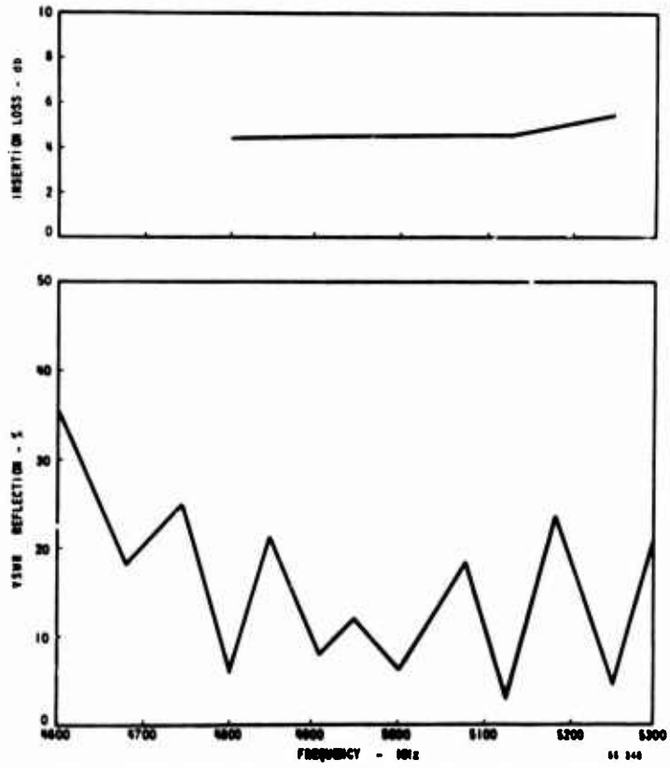

Figure 57. QK1329 Test Vehicle No. A-5 Circular C-Band SWS Serial No. C-125 Insertion Loss and VSWR

2.5.4.2 QKA1329 No. A-6

Tube no. A-6 was also sealed in and evaluated. A curve of the rf match and insertion loss of this tube is shown in Figure 58. The tube was first operated under pulsed conditions at a 10% duty cycle. The operation under these conditions was found to be comparable to previous tubes. The tube was then operated under cw conditions and two peculiarities were noted in the operation. First a power sag of approximately 10 watts was matched after 2 to 3 minutes of operation. This occurred every time the tube was turned on, indicating that the effect was thermal in nature. Secondly the average rf power was approximately 20 watts less than the peak rf power recorded under pulse conditions. A performance curve of the cw operation is shown in Figure 59.

It has been noted that the mode boundary in this and in other tubes reported appears to occur at a higher value of sole voltage than would be expected in a conventional C-band tube. Whether this is a characteristic of tubes utilizing a photodeposited slow-wave structure has not been studied up to this time, but since the effort has been directed mainly toward achieving performance with reliable structures, rather than toward improving tube performance, these tubes should not be considered as typical.

A life test of this tube was initiated and the results are discussed in Section 2.6.1 of this report.

2.5.4.3 QKA1329 No. A-7

The basic design of the test vehicle featured two outputs and an external attenuator, so that insertion loss could be measured on the test vehicles. There was an interest as to the possibility of an internal attenuator. Tube No. QKA1329 A-7 was constructed featuring a thin film internal attenuator. The last 20 fingers were attenuated in a triangular pattern (Figure 60) by evaporating molybdenum to a thickness of approximately 300 Å.

The initial pulsed performance of the tube is shown in Figure 61. After approximately 4 hours operation at the 25% duty cycle, a VSWR was taken (see Figure 62) which indicated no deterioration of the delay line or attenuator.

The tube was then operated in the cw mode for approximately 4 hours, during which time the tube performance appeared similar to the pulsed operation. After this, the tube was removed from the test station for evaluation of the next tube. The tube was later returned to the test station and the evaluation at cw continued. During operation, the power showed a definite deterioration over that obtained previously, and when the level reached 10 watts the tube was sent for scrap analysis. Figure 63 indicates the voltage reflection before and after breaking the vacuum seal. Since the reflection increased after exposure to air, it can be assumed that the delay line is less attenuative. However, the physical appearance of the delay line and internal attenuator was excellent, from both the adherence and cleanliness. No explanation could be found for the change in performance.

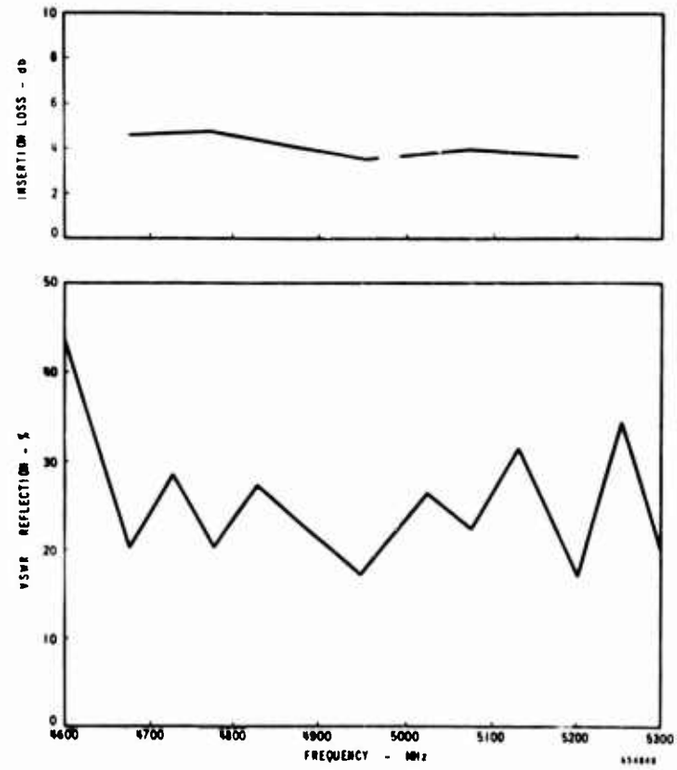

Figure 58. QK1329 Test Vehicle No. A-6 Circular C-Band SWS Serial No. C-133R Insertion Loss and VSWR

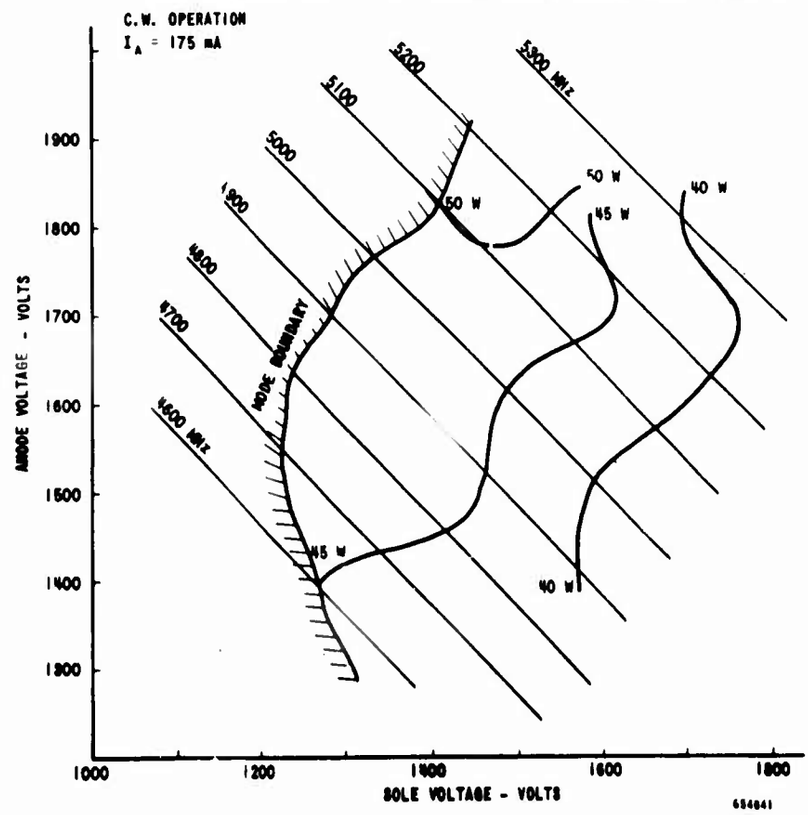

Figure 59. QKA1329 Test Vehicle No. A-6 Performance Chart Power Contours

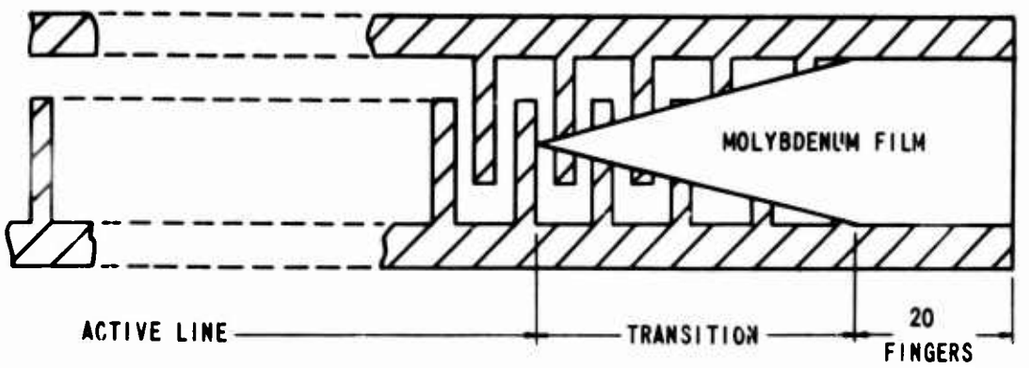

Figure 60. Test Vehicle A-7 Showing Attenuated SWS

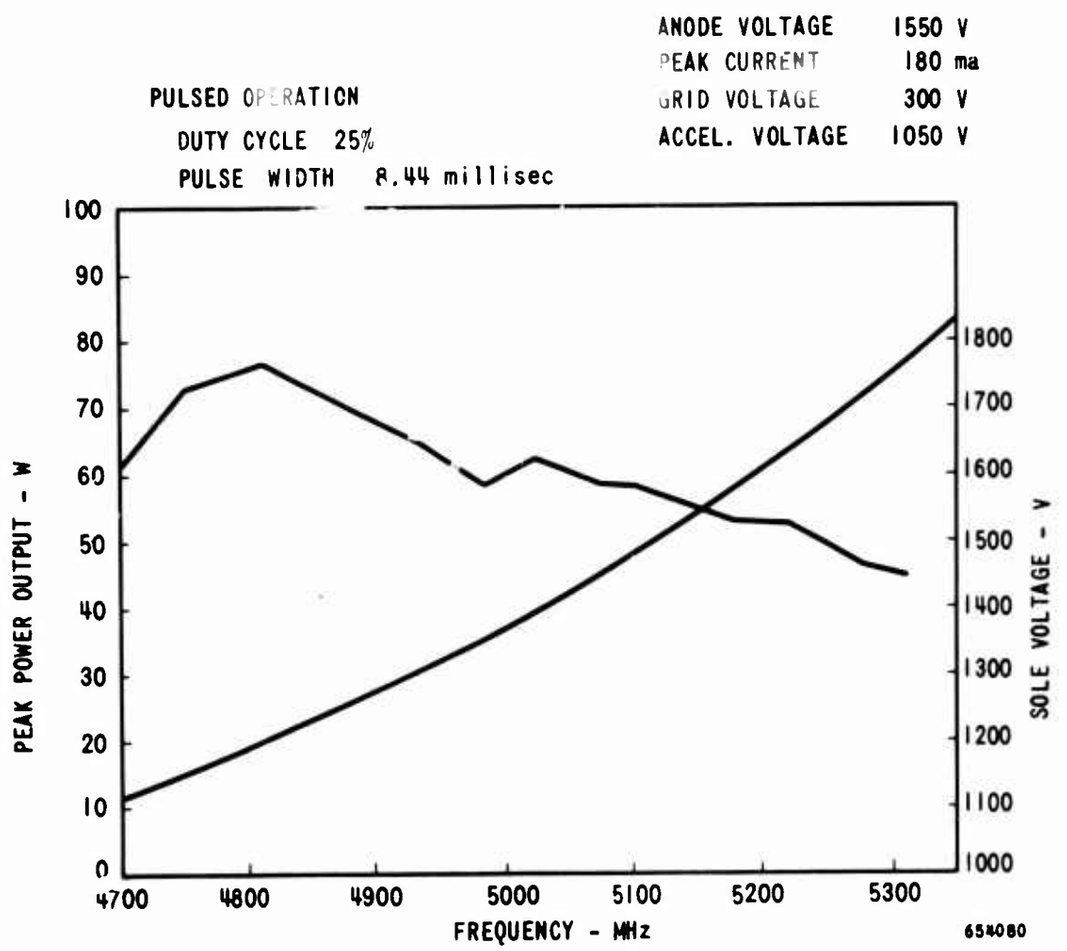

Figure 61. CKA1329 Test Vehicle No. A-7
Electromagnet Operation

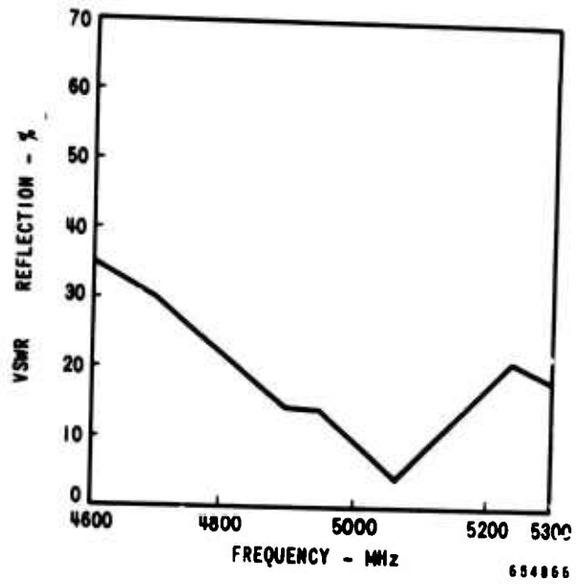

Figure 62. QK1329 Test Vehicle No. A-7
Serial No. C-140 VSWR

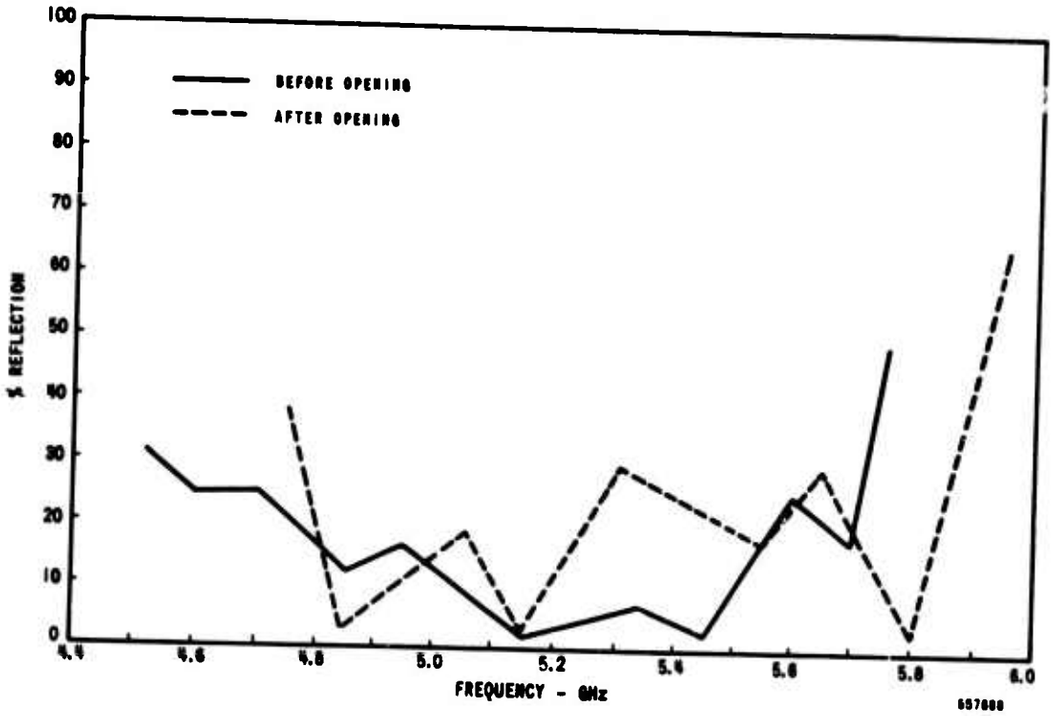

Figure 63. Voltage Reflection Before and After
Opening QKA1329 No. A-7
SWS Serial No. 140

2.5.4.4 QKA1329 No. A-8

This tube, constructed in a similar manner to QKA1329 No. A-6, developed a leak during the initial process. The leak was repaired and evaluation was started by pulsing the tube at a 25% duty cycle. Initial performance was satisfactory but the power soon deteriorated. An insertion loss was taken and found to be 20 db. The tube was scrap-analyzed. A black deposit was observed on the delay line. Both spectrographic analysis and chemical analysis failed to positively identify this deposit. Traces of iron came from the etching process which includes ferric chloride. Another anode assembly was tested in which the anode was washed in distilled water. The water was tested by titration with silver nitrate for chloride residual which was indeed present. The cleansing process was revised to more thoroughly remove these clorides. As this is the first time that this has occurred, this particular anode assembly may not have been properly cleaned. Figure 64 shows VSWR and insertion loss for this tube.

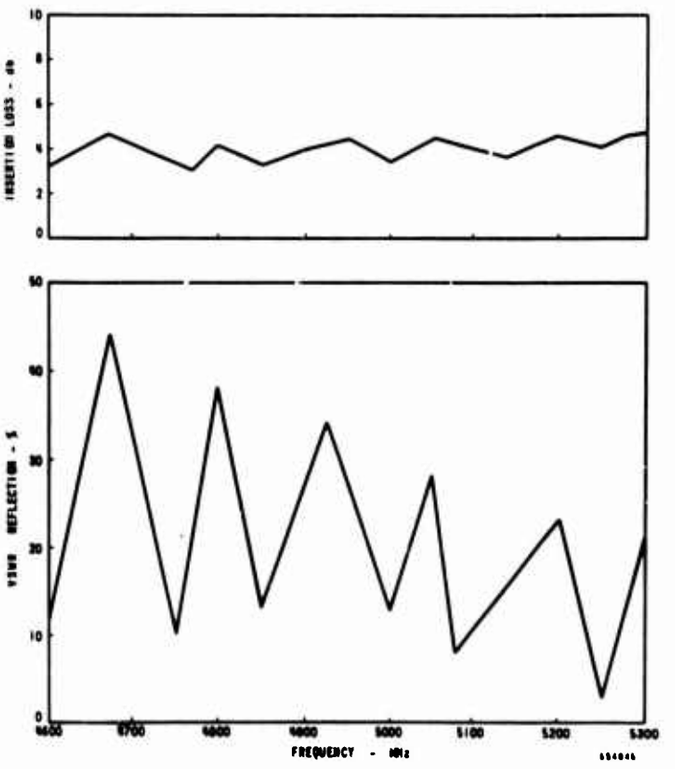

Figure 64. QK1329 Test Vehicle No. A-8 Circular C-Band SWS Serial No. C-150R Insertion Loss and VSWR

2.5.4.5 QKA1329 No. A-9

This tube failed due to a high VSWR at cold test prior to tube bakeout. The tube was scrap-analyzed and was found to have a finger lifted from the ceramic substrate at the output connection. Further investigation showed that the cleaning process initiated after the failure of tube No. A-8 (i.e., cleaning in boiling distilled water) had, in fact, undercut the bond area between the SWS and the substrate. The undercutting effect was due to the slight concentration of the etchant at this elevated temperature. This caused failure of the bond and eventually the finger was lifted by mechanical stresses set up during the sealing-in procedure. After this failure, the cleaning process was modified to use cold distilled water for rinsing, with more frequent changes of water during the processing.

2.5.4.6 QKA1329 No. A-10

This was the last tube sealed in during the program, and, with the failure of tube No. A-9, was expected to be the life test tube. The structure was cleaned and mechanically sound after the cleaning process. The tube was sealed in and processed in the usual manner.

Initial operation of the tube under pulsed operation for outgassing of the SWS appeared normal. The tube was then operated under cw conditions at slowly increasing levels of anode current, to continue the outgassing of the structure. Again, the operation appeared normal, with power output varying between 40 and 50 watts over the operating band. After 3 or 4 hours of cw operation at rated current, during which time the operating parameters were being adjusted to improve the tube performance and the operating points were being selected for life test operation, the power output of the tube suddenly started to decay. When the power level dropped below 10 watts (after about 12 hours), further testing was stopped and the tube was scrap-analyzed.

The failure mechanism of this tube was immediately obvious; the beam had struck the electron beam welded area of the output center conductor and had sprayed copper over the spacing between the first 3 to 4 fingers. This could be seen by the shadow pattern of the deposit, which was directly in the line of sight of the center conductor weld.

This failure points out the need for a redesign of the center conductor to delay line junction. Since it has been shown that a wide first finger is not detrimental to tube operation, a larger hole could be made through the ceramic substrate. This would allow a conventional ceramic-to-metal braze of the center conductor (the present hole is too small for proper metalizing) thus eliminating the need for the present electron-beam-welded joint. Such a redesign should eliminate this type of failure in future tubes.

The use of thin-wall tubing in the making of I.D. ceramic-to-metal seals is quite common and is, in fact, used in the center conductor of the rf output of this tube. The mechanical stresses are taken up in the yielding of the tubing, a distinct advantage over the case of a solid pin where the stresses are imparted to the ceramic and will cause it to crack. The tubing must be of such size that braze material does not fill it, thus making, in effect, a solid pin.

2.6 Life Test (Ref: Appendix A, Section IB3b(8))

2.6.1 First Life Test Tube (QKA1329 No. A-6)

Tube no. A-6 was assigned to life test evaluation with an objective of 100 hours minimum. The decision was made to accumulate the first 100 hours of life with the VacIon pump operating so that in the event failure occurred due to sputtering, the tube pressure would be known. At the end of 100 hours, the pump would be turned off and the test continued to tube failure.

Figure 65 shows the power variation with life up to the point where the tube failed at 268 hours. Power variation up to that time was in the order of 2 or 3 watts. At the time of failure, the tube exhibited a sudden drop in power accompanied by the occurrance of positive sole current indicating emission from the sole. After the tube was shut down, comparable operation could be obtained for a period of 4 to 5 minutes after which a drop in power accompanied by sole current again occurred.

The tube was scrap-analyzed and a photograph of the anode assembly and sole gun assembly are shown in Figures 66 and 67.

A black deposit can be seen on the substrate over the front of the delay line. Opposite the area there is evidence of discoloration of the sole but spectroscopic examination, electron beam probing and chemical analysis failed to reveal the identity of this deposit. It is suspected that it may be due to iron, as explained in Section 2.5.4.4 of this report. The bond of the copper delay line to the substrate was intact.

Insertion loss measurements were made on the structure prior to and after initial processing. An increase from4 to 5 dB (see Figure 44) across the band to values of 5 to 6 dB were noted prior to the start of tube evaluation. A period of evaluation then occurred during which time the tube parameters and magnetic fields were adjusted and trimmed prior to the selection of the operating parameters for life test. Considerable variations in performance were encountered during the evaluation due to the adjustment prccess which lasted about two days.

It was after this period of time that the life test was started, but unfortunately no cold test measurements were taken at this time, and in fact were not taken again until the tube was opened to air for scrap analysis after life test, at which time the values correlated quite well with the previous readings taken. This differed from later tubes in which the presence of a black deposit similar in appearance resulted in an extremely high insertion loss.

The tube performance characterized by a flat power curve with life, tends to confirm this, since obviously such performance would not be possible with a high insertion loss such as occurred in the later tubes.

It has not been possible, because of the many unknowns involved, to obtain an explanation of the exact mechanism of failure of this tube.

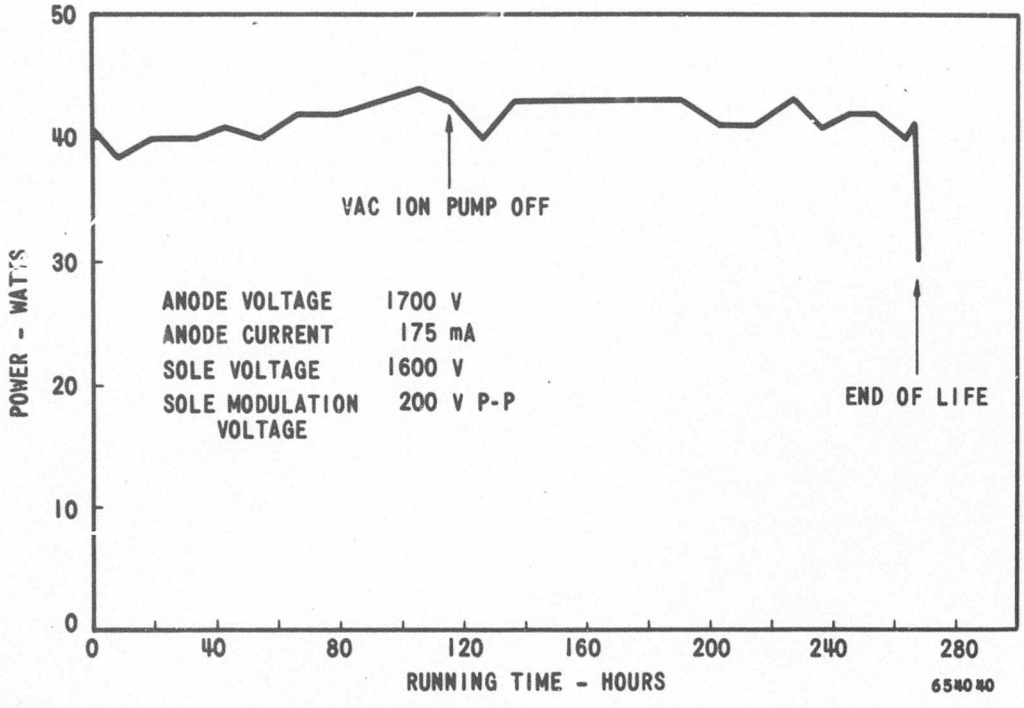

Figure 65. QKA1329 Test Vehicle No. A-6
Power Variation with Life

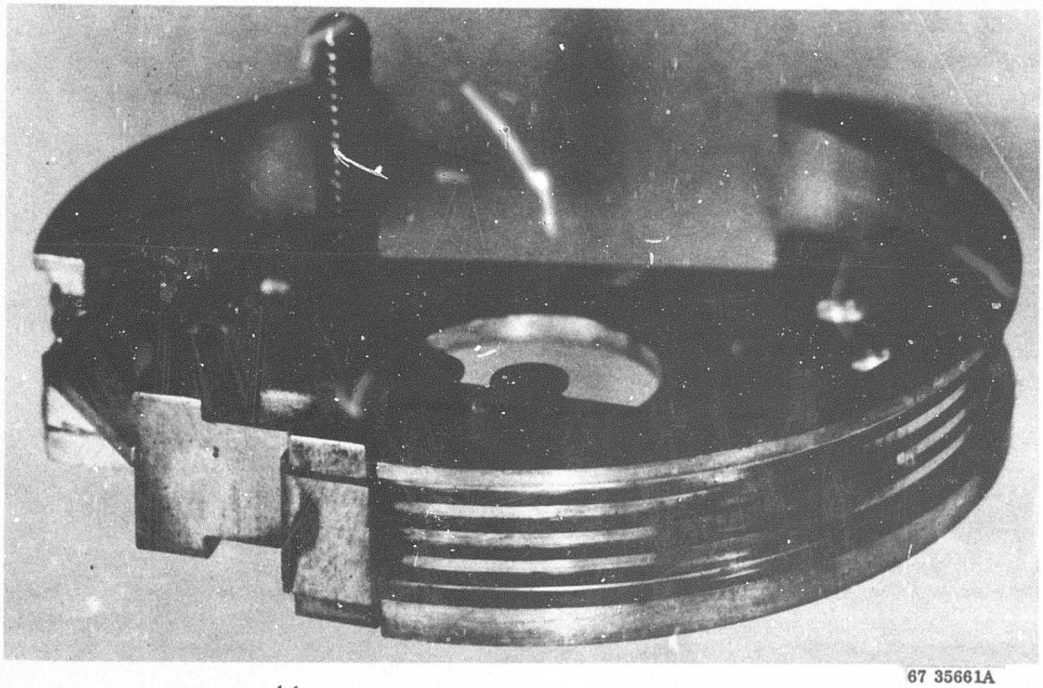

67 35661A

Figure 66. QKA1329 Tube No. A-6 Sole

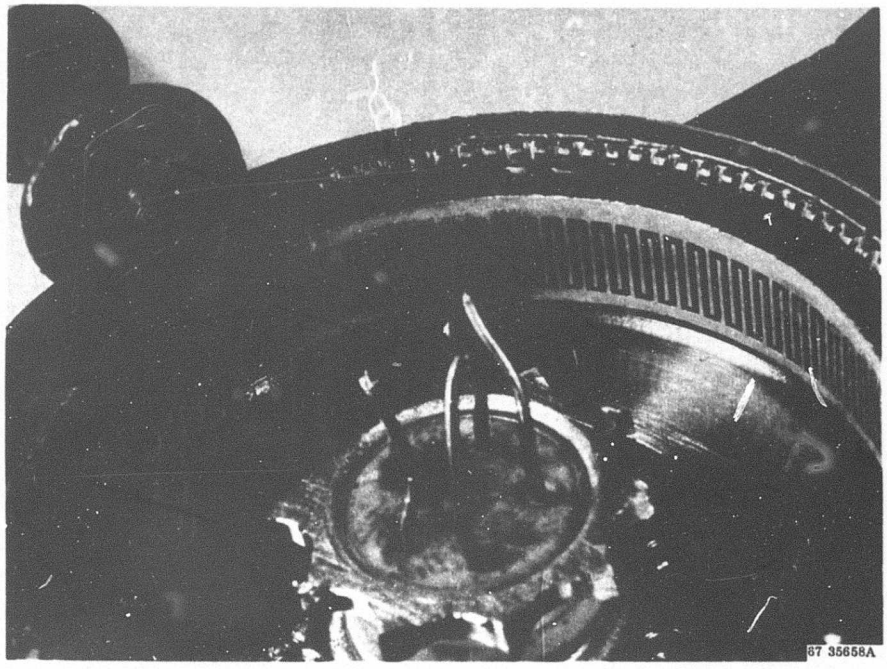

Figure 67. QKA1329 Tube No. A-6 Anode

2.6.2 Second Life Test Tube

At the time of the revision of the Statement of Work (Appendix A) on 8 June 1967, when the number of tubes to be submitted to life test was increased from one to two, Raytheon had sufficient structures on hand to manufacture three more test vehicles. It was felt that this was sufficient to assure that one tube could be submitted to life test. The three tubes were built (No. A-8, A-9 and A-10), but all failed prematurely before the actual accumulation of formal life test data could begin.

Since the lead time for procurement of further BeO substrates is 2 to 3 months, it is considered inadvisable to build more test vehicles under this contract.

2.6.3 Summary of Life Test Results

Prior to the initiation of life test, it was suspected that the two main deterrents to extend life of an M-type BWO with photodeposited delay lines would be either sputtering of the sole material to the delay line or failure of the SWS-to-substrate bond during prolonged operation. In actual fact, however, neither condition proved to be the limiting factor in any of the life test tubes, which shows that expected operation life should be comparable to many conventional tubes.

Analysis of the results of tube No. A-6 confirms this expectation, since the life of the tube was terminated by the appearance of secondary emission from the sole element of the tube. While it is true that the alumina coating used to inhibit sputtering has a higher secondary emission ratio than pure copper (this has been measured between 2 and 5 for alumina films as against 1.3 for copper), all evidence points to the fact that this value decreased with life, and therefore, were the secondaries associated directly with the alumina film, the secondary emission current would have been present initially.

The second failure was attributed to a residue of etchant on the substrate, causing high attenuation of the delay line. An additional cleaning process used on subsequent assemblies prevented re-occurance of this condition on the next tube.

The third failure was due to the impingement of the beam on the center conductor weld. An earlier discussion (see Section 2.5.4.6) showed where a redesign of this connection would preclude further failure of this type.

In summation then, none of the failures have been attributed to insurmountable problems connected with the presence of a photocopied SWS in the tube. The premature failures of the last two tubes point out the need for a refinement of the mechanical design of the test, however there are insufficient parts and materials to accomplish this during the scope of this program.

2.7 Delivery of Slow-Wave Structures (Ref: Appendix A, Section IB3b(7))

2.7.1 Circular C-Band Slow-Wave Structure

Two of the acceptable slow-wave structures and two anode assemblies featuring these slow-wave structures were delivered at the conclusion of this contract.

2.7.2 Linear Ku-Band Slow-Wave Structures (Ref: Appendix A, Section IB3b(9))

Two of the acceptable K-band linear slow-wave structures were delivered at the conclusion of the contract.

3. CONCLUSIONS

3.1 Accomplishments

At the beginning of this program there were two major problems to be solved prior to using photocopied SWS in microwave tubes. The first was development of a bond of the copper SWS to the beryllia substrate; the second was a method of inhibiting sputtering of the sole material to the delay line, which was causing premature failure of the tube.

The decision was made to develop a bond to beryllia, even though a bond to other materials (specifically, some forms of alumina) would possibly be simpler. The greater thermal dissipation capabilities of the beryllia made it a much more desirable material with versatility in a wider range of power levels of electron tubes.

This led first to the development of the CuO_x bond, which was successful in earlier tubes, but was found to be quite critical in the control of certain parameters. The development of the TiO_x bond followed and markedly reduced the number of bond failures.

The second major unknown was the effect of sputtering on tube life. For this purpose an alumina film was used on the sole and its success was demonstrated by life testing one tube for a period of 260 hours before failure.

Since the solution of these problems there appear to be no major obstacles to the use of photodeposited SWS in microwave tubes.

3.2 Comparison of Conventional and Photocopied Delay Lines (C-Band)

The use of a photocopied delay line on a ceramic substrate, in this case, beryllia, offers certain advantages over the conventional machined delay line particularly in the case where the final tube objective requires low cost, small size, rugged construction and a maximum power-to-weight ratio.

For example, if we compare a photocopied line to a conventional SWS which is electrically equivalent in its dispersion characteristics and coupling impedance, we can arrive at the following dimensions:

Dimension	Photocopied Tube (in.)	Conventional Tube (in.)
Pitch	0.030	0.030
Finger Length	0.198	0.380
Finger Thickness	0.015	0.015
Finger Spacing	0.015	0.015
Finger Cross Section	0.015 x 0.003	0.015 x 0.030

A cross-sectional view of the delay line is shown in Figure 68.

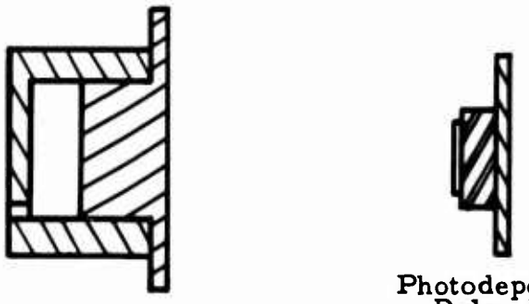

Figure 68. Cross Sectional View of the QK1329 Delay Line

If we calculate the maximum power dissipation capabilities of the two structures, we see that, for equivalent delay lines, the photocopied line on beryllia is capable of dissipating 5 to 6 times the power that can be dissipated by an electrically equivalent conventional delay line. When we consider that there is approximately a 40% weight reduction with the dielectrically loaded line, we realize that there is an increase in watts per pound of from 8 to 10 times.

This is not meant to imply that a tube designed for 50 watt operation could be operated at 300 watts. What is meant is that the delay line dissipation limitation, which is often, particularly in high frequency, the limiting factor in power output, can be raised to a higher limit than could previously be attained with conventional crowns.

Other advantages inherent to the photodeposited type of SWS are as follows:

1. Ability to withstand greater environmental requirements because the fingers are totally supported by the beryllia substrate.

2. Lower manufacturing costs since the photocopied line is ideally suited to batch manufacture and the final result is a perfectly matched set of crowns ready for use in a tube.

3.3 Problem Areas

Two areas which have caused problems in the construction and evaluation of test vehicles are:

1. Welding of the center conductor of the coaxial output to the slow-wave structure.

2. Cracking of the beryllia substrate during processing.

It is felt that both problems could be solved in a mechanical redesign of the anode structure. However, due to the long lead time required for delivery of beryllia, it was impossible to delay the program for sufficient time to accomplish such a redesign. Instead, a "waffle-type" braze was used to reduce the cracking, and electron beam welding was used for the center-conductor-to-SWS junction.

3.4 Recommendations

While this program has accomplished its main objectives - i.e., proving the feasibility of using photocopied SWS in microwave tubes in general and M-type BWO's in particular, the test vehicles constructed and evaluated did not explore to their limits the advantages to be obtained.

For example, while the test vehicles were quite small, full advantage was not taken of the size reduction possible. Also, the upper limits of thermal dissipation capability have not been investigated. The design techniques of the delay line itself should be refined with the objective the design and development of an efficient miniature, high-power, d tube for airborne use.

APPENDIX A

STATEMENT OF WORK

APPENDIX A

STATEMENT OF WORK

EXHIBIT "A"

I. DETAILED DESCRIPTION

A. Purpose and Objective

1. The contractor shall develop manufacturing methods, processes, and techniques for improving Slow Wave Structures (SWS) in the "C" Frequency Band. The selected fabrication technique must be adaptable to production "K" Band SWS. Improving means developing a new technique of fabrication that will increase reproducibility, versatility, and reliability while reducing size, weight, and unit cost, etc.

2. The contractor shall furnish the necessary supplies and services required to establish and evaluate a manufacturing technique and facility for fabricating photocopied ceramic-mounted SWS for microwave tubes. The contractor shall provide process and design specifications permitting tube manufacturers to apply this technique to applicable microwave tubes. The supplies and services rendered shall be in accordance with this work statement and Exhibit "C".

3. The contractor shall report to interested government and industrial agencies the improved SWS fabrication technology developed in the course of this effort.

B. Scope

1. Phase I

a. Objective - Material analysis, program planning, and SWS design and evaluation.

b. Criteria and Approach

(1) The contractor shall develop a Management Control Plan network showing significant events in the course of the program. This plan shall be included as an attachment to the first Monthly Progress Letter and shall be updated in subsequent MPL's.

(2) The contractor shall develop and analyze methods of producing SWS's using the following as a guide.

(a) Analyze and select materials, techniques and methods for photocopying SWS on a ceramic substrate.

(b) Establish a facility to manufacture prototype photocopied SWS.

(c) Manufacture and evaluate various linear prototype C-Band SWS. The evaluation shall consider both ceramic bonding techniques and the basic electrical characteristics of the SWS.

(d) Design, fabricate, and cold test prototype linear Ku-Band SWS to demonstrate the applicability of photocopied ceramic SWS to this frequency range. The prototypes shall be designed to have a 10% bandwidth centered about 14 Gigacycles.

(e) Develop an initial technique for photocopying circular C-Band SWS. Fabricate and evaluate SWS, with variations in techniques to obtain accurate and reproducible SWS.

(f) Demonstrate that a circular ceramic mounted C-Band SWS is compatible with the tube environment by mounting a SWS in a simulated tube environment and subjecting the assembly to the vibration and shock tests of Exhibit "C".

(3) The contractor shall develop and evaluate an electrical design method of ceramic mounted SWS using the following steps as a guide.

(a) Review past theoretical studies on design of ceramic mounted SWS.

(b) Develop an initial design for a C-Band ceramic mounted SWS to operate in the selected test vehicle with characteristics that conform to Exhibit "C". Modify the selected test vehicle to accept these structures.

(c) Fabricate, evaluate in the test vehicle, and modify sufficient numbers of circular, ceramic mounted SWS to determine a final electrical design for the SWS. The test vehicle with ceramic SWS installed shall meet the electrical specifications of Exhibit "C".

(d) Prepare and submit for approval the design specification for the SWS.

(4) Certified test data on the above work shall be compiled and submitted for approval before any funds are obligated against subsequent phases.

2. Phase II

a. Objective - Develop a plan for an unbalanced pilot line to produce ceramic mounted SWS.

b. Criteria and Approach - Upon receipt of written approval of prior work, the contractor shall develop a plan for a pilot line facility and manner of operation to consistently fabricate the approved SWS in an economical and reproducible manner. The line shall be designed to produce ten SWS per hour. The following items shall be included in the plan:

(a) A sketch showing equipment layout and flow of materials.

(b) A description of equipment, fabrication technique, and recommended rates of production.

(c) Quantity, nomenclature, and price of each equipment.

(d) Description of proposed quality control equipment and methods.

3. Phase III

a. Objective - Establish an unbalanced pilot line and demonstrate the acceptability of the product.

b. Criteria and Approach - Upon receipt of approval of Phase I work, the contractor shall establish a pilot line and operate same to prove-in the methods and procedures used in the line.

1. A minimum quantity of machinery and test equipment shall be used to demonstrate the capability of the pilot line.

2. In line Quality Control Procedures and techniques shall be established and evaluated to insure that high yield, high quality and high reproducibility shall be maintained.

3. To demonstrate the adaptability of the pilot line, 18 circular C-band and five linear K-band, SWS will be fabricated.

4. All SWS produced on the pilot line will be evaluated electrically. Six C-band SWS will be subjected to environmental evaluation.

5. Five miniature M-BWO test vehicle seal-ins will be fabricated using C-band SWS produced on pilot line.

6. Operate and evaluate the test vehicles to determine usability of the ceramic supported SWS.

7. Two (2) of the acceptable C-band SWS's shall be delivered to MATE.

8. Two test vehicles featuring a ceramic mounted SWS shall be life tested for 100 hours or tube failure which ever comes first.

9. Two (2) of the acceptable linear K-band SWS's shall be delivered to MATE.

II. OTHER

A. Approvals

1. Data specified to be submitted for approval at the end of all Phases shall be submitted to MATE through the Procurement Contracting Officer.

2. The contractor shall not proceed with any phase requiring approval without such approval being received from the Procurement Contracting Officer through MATE.

APPENDIX B

MANAGEMENT CONTROL PLANS

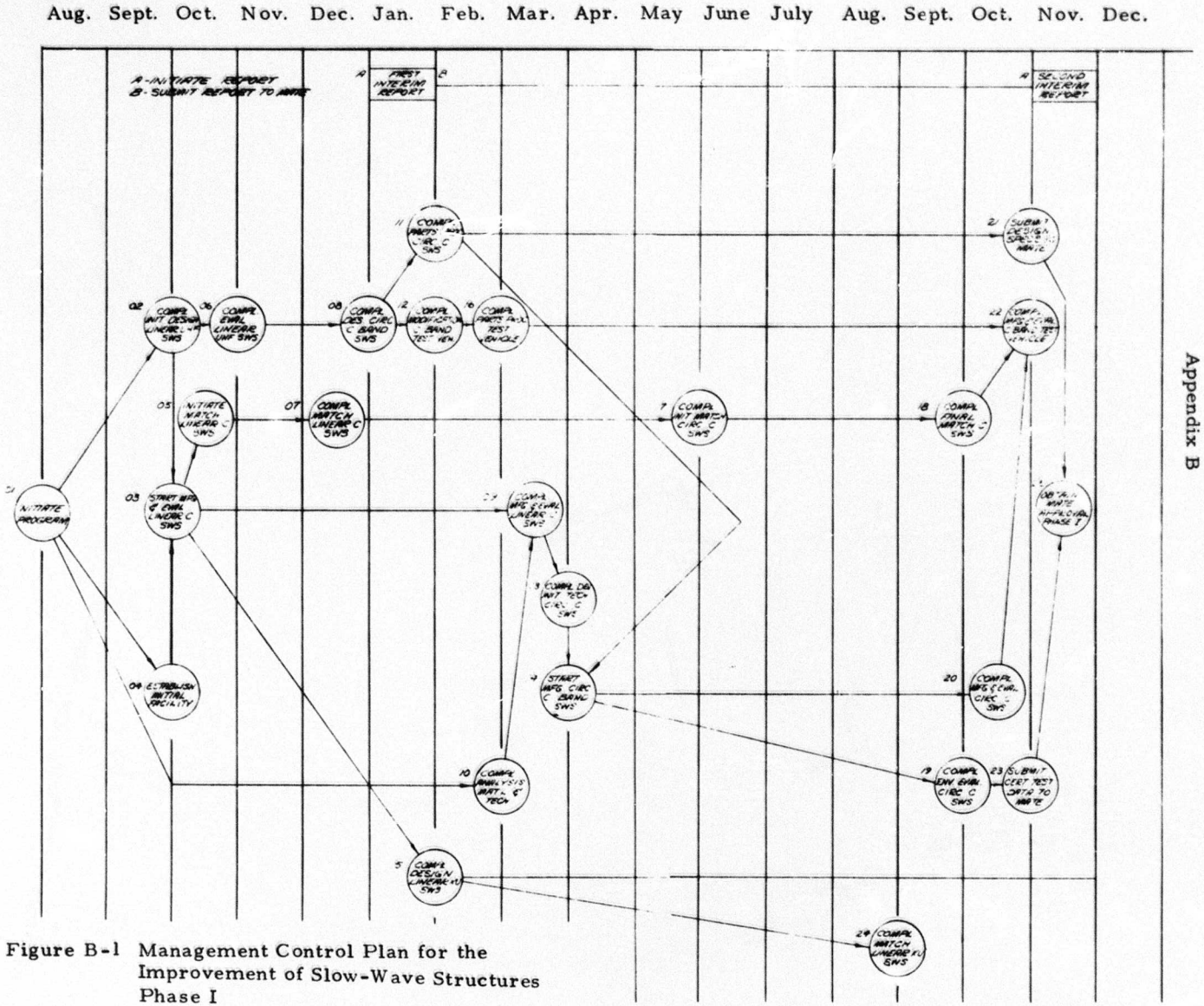

Figure B-1 Management Control Plan for the Improvement of Slow-Wave Structures Phase I

D88780-1

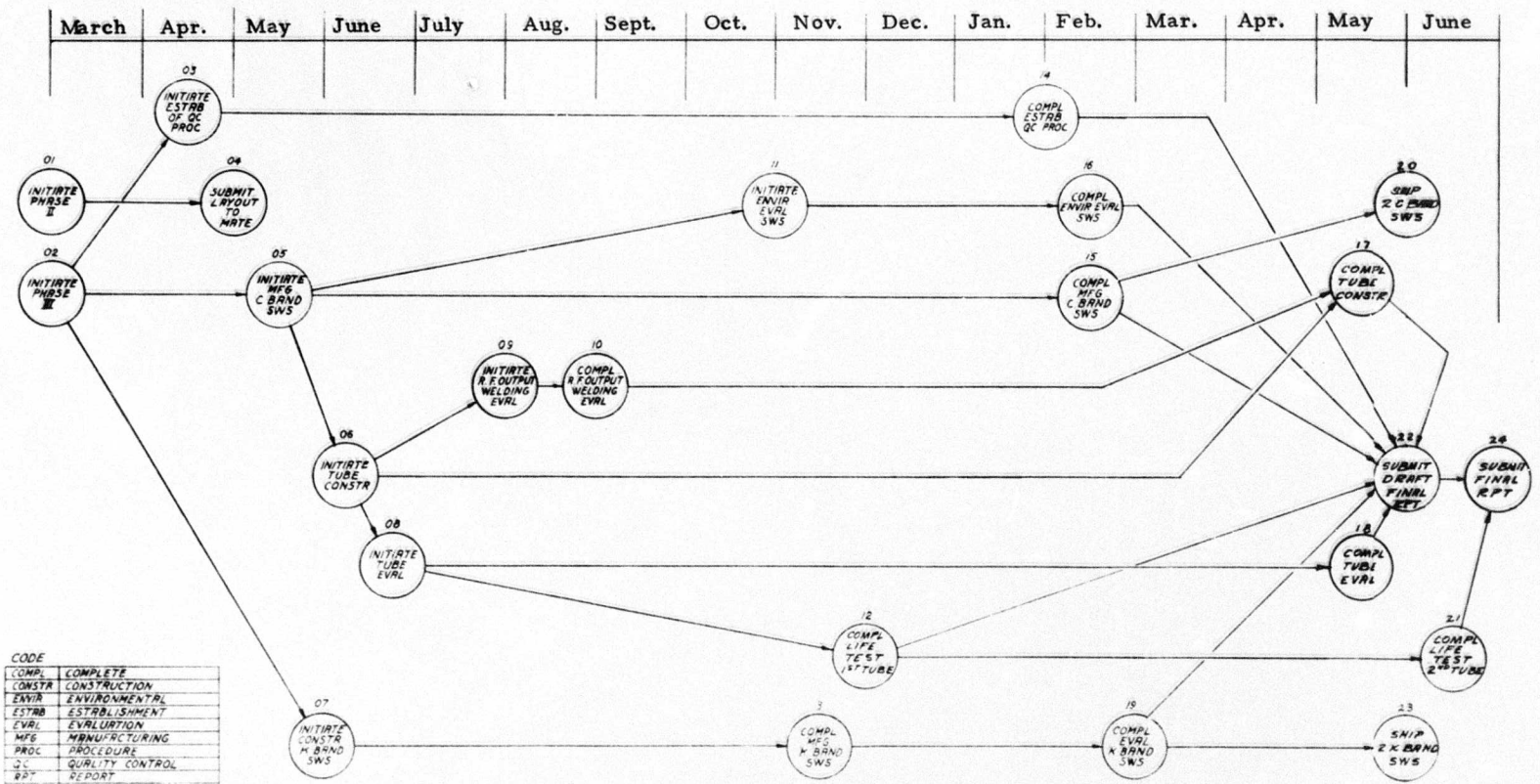

Figure B-2 Management Control Plan for the Improvement of Slow-Wave Structures Phase II and Phase III

C651183-1

APPENDIX C

PHOTO-ETCH EQUIPMENT

APPENDIX C

PHOTO-ETCH EQUIPMENT

Cleaning Equipment

The following pieces of equipment are available for cleaning:

(1) Ramco Model A15E Vapor Degreaser

Size - 15 x 15 x 24 inches
Capacity - 3 gallons
Power requirement - 600 watts, 110 volts

(2) Sonoblaster Vapor Degreaser Series 600

Size - 12 x 8 x 13 inches
Capacity - 1 gallon, water-cooled
Power requirement - 300 watts, 110 volts

(3) Sonoblaster Ultrasonic Cleaner Series 200

Size - Tank 4-1/2 inch diameter, 9 inches high, power supply 9 x 8 x 8 inches
Capacity - 1 litre
Power requirement - 200 watts, 110 volts

(4) American Timex Ultrasonic Washer

Size - 13 x 9 x 8 inches
Power requirement - 200 watts, 110 volts.

Vacuum Evaporator

Make - High Vacuum Equipment Corporation, Hingham, Massachusetts
Model - C0018
Bell type and size - 18-inch diameter, 30 inches high, pyrex glass.

Components - Kinney Mechanical Roughing Pump, Cold Trap, - six electrical fed-through connections, eight thermocouple feed-through connections, one rotary mechanical feed-through, one high-voltage feed-through.

The mechanical pumps are located on the outside of the room partitions to keep the oil vapors outside the clean room areas.

Electroplating Facilities

Because of the small size of the pieces to be electroplated, this operation is carried out in a glass beaker. In addition to electrical meters to measure the plating current and voltage, the only piece of equipment used in this process is a Model EFB Electron Products dc power supply. This has dual ranges of 0 - 16 volts at 8 amperes and 0 - 32 volts at 4 amperes.

Spin Coating Machine

This is a Raytheon-fabricated piece of equipment and consists of a Boston Gear Company type 29005 dc motor and a type R-12 speed control. The motor is supported in a vertical position and provided with a turntable surrounded by an enclosure and fitted with a cover. Speeds from 0 to 2300 rpm can be selected as desired. The overall dimensions of the turntable portion are 12 x 12 x 15 inches. The turntable is 8 inches in diameter.

Dry Box

This is an isolette type of enclosure kept under a slight positive pressure of dry nitrogen gas and having windows provided with Kodagraph sheeting filters. Access is through arm holes and hinged doors.

Oven

This is a Bockel thermostatically controlled convection-type oven.

Specifications

Size 12 x 12 x 12 inches
Temperature range - room temperature to 300°C
Power requirement - 600 watts, 110 volts.

Exposure Machine

This is a NU-ARC Type FT-18M Plate Maker and consists of a flip-top, single-sided vacuum print frame, vacuum pump, and magnetic amplifier motor-driven carbon arc lamp, with built-in timer. This equipment is integrated in a chest-type enclosure supported on a floor stand. The power requirement is 200 watts at 110 volts.

Development

Processing is carried out in glass beakers. Spray rinsing is done with a Thayer and Chandler Model E air brush with attached one-ounce fluid container.

Etch Machine

Masters Model S Splash Etcher.
Dimensions - 20 x 30 x 40 inches
Capacity - 5 gallons
Power requirement - 100 watts at 110 volts.

APPENDIX D

MEASUREMENT PROCEDURE FOR (c/v_o) VS λ CURVE

Discussion

An interdigital line which is shorted at either end by an image plane, when weakly coupled to a power source, is resonant at an integral number of half guide wavelengths. This resonance condition is determined by the guide wavelength λ_g and by the physical length of the circuit according to

$$n \frac{\lambda_g}{2} = Np \quad (n = 1, 2, 2, ----) \tag{D. 1}$$

where

λ_g = guide wavelength
N = number of pitches
P = pitch of the structure

In an interdigital delay line the phase shift per pitch is given by the expression

$$\theta = \frac{2\pi}{\lambda_g} P \tag{D. 2}$$

where

θ = phase shift per pitch.

The expression for (c/v_o) of an interdigital delay line, which is the ratio of the velocity of light to the phase velocity of the rf wave, can be expressed as

$$c/v_o = \frac{\lambda}{2p} - \frac{\theta}{\pi}\left(\frac{\lambda}{2p}\right) \tag{D. 3}$$

where

λ = free-space wavelength
θ = phase shift per pitch

This can be rewritten as

$$c/v_o = \frac{\lambda}{2p}\left(1 - \frac{\theta}{\pi}\right) \tag{D. 4}$$

Substituting the value of λg from (D. 1) into the expression for θ (D. 2) yields the following expression

$$\frac{\theta}{\pi} = \frac{n}{N} \tag{D. 5}$$

Substituting this value into expression (D. 4) gives an expression for (c/v_o) where all the quantities are measurable experimentally; namely,

$$\frac{c}{v_o} = \frac{\lambda}{2p} \quad 1 - \frac{n}{N} \qquad \text{(D. 6)}$$

Test Procedure

The test setup for measuring the quantities in Eq. (D. 6) is shown in Figure D-1. The signal from the oscillator is varied until a resonance is detected on the oscilloscope. Its frequency is noted and the resonance number then found by probing the field pattern near the structure and identifying the number by counting the peaks in the pattern. The values obtained are substituted in equation (D. 6) to find the (c/v_o) vs λ relationship.

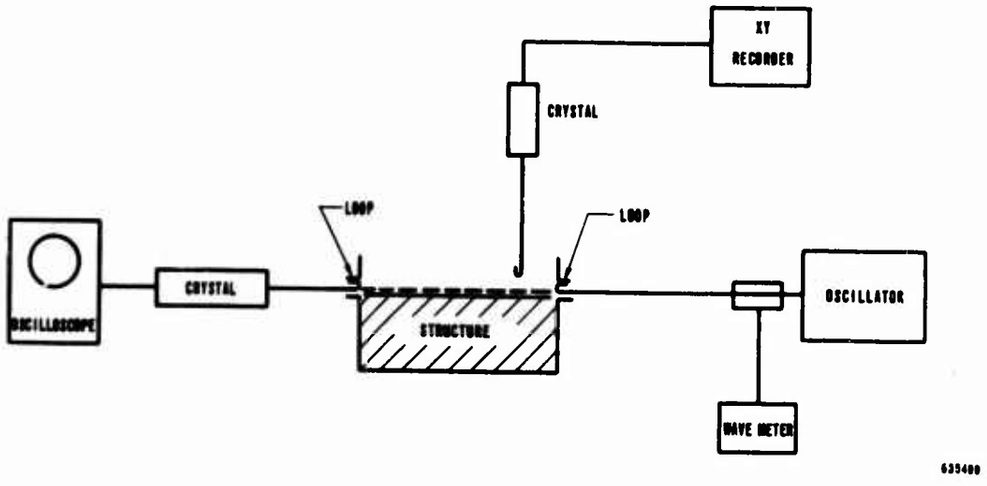

Figure D-1. C/V_o vs λ Test Set-Up

APPENDIX E

MEASUREMENT PROCEDURE FOR COUPLING IMPEDANCE

The coupling impedance is a measure of the strength of the field in the interaction space for a given power flow, and is defined as

$$R_c = \frac{|E_{RF}|}{2\,\Gamma_o^2 p} \qquad \text{(E. 1)}$$

where

p = power flow on the SWS
$|E_{RF}|$ = magnitude of rf field component at the beam position
Γ_o = propagation constant.

A low value of coupling impedance results in a long delay line as the starting current varies inversely with the coupling impedance, which means the number of fingers must be increased to lower the starting current to approximately 1/3 of the operating current. If the coupling impedance is too low, there will be little or no control of the beam by the rf wave, resulting in a low-efficiency tube.

The quantities in equation (E. 1) are difficult to measure directly, therefore an indirect method of measuring the coupling impedance at the surface of the line has been evol[illegible], with the assumption made that the value decreased exponentially to the calculated beam position. The method used in this case was the frequency perturbation method. It is based on the detection of resonances of a shorted section of delay line as discussed in Appendix D. Then a dielectric sheet is placed parallel to the line a small distance away. This causes the resonant frequencies to move downward, and this shift in frequency can then be related to the coupling impedance of the line through the following expression:

$$R_{c(o)} = 377 \left(\frac{c}{vg}\right) \frac{e^{2\,\Gamma_o a}}{\Gamma_o \ell} \frac{1+\epsilon_r}{1-\epsilon_r} \frac{\Delta f}{f} \qquad \text{(E. 2)}$$

where

$\left(\frac{c}{vg}\right)$ = delay ratio of group velocity

Γ_o = propagation constant
a = distance from the line to the dielectric
ℓ = width of the circuit
ϵ_r = dielectric constant of the dielectric sheet
Δf = frequency shift
f = frequency

The test setup is identical to that described in Appendix D, and the values obtained can be substituted into equation (E. 2) to determine the coupling impedance.

APPENDIX F

INSERTION LOSS MEASUREMENTS

APPENDIX F

INSERTION LOSS MEASUREMENTS

The measurement of the insertion loss of a delay line cannot be made by the usual substitution technique since the reflection from the output is also included in the results obtained. A method has been developed by CW Beaty[1] in which the dissipative and reflective components of attenuation are measured separately.

It can be shown that the total attenuation in any linear passive device inserted in a transmission line can be expressed by:

$$A_T = A_D + A_R \qquad \text{(F. 1)}$$

where

A_T = total attenuation

A_D = dissipative component

A_R = reflected component

The measure of the dissipative component involves the measurement of the power ratio $(\frac{Po\ in}{Po\ out})$ or its reciprocal, the efficiency, N_m, of the attenuator when terminated in a matched load. A convenient method exists for the measurement of N_m, by the use of a Smith chart. The efficiency, N_m, is equal to the radius of a circular locus, obtained by plotting the maximum and minimum values of VSWR as the position of a sliding short circuit is varied at the termination of the line. A_D then is given by the expression:

$$A_D = 10 \log_{10} \frac{Pin}{Pout} = 10 \log_{10} \frac{1}{N_m} = 10 \log_{10} \frac{I}{R} \qquad \text{(F. 2)}$$

where

P = power

N_m = efficiency

R = radius of circle on a Smith chart

$$= \frac{\sigma \text{ max. } \sigma \text{ min } -1}{(\sigma \text{ max} + 1)(\sigma \text{ min} + 1)} \qquad \text{(F. 3)}$$

The reflective component A_R can be found by measurement of the VSWR of the device when terminated in a matched load from the expression

$$A_R = 10 \log_{10} (\sigma_m + 1)^2 \qquad \text{(F. 4)}$$

where σm = VSWR of the device.

---

[1] Determination of Attenuation from Impedance Measurements Proc. of IRE August 1950 CW Beatty.

Therefore the total attenuation of the device can be expressed as the sum of (F.2) and F.4)

$$A_T = 10 \log_{10} \frac{1}{R} + 10 \log_{10} \frac{(\sigma + 1)^2}{4 \sigma_m} \qquad \text{(F.5)}$$

The test setup for measurement of the required values is shown in Figure F-1. In the measurement of A_D, it should be noted that the device is reversed from its normal orientation as noted in the diagram.

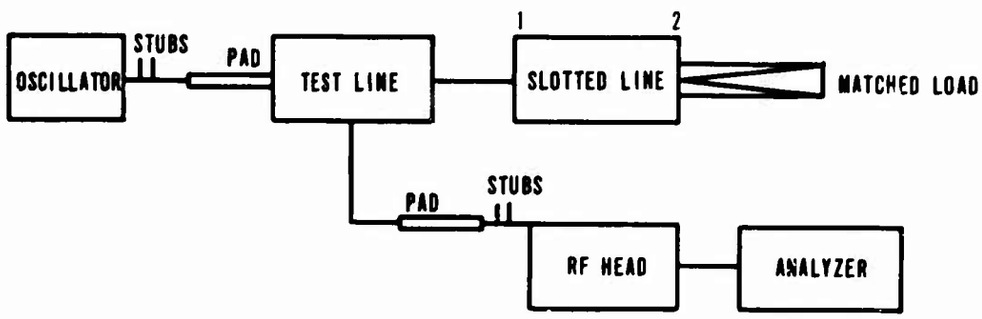

(a) Measurement of A_R

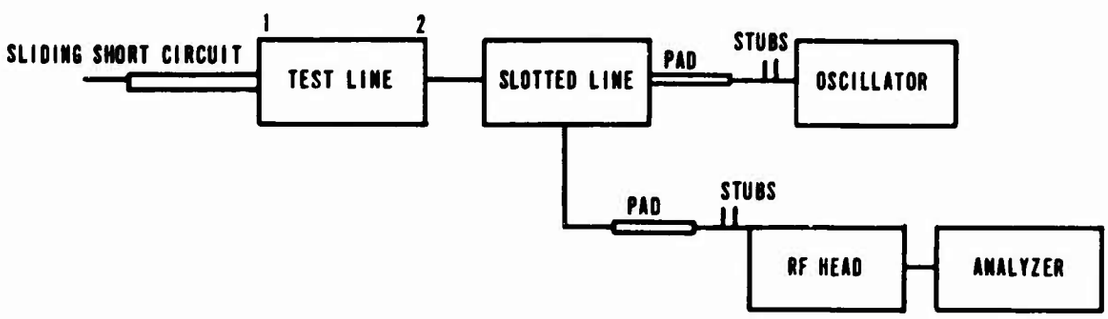

(b) Measurement of A_D

635500

Figure F-1. Set-Ups for Measurements of Insertion Loss

APPENDIX G

DESIGN SPECIFICATION DRAWINGS

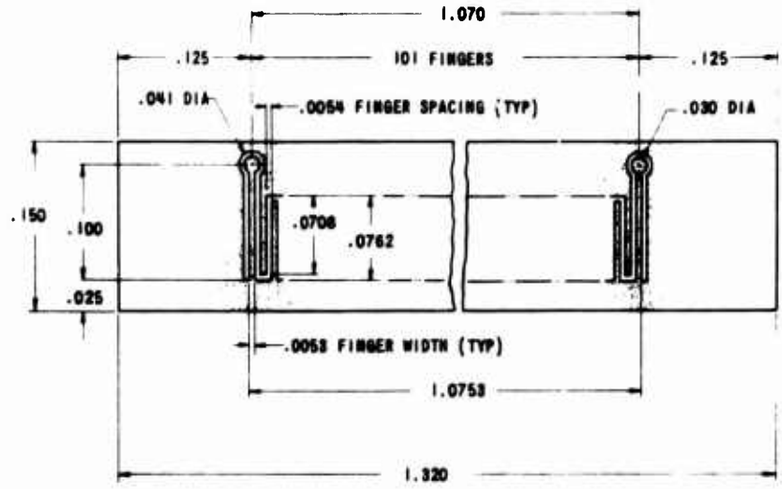

NOTES:

1. NEGATIVE FOR ABOVE PATTERN SHOULD HAVE TRANSPARENT BACKGROUND AND FINGERS, AND OPAQUE SPACES.
2. NEGATIVE TO BE SUPPLIED ON 1/4 THICK HIGH RESOLUTION GLASS PLATE.

636150

Figure G-1. Linear Ku-Band Slow-Wave Structure

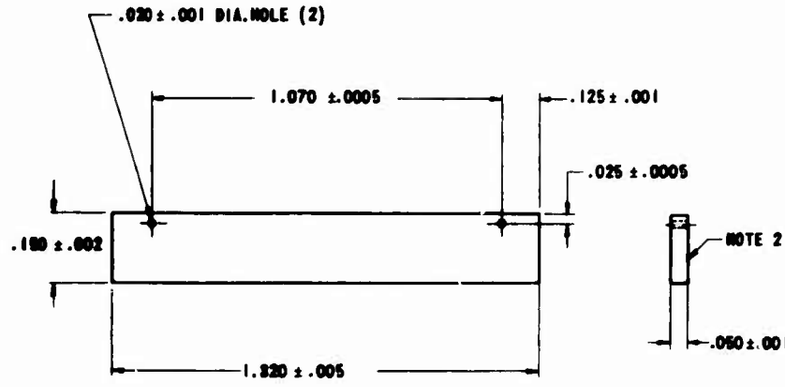

NOTES:

1. PIECE TO BE FLAT TO 6-8 LIGHT BANDS.
2. ONE SURFACE ONLY TO BE FINISHED TO 3 TO 5 MICROINCH.

636148

Figure G-2. Substrate Material: Beryllia 99% Pure, 95% Min Density

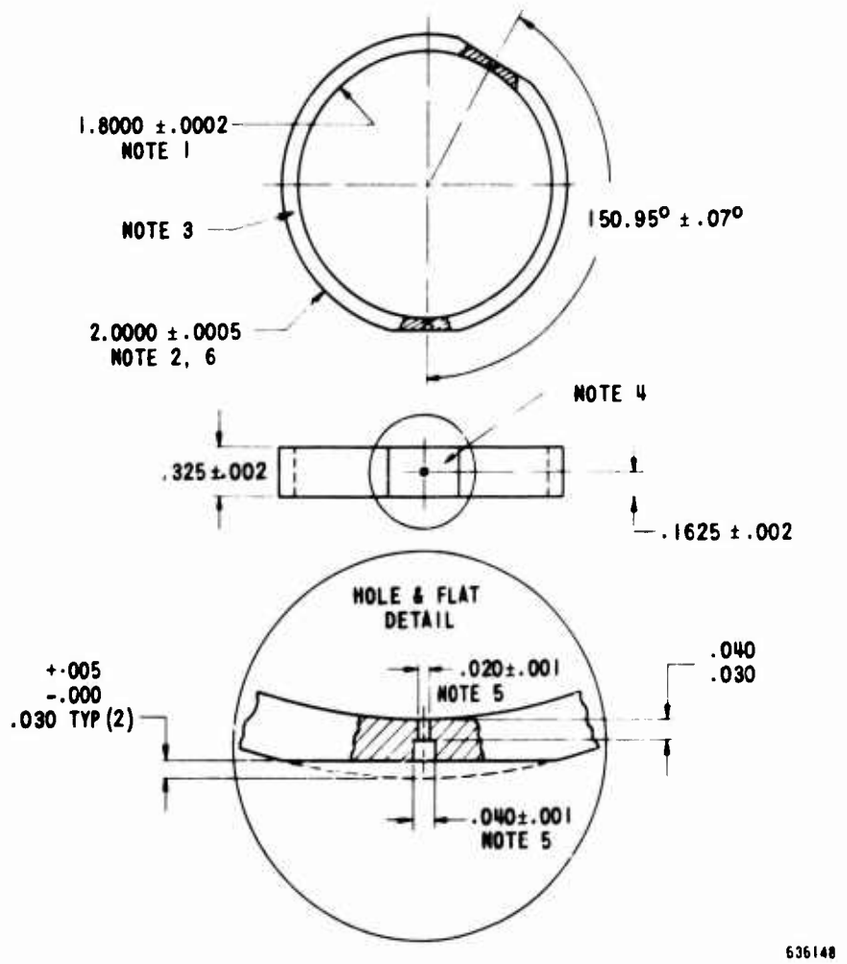

NOTES:

1. I.D. SURFACE FINISH TO BE 15 MICRO INCH OR BETTER, NOT METALIZED.
2. O.D. SURFACE FINISH TO BE 50 MICRO INCH, AND METALIZED (SEE NOTE 4).
3. CYLINDER ENDS TO BE FINISHED 50 MICRO INCH, AND METALIZED.
4. THIS SURFACE TO BE FINISHED TO 50 MICRO INCH, BUT NOT METALIZED.
5. INTERIOR OF .020 HOLES TO BE METALIZED FOR .025 MIN LENGTH .040 DIA HOLES TO BE UNMETALIZED.
6. DIA AFTER METALIZING TO BE 2.0030 MAX.

Figure G-3. Cylinder for Circular SWS
Material: Beryllia, 99% Pure, 95% Min. Density

Security Classification

DOCUMENT CONTROL DATA - R&D

(Security classification of title, body of abstract and indexing annotation must be entered when the overall report is classified)

1. ORIGINATING ACTIVITY (Corporate author) Raytheon Company Microwave and Power Tube Division Waltham, Massachusetts	2a. REPORT SECURITY CLASSIFICATION Unclassified 2b GROUP

3. REPORT TITLE

Development of Manufacturing Methods for Improved Delay Lines

4. DESCRIPTIVE NOTES (Type of report and inclusive dates)

Final Report 23 December 1963 - 31 May 1967

5. AUTHOR(S) (Last name, first name, initial)

Hendry, Frank M., Mannette, Russell T., Shaw, Beverly A.

6. REPORT DATE	7a. TOTAL NO. OF PAGES	7b. NO. OF REFS
August 1967	150	None

8a. CONTRACT OR GRANT NO.	9a. ORIGINATOR'S REPORT NUMBER(S)
AF33(615)-2044 b. PROJECT NO. MMP Project 8-142 c. d.	PT-1437 9b. OTHER REPORT NO(S) (Any other numbers that may be assigned this report) AFML-TR-67-281

10. AVAILABILITY/LIMITATION NOTICES This document is subject to special export controls and each transmittal to foreign governments or foreign nationals may be made only with prior approval of the Air Force Materials Laboratory, W-PAFB, Ohio 45433. In DDC.

11. SUPPLEMENTARY NOTES	12. SPONSORING MILITARY ACTIVITY
	Air Force Materials Laboratory Wright Patterson AFB, Ohio 45433

13 ABSTRACT

During the three phases of this program the following major objectives were accomplished:

1. A facility was established to manufacture photocopied slow-wave structures.

2. A bonding technique was developed between the metallic slow-wave structure and a beryllia substrate, capable of withstanding the processing and operating conditions of the test vehicles.

3. Ten test vehicles have been constructed and evaluated to demonstrate the reliability of the finished C-band slow-wave structure.

4. One test vehicle has been life tested and accumulating 260 hours before failure.

5. Structures have been evaluated at cold test both at C-band and K-band, demonstrating the wide versatility of the technique.

6. Structures have been environmentally evaluated at an acceleration of 20 g's over a frequency range of 55 to 2000 Hz.

This abstract is subject to special export controls and each transmittal to foreign governments or foreign nationals may be made only with prior approval of the Air Force Materials Laboratory, W-PAFB, Ohio 45433.

DD FORM 1 JAN 64 1473

Security Classification

Unclassified

Security Classification

14 KEY WORDS	LINK A		LINK B		LINK C	
	ROLE	WT	ROLE	WT	ROLE	WT
Photocopied slow-wave structure Development of bonding technique Beryllia substrate Reliability and environmental evaluation "M"-Type Backward Wave Oscillator Linear Circular						

INSTRUCTIONS

1. **ORIGINATING ACTIVITY:** Enter the name and address of the contractor, subcontractor, grantee, Department of Defense activity or other organization *(corporate author)* issuing the report.

2a. **REPORT SECURITY CLASSIFICATION:** Enter the overall security classification of the report. Indicate whether "Restricted Data" is included. Marking is to be in accordance with appropriate security regulations.

2b. **GROUP:** Automatic downgrading is specified in DoD Directive 5200.10 and Armed Forces Industrial Manual. Enter the group number. Also, when applicable, show that optional markings have been used for Group 3 and Group 4 as authorized.

3. **REPORT TITLE:** Enter the complete report title in all capital letters. Titles in all cases should be unclassified. If a meaningful title cannot be selected without classification, show title classification in all capitals in parenthesis immediately following the title.

4. **DESCRIPTIVE NOTES:** If appropriate, enter the type of report, e.g., interim, progress, summary, annual, or final. Give the inclusive dates when a specific reporting period is covered.

5. **AUTHOR(S):** Enter the name(s) of author(s) as shown on or in the report. Enter last name, first name, middle initial. If military, show rank and branch of service. The name of the principal author is an absolute minimum requirement.

6. **REPORT DATE:** Enter the date of the report as day, month, year; or month, year. If more than one date appears on the report, use date of publication.

7a. **TOTAL NUMBER OF PAGES:** The total page count should follow normal pagination procedures, i.e., enter the number of pages containing information.

7b. **NUMBER OF REFERENCES:** Enter the total number of references cited in the report.

8a. **CONTRACT OR GRANT NUMBER:** If appropriate, enter the applicable number of the contract or grant under which the report was written.

8b, 8c, & 8d. **PROJECT NUMBER:** Enter the appropriate military department identification, such as project number, subproject number, system numbers, task number, etc.

9a. **ORIGINATOR'S REPORT NUMBER(S):** Enter the official report number by which the document will be identified and controlled by the originating activity. This number must be unique to this report.

9b. **OTHER REPORT NUMBER(S):** If the report has been assigned any other report numbers *(either by the originator or by the sponsor)*, also enter this number(s).

10. **AVAILABILITY/LIMITATION NOTICES:** Enter any limitations on further dissemination of the report, other than those imposed by security classification, using standard statements such as:

(1) "Qualified requesters may obtain copies of this report from DDC."

(2) "Foreign announcement and dissemination of this report by DDC is not authorized."

(3) "U. S. Government agencies may obtain copies of this report directly from DDC. Other qualified DDC users shall request through _____."

(4) "U. S. military agencies may obtain copies of this report directly from DDC. Other qualified users shall request through _____."

(5) "All distribution of this report is controlled. Qualified DDC users shall request through _____."

If the report has been furnished to the Office of Technical Services, Department of Commerce, for sale to the public, indicate this fact and enter the price, if known.

11. **SUPPLEMENTARY NOTES:** Use for additional explanatory notes.

12. **SPONSORING MILITARY ACTIVITY:** Enter the name of the departmental project office or laboratory sponsoring *(paying for)* the research and development. Include address.

13. **ABSTRACT:** Enter an abstract giving a brief and factual summary of the document indicative of the report, even though it may also appear elsewhere in the body of the technical report. If additional space is required, a continuation sheet shall be attached.

It is highly desirable that the abstract of classified reports be unclassified. Each paragraph of the abstract shall end with an indication of the military security classification of the information in the paragraph, represented as *(TS)*, *(S)*, *(C)* or *(U)*.

There is no limitation on the length of the abstract. However, the suggested length is from 150 to 225 words.

14. **KEY WORDS:** Key words are technically meaningful terms or short phrases that characterize a report and may be used as index entries for cataloging the report. Key words must be selected so that no security classification is required. Identifiers, such as equipment model designation, trade name, military project code name, geographic location, may be used as key words but will be followed by an indication of technical context. The assignment of links, rules, and weights is optional.

Unclassified

Security Classification